

POLYMERIC SURFACE MODIFICATION OF METALLIC MEDICAL IMPLANTS
FOR ENHANCED STABILITY AND DELIVERY OF THERAPEUTIC AGENTS

By

MARGARET W. KAYO

A DISSERTATION PRESENTED TO THE GRADUATE SCHOOL
OF THE UNIVERSITY OF FLORIDA IN PARTIAL FULFILLMENT
OF THE REQUIREMENTS FOR THE DEGREE OF
DOCTOR OF PHILOSOPHY

UNIVERSITY OF FLORIDA

2005

Copyright 2005

by

Margaret W. Kayo

This dissertation is dedicated to my family and the close friendships I have made here...

ACKNOWLEDGMENTS

I thank my advisor, Dr. Eugene Goldberg, for his support and leadership, in addition to his confidence in my abilities. My thanks are also extended to my advisory committee, Dr. Anthony Brennan, Dr. Chris Batich, Dr. James Seeger and Dr. Kenneth Wagener. I would also like to acknowledge the expertise of Eric Lambers, Gary Scheffeile, Paul Martin, Dr. Won-Seok Kim, Dr. Mike Ollinger, Dr. David Norton, Mat Ivill, Dr. Harmut Derendorff, Dr. Vipul Kumar, Dr. Samuel Farrah and Dr. George Lukasik.

Thanks are extended to the following people for their technical support and friendships: Dr. Daniel Urbaniak, Amanda York, Adam Reboul, Adam Feinberg, Dr. Chris Widenhouse and Jennifer Wrighton.

I thank the following people for their friendship and humor Samesha Barnes, Dr. Brett Almond, Dr. Clayton Bohn, Iris Enriquez, Jim Schumacher, Anika Odukale, Jompo Molye, Tara Wahsington, Amin Elachchabi, Michelle Carman, Leslie Wilson, Thomas Estes, and Jim Seliga. Finally, I would like to thank my mother, Cecilia Kayo Bressan, father, David Kayo, stepfather, Ronald Bressan, sister, Rebekah Kao and brother, Jonathan Kayo for their confidence in my ability to succeed.

TABLE OF CONTENTS

	<u>page</u>
ACKNOWLEDGMENTS	iv
LIST OF TABLES	viii
LIST OF FIGURES	x
ABSTRACT	xv
CHAPTER	
1 INTRODUCTION	1
2 BACKGROUND	4
Introduction.....	4
Endovascular Stents.....	5
Sirolimus (Rapamycin) Eluting Stents	10
Paclitaxel Eluting Stents	11
17 β -estradiol Eluting Stents	12
Dexamethasone Eluting Stents	13
Drug Release from Silicone.....	14
Keratome Blades.....	15
Materials for Coatings and Implantable Medical Devices	15
Significance	20
3 METAL ALKOXIDE TREATMENTS AND LOW DOSE GAMMA SURFACE MODIFICATION OF STAINLESS STEEL.....	21
Introduction.....	21
Metal Alkoxide Treatments	21
Materials and Methods	23
Preparation of 316L stainless steel substrates	23
Treating 316L stainless steel with metal alkoxides.....	23
Chromium alkoxide degradation study	24
Analysis.....	24
Results and Discussion.....	24
Summary.....	31

Low Dose Gamma Irradiation Grafting of Polymers to Metal Alkoxide Treated	
Substrates	32
Materials and Methods	33
Preparation and treatment of 316L stainless steel substrates	33
Preparation of monomer solutions	34
Gamma irradiation of substrates	34
Analysis.....	35
Results and Discussion	36
Summary.....	52
4 PULSED LASER ABLATION DEPOSITION (PLAD) AND RF PLASMA	
POLYMERIZATION DEPOSITION	55
Introduction.....	55
Pulsed Laser Ablation Deposition (PLAD).....	55
Materials and Methods	57
Preparation of silicone targets and substrates	57
Pulsed laser ablation deposition chamber	58
Analysis.....	59
Results and Discussion	59
Summary.....	66
RF Plasma Surface Modification.....	67
Materials and Methods	68
Preparation of substrate, monomers, and comonomer	68
Monomer RF plasma.....	69
Analysis.....	70
Results and Discussion	70
Summary.....	74
5 SOLUTION POLYMERIZATION COATING SURFACE MODIFICATION.....	76
Introduction.....	76
Materials and Methods	77
Preparation and Treatment of 316L Stainless Steel Substrates	77
Preparation of Monomer Solutions	77
Preparation of Silicone Component Solutions	77
Solution Polymerization (SP) Coating of Substrates.....	78
Analysis	78
Results and Discussion	79
Summary	89
6 LOADING AND RELEASE OF THERAPUETIC AGENTS FROM SURFACE	
MODIFIED METAL ALKOXIDE TREATED STAINLESS STEEL.....	91
Introduction.....	91
Materials and Methods	92
Preparation of Substrates and Coatings.....	92

Post Loading Ofloxacin and Dexamethasone.....	93
Drug Loading Solution Depletion Study.....	94
Release of Drugs from Surface Modified 316L Stainless Steel.....	94
Preparation of Bacterial Cultures for Zone of Inhibition.....	96
Analysis.....	96
Results and Discussion.....	97
Summary.....	105
7 CONCLUSIONS.....	107
8 FUTURE WORK.....	110
LIST OF REFERENCES.....	112
BIOGRAPHICAL SKETCH.....	118

LIST OF TABLES

<u>Table</u>	<u>page</u>
2.1 - Metal alkoxide chromium complex constituents.....	18
2.2 - Silicone curing systems	19
3.1 – Volan [®] L solution and Silver Acrylate mixed solvent solution composition.	24
3.2 – XPS analysis for air dried samples without rinsing: % Cr2p3 and % C1s relative to % O1s, Fe2p3 and Cl2p. All conditions were examined on 316L stainless steel.....	27
3.3 – MPC XPS elemental surface composition (%) and rehydrated contact angle of surfaces for dose of 0.1 Mrads. MPC* refers to theoretical concentrations of elemental composition.....	49
3.4 – NVP XPS elemental surface composition (%) and rehydrated contact angle of surfaces for dose of 0.1 Mrads. NVP* refers to theoretical concentrations of elemental composition.....	49
3.5 – KSPA XPS elemental surface composition (%) and rehydrated contact angle of surfaces for dose of 0.1 Mrads. KSPA* refers to theoretical concentrations of elemental composition.....	51
4.1 – Contact angle of MED 6820 depositions at various fluences on untreated 316L stainless steel.	60
4.2 – XPS elemental analysis (%) of PLAD coated samples on untreated 316L stainless steel.	64
4.3 – XPS elemental analysis (%) of PLAD coated samples on Volan [®] treated 316L stainless steel.	65
4.4 – XPS elemental analysis (%) of 5 minute monomer RF plasma modification of untreated, Volan [®] L and Quilon [®] L treated 316L stainless steel.	74
5.1 – XPS analysis of SP coated Volan [®] L and untreated 316L stainless steel.....	89

6.1 – Coating and metal alkoxide treatment conditions investigated for drug release where Oflox and Dex refers to ofloxacin and dexamethasone, respectively. 2% V-L refers to 2 % v/v Volan [®] L.	94
6.2 – Ofloxacin depletion UV-Vis absorption measurements in terms of concentration with adjustments for surface area and conversions, all values are reported as averages.	97
6.3 – Dexamethasone depletion UV-Vis absorption measurements in terms of concentration with adjustments for surface area and conversions, all values are reported as averages.	98

LIST OF FIGURES

<u>Figure</u>	<u>page</u>
2.1 - Illustration of balloon angioplasty and stenting. Adapted from ADAM, Inc.....	6
2.2 - Histological section of restenotic arteries following balloon angioplasty and stenting. ¹⁰ Indolfi et al. 2003	8
2.3 - Various stents. A) CYPHER [®] sirolimus-eluting coronary stent by Cordis Corporation, B) Stent by Boston Scientific Corporation, C) Stent by Medtronic, Inc.....	11
2.4 - Volan [®] and Volan [®] L bonding agent, chromium (III) methacrylate.....	17
2.5 - Quilon [®] L bonding agent, chromium (III) fatty acid where R=C ₁₄₋₁₈	17
2.6 – Hydrophilic monomer structures: 2-methacryloyloxyethyl phosphorylcholine (MPC), N-vinyl pyrrolidone (NVP), N,N-dimethylacrylamide (DMA), and potassium 3-sulfopropyl acrylate (KSPA).	19
2.7 - Silicone vinyl addition curing system	20
3.1 – Silver Acrylate (Gelest, Inc., Morrisville, PA).	23
3.2 – XPS survey of PET.	26
3.3 – XPS spectra of Ag3d5 of silver acrylate treatment on 316L stainless steel.	28
3.4 – XPS C1s and O1s spectra of: A) Previously-opened 2% Quilon [®] L treatment on 316 L stainless steel, B) Newly-opened 2% Quilon [®] L treatment on 316 L stainless steel, and C) 316L stainless steel control.....	30
3.5 – XPS C1s and O1s spectra of: A) Previously-opened 2% Volan [®] treatment on 316 L stainless steel, B) Newly-opened 2% Volan [®] treatment on 316 L stainless steel, and C) 316L stainless steel control.	31
3.6 - ⁶⁰ Co gamma irradiator and rotating sample stage.	35
3.7 – Contact angle stability of untreated 316L stainless steel irradiated to 0.1 and 0.15 Mrads in 10% NVP / Ultrapure [™] water solutions.....	36

3.8 – Contact angle stability of untreated 316L stainless steel irradiated to 0.1 and 0.15 Mrads in 10% MPC / Ultrapure™ water solutions.	37
3.9 – Contact angle stability of untreated 316L stainless steel irradiated to 0.1 and 0.15 Mrads in 2.5% DMA / Ultrapure™ water solutions.	37
3.10 – Contact angle stability of untreated 316L stainless steel irradiated to 0.1 and 0.15 Mrads in 10% KSPA / Ultrapure™ water solutions.	38
3.11 – Contact angle stability of untreated 316L stainless steel irradiated to 0.1 and 0.15 Mrads in 9.5% NVP / 0.5% DMA / Ultrapure™ water solutions.	38
3.12 – Contact angle stability of untreated 316L stainless steel irradiated to 0.1 and 0.15 Mrads in 9.5% MPC / 0.5% DMA / Ultrapure™ water solutions.	39
3.13 – Contact angle stability of untreated 316L stainless steel irradiated to 0.1 and 0.15 Mrads in 9.5% KSPA / 0.5% DMA / Ultrapure™ water solutions.	39
3.14 – Contact angle stability of Quilon® L treated 316L stainless steel irradiated to 0.1 and 0.15 Mrads in 10% NVP / Ultrapure™ water solutions.	40
3.15 – Contact angle stability of Quilon® L treated 316L stainless steel irradiated to 0.1 and 0.15 Mrads in 10% KSPA / Ultrapure™ water solutions.	40
3.16 – Contact angle stability of Quilon® L treated 316L stainless steel irradiated to 0.1 and 0.15 Mrads in 9.5% NVP / 0.5% DMA / Ultrapure™ water solutions.	41
3.17 – Contact angle stability of Quilon® L treated 316L stainless steel irradiated to 0.1 and 0.15 Mrads in 9.5% KSPA / 0.5% DMA / Ultrapure™ water solutions.	41
3.18 – Contact angle stability of Volan® treated 316L stainless steel irradiated to 0.1 and 0.15 Mrads in 10% NVP / Ultrapure™ water solutions.	42
3.19 – Contact angle stability of Volan® treated 316L stainless steel irradiated to 0.1 and 0.15 Mrads in 10% KSPA / Ultrapure™ water solutions.	42
3.20 – Contact angle stability of Volan® treated 316L stainless steel irradiated to 0.1 and 0.15 Mrads in 9.5% NVP / 0.5% DMA / Ultrapure™ water solutions.	43
3.21 – Contact angle stability of Volan® treated 316L stainless steel irradiated to 0.1 and 0.15 Mrads in 9.5% KSPA / 0.5% DMA / Ultrapure™ water solutions.	43
3.22 – Contact angle stability of Volan® L treated 316L stainless steel irradiated to 0.1 and 0.15 Mrads in 10% NVP / Ultrapure™ water solutions.	44
3.23 – Contact angle stability of Volan® L treated 316L stainless steel irradiated to 0.1 and 0.15 Mrads in 10% KSPA / Ultrapure™ water solutions.	44

3.24 – Contact angle stability of Volan [®] L treated 316L stainless steel irradiated to 0.1 and 0.15 Mrads in 9.5% NVP / 0.5% DMA / Ultrapure [™] water solutions.	45
3.25 – Contact angle stability of Volan [®] L treated 316L stainless steel irradiated to 0.1 and 0.15 Mrads in 9.5% KSPA / 0.5% DMA / Ultrapure [™] water solutions.	45
3.26 – Contact angle stability of Quilon [®] L treated 316L stainless steel irradiated to 0.1 and 0.15 Mrads in 10% MPC / Ultrapure [™] water solutions.	46
3.27 – Contact angle stability of Quilon [®] L treated 316L stainless steel irradiated to 0.1 and 0.15 Mrads in 9.5% MPC / 0.5% DMA / Ultrapure [™] water solutions.	46
3.28 – Contact angle stability of Volan [®] treated 316L stainless steel irradiated to 0.1 and 0.15 Mrads in 10% MPC / Ultrapure [™] water solutions.	47
3.29 – Contact angle stability of Volan [®] treated 316L stainless steel irradiated to 0.1 and 0.15 Mrads in 9.5% MPC / 0.5% DMA / Ultrapure [™] water solutions.	47
3.30 – Contact angle stability of Volan [®] L treated 316L stainless steel irradiated to 0.1 and 0.15 Mrads in 10% MPC / Ultrapure [™] water solutions.	48
3.31 – Contact angle stability of Volan [®] L treated 316L stainless steel irradiated to 0.1 and 0.15 Mrads in 9.5% MPC / 0.5% DMA / Ultrapure [™] water solutions.	48
3.32 – MPC grafted on treated and untreated 316L SS. XPS elemental spectra for N1s and P2p. A) 2% Volan [®] L treated, B) 2% Quilon [®] L treated, and C) untreated.	50
3.33 – SEM of cleaned 316L stainless steel at 5000x.	51
3.34 – SEM of 10% v/v MPC gamma irradiation grafted (0.1 MRads) coating on Volan [®] L activated 316L stainless steel at 5000x.	52
4.1 – Illustration of PLAD system setup. ⁶⁰	57
4.2 – FTIR-ATR spectra of MED 6820 deposited at a fluence of 400 mJ/cm ² on silicon wafer.	62
4.3 – FTIR-ATR spectra of MED 6820 deposited at a fluence of 400 mJ/cm ² on 2% Volan treated 316L stainless steel.	62
4.4 – FTIR-ATR spectra of MED 6820 deposited at a fluence of 200 mJ/cm ² on 2% Volan treated 316L stainless steel.	63
4.5 – FTIR-ATR spectra of MED 6820 deposited at a fluence of 125 mJ/cm ² on 2% Volan treated 316L stainless steel.	63
4.5 – SEM of 316L stainless steel at 500x.	65

4.6 – SEM of MED6820 PLAD coated at fluence of 300 mJ/cm ² onto untreated 316L stainless steel at 500x.	66
4.7 – Initial contact angle measurements for NVP, DMA and NVP/DMA RF plasma surface modifications on untreated 316L stainless steel.	71
4.8 – Initial contact angle measurements for NVP, DMA and NVP/DMA RF plasma surface modifications on 2% v/v Quilon [®] L treated 316L stainless steel.	71
4.9 – Initial contact angle measurements for NVP, DMA and NVP/DMA RF plasma surface modifications on 2% v/v Volan [®] L treated 316L stainless steel.	72
4.10 – Rehydrated contact angle measurements for NVP, DMA and NVP/DMA RF plasma surface modifications on untreated 316L stainless steel.	72
4.11 – Rehydrated contact angle measurements for NVP, DMA and NVP/DMA RF plasma surface modifications on 2% v/v Quilon [®] L treated 316L stainless steel.	73
4.12 – Rehydrated contact angle measurements for NVP, DMA and NVP/DMA RF plasma surface modifications on 2% v/v Volan [®] L treated 316L stainless steel.	73
5.1 – Initial contact angle measurements for 10% and 25% v/v monomer SP coated untreated 316L stainless steel.	80
5.2 – Initial contact angle measurements for 10% and 25% v/v monomer SP coated Volan [®] L treated 316L stainless steel.	80
5.3 – Contact angle measurements immediately after dehydration for 10% and 25% v/v monomer SP coated untreated 316L stainless steel.	81
5.4 – Contact angle measurements immediately after dehydration for 10% and 25% v/v monomer SP coated Volan [®] L treated 316L stainless steel.	81
5.5 – Rehydrated contact angle measurements for 10% and 25% v/v monomer SP coated untreated 316L stainless steel.	82
5.6 – Rehydrated contact angle measurements for 10% and 25% v/v monomer solution coated Volan [®] L treated 316L stainless steel.	83
5.7 – Contact angle measurements for 10% and 25% v/v NVP SP coated untreated 316L stainless steel.	83
5.8 – Contact angle measurements for 10% and 25% v/v NVP SP coated Volan [®] L treated 316L stainless steel.	84
5.9 – Contact angle measurements for 10% and 25% v/v MPC SP coated untreated 316L stainless steel.	84

5.10 – Contact angle measurements for 10% and 25% v/v MPC SP coated Volan [®] L treated 316L stainless steel.....	85
5.11 – Contact angle measurements for 10% v/v KSPA SP coated untreated 316L stainless steel.....	85
5.12 – Contact angle measurements for 10% v/v KSPA SP coated Volan [®] L treated 316L stainless steel.....	86
5.13 – FTIR-ATR spectra of MED 6820 medical grade silicone.....	87
5.14 – FTIR-ATR spectra of MED 6820 SP coated untreated 316L stainless steel.....	87
5.15 – FTIR-ATR spectra of MED 6820 SP coating on Volan [®] L treated 316L stainless steel.....	88
6.1 – Molecular structures for ofloxacin and dexamethasone.....	92
6.2 – Ofloxacin release from 25% v/v NVP SP coated Volan [®] L and untreated 316L stainless steel compared with unmodified controls.....	100
6.3 – Ofloxacin release from 25% v/v MPC SP coated Volan [®] L and untreated 316L stainless steel compared with unmodified controls.....	100
6.4 – Dexamethasone release from 25% v/v MPC SP coated Volan [®] L and untreated 316L stainless steel compared with unmodified controls.....	101
6.5 – Dexamethasone release from 10% v/v MPC gamma irradiation graft coated Volan [®] L and untreated 316L stainless steel compared with unmodified controls.....	102
6.6 – Dexamethasone release from 45% v/v MED6820 SP coated Volan [®] L and untreated 316L stainless steel compared with unmodified controls.....	103
6.7 – Zone of inhibition of ofloxacin release from 25% NVP solution coated Volan [®] L treated 316L stainless steel. Left-S.Aureus. Right-S.Epidermidis.....	104
6.8 – Zone of inhibition of ofloxacin release from 25% NVP solution coated untreated 316L stainless steel. Left-S.Aureus. Right-S.Epidermidis.....	104
6.9 – Zone of inhibition of ofloxacin release from 2% silver acrylate functionalized 316L stainless steel. Left-S.Aureus. Right-S.Epidermidis.....	104

Abstract of Dissertation Presented to the Graduate School
of the University of Florida in Partial Fulfillment of the
Requirements for the Degree of Doctor of Philosophy

POLYMERIC SURFACE MODIFICATION OF METALLIC MEDICAL IMPLANTS
FOR ENHANCED STABILITY AND DELIVERY OF THERAPEUTIC AGENTS

By

Margaret W. Kayo

August 2005

Chair: Eugene P. Goldberg

Major Department: Materials Science and Engineering

Complications associated with implantable devices have led to research focused on enhancing surface properties to improve device biocompatibility. Implants such as endovascular stents and surgical contact devices such as keratome blades are examples of medical devices that can potentially benefit from enhanced surface properties. Drug delivery from stent surface modifications has been shown to reduce or control wound healing response to such implants and enhance wound healing with inhibition of restenosis. Surface modifications that provide therapeutic effects through the incorporation and localized action of drugs represent an important area of research for improved medical devices.

In the study reported here, novel surface modifications of 316L stainless steel have been prepared with surface functionalized metal alkoxides. The general objective has been to develop new surface treatments pertinent to metal stents and surgical blades. The surface modification techniques used in this research included gamma radiation grafting,

solution polymerization coating, thin film deposition by pulsed laser ablation deposition (PLAD) and radio frequency plasma (RF plasma). The monomers used in these metal coating systems were designed to produce stable hydrophilic surfaces; N-vinylpyrrolidone (NVP), 2-methacryloyloxyethyl phosphorylcholine (MPC), N,N-dimethylacrylamide (DMA), and potassium 3-sulfopropyl acrylate (KSPA). Medical grade silicones were also studied as coatings on 316L stainless steel using PLAD and solution polymerization coating methods. Emphasis of the research was on the evaluation of new metal alkoxide activated stainless steel surfaces with untreated stainless steel to enhance surface modification stability. Improved hydrophilic surface modifications of metal alkoxide treated stainless steel were demonstrated to be stable and lubricious. Surfaces were characterized by contact angle goniometry, FTIR-ATR, XPS and SEM.

Various conditions were also investigated to develop methods for incorporating therapeutic agents into modified device surfaces. The drugs studied included ofloxacin, an antimicrobial agent, and dexamethasone, an anti-inflammatory agent. Loading and release of these drugs into PBS and human blood plasma were examined by UV-Vis and HPLC.

In summary, new coating systems and practical process procedures were developed to enhance the coating stability on 316L stainless steel surfaces and to effectively deliver therapeutic agents.

CHAPTER 1 INTRODUCTION

The manufacture and sale of implantable devices, such as endoluminal stents and keratome blades, represent a growing industry in medical treatments that extend and enhance the quality of life for patients. While manufacturing continues to advance, many complications remain associated with the biocompatibility of these devices. Material-tissue interactions play a central role in the bioacceptance of a device. Surface modification of a medical device is an effective approach to reducing and controlling post-interventional complications such as inflammation, thrombosis, and restenosis and to enhance biocompatibility between device materials and local host tissue.

The research presented here was aimed at exploring various new coatings involving several hydrophilic vinyl monomers and resin reinforced silicone applied in conjunction with an assortment of metal alkoxide coupling agents through several novel coating techniques that have been shown to modify surfaces effectively.

316L Stainless steel is widely used in the medical device industry due to its desirable mechanical properties, low carbon content and high corrosion resistance. Despite these beneficial characteristics, 316L stainless steel surfaces elicit an inflammatory and thrombotic cascade when implanted in a blood rich environment in the human body. For this reason, surface modification is an ideal method to improve the biocompatibility of 316L stainless steel. Several approaches to modifying metallic substrates have been investigated and will be presented in this body of work as will the problems associated with various coating techniques.

A problem inherent to most coatings for medical devices is stability of coatings over time and when exposed to a variety of storage environments and inadequate adhesion of the coatings to substrates. The use of a novel coupling system for biomedical device applications to enhance binding at the polymer and metal interface may resolve these issues. Metal alkoxides with either methacrylate functionality or fatty acid pendant groups were investigated in this research.

The research presented here used metal alkoxide coupling systems to enhance the binding of polymer coatings to metal substrates employing a wide variety of surface modification techniques. Because these coupling systems have not been used in the biomedical device industry, their incorporation into medical device surface modification techniques is a novel approach for developing stable coatings with the potential to release therapeutic agents from the coatings.

Chapter 2 presents a review of the biological complications associated with medical implants, examples of device complications from clinical studies and the materials and technologies that have led to this work. Backgrounds of individual surface modification techniques will be addressed at the beginning of each respective chapter.

Chapter 3 focuses on the development of metal alkoxide coupling and coating systems and the use of gamma irradiation for initiating surface reactions in monomer solutions for modification of metal substrates. The incorporation of metal alkoxide pretreatments is shown to enhance the stability of the hydrophilic monomers investigated when grafted by gamma initiation.

Chapter 4 covers the use of Pulsed Laser Ablation Deposition (PLAD) and monomer RF-plasma. Both techniques require vacuum systems and rely on ionizing the

surfaces with laser and radio frequency generated plasma, respectively. In PLAD, the influence of chamber oxygen content on coating composition is explored. New coating conditions are investigated with RF-plasma utilizing individual monomers as well as a combination. Additionally, the effectiveness of these surface modification techniques are investigated with metal alkoxide coupling systems.

Chapter 5 describes the effectiveness of metal alkoxide treatments with solution polymerization coating. In addition to vinyl monomer solutions, dilute reactive resin reinforced silicone solutions were also investigated in these coating systems.

Chapter 6 highlights sustained release studies demonstrating the potential of metal alkoxide coupling systems to enhance coating stability for drug delivery applications. Release of both an antimicrobial and anti-inflammatory drug was investigated with various gamma irradiated and solution coated systems.

Chapters 7 and 8 review the conclusions drawn from the studies in each chapter and identify avenues for future studies, respectively.

This body of work is intended to advance the understanding and application of chromium alkoxide coupling systems to enhance polymer coating stability on stainless steel surfaces with the potential to release drugs. Biocompatibility is not tested in this work, while demonstrating biocompatibility is the long-term goal for the coating systems developed here.

CHAPTER 2 BACKGROUND

Introduction

The manufacturing of implantable medical devices has revolutionized treatment and quality of life for patients. The strides made in implantable medical device research have led to a focus on developing surfaces that afford these devices greater biocompatibility in the human body. For example, surface modifications and compositional developments of endoluminal stents have reduced restenosis rates. Additionally, developments in keratome blade sharpness and composition have decreased trauma after intraocular lens implantation. However, most materials are not readily accepted by the body and often cause a foreign body response in addition to inflammatory trauma associated with the process of implantation.¹ How well a device is accepted by a patient's biology is largely governed by chemical or structural surface interactions between the implanted material and surrounding tissue.¹

Immediately after a device has been implanted or is in contact with live biological tissue, an inflammatory response ensues beginning with the adsorption of a protein monolayer.¹ Monocytes, leukocytes, macrophages, cytokines and other chemical mediators are signaled to migrate to the injured site and serve to heal or rebuild the tissue. This initial response can last from minutes to several days depending on the host response to the implant or type of trauma followed by a chronic response and granulation. When injured tissue cannot be healed or rebuilt often due to the presence of a foreign body

(implant), local inflammatory cells begin fusing together forming giant cells in an attempt to wall off the site, which is an end stage healing response.¹

Thrombosis is a blood compatibility complication associated with most intravascular implant materials that may otherwise be inert. When these materials are used for implantable medical devices, platelet activation coupled with inflammation begins the thrombotic cascade. Thrombosis is initiated by protein adsorption onto a surface in contact with blood, which causes an irreversible platelet aggregation releasing a host of factors to essentially coagulate and “plug” an injured site to prevent excessive blood loss.¹⁻⁴

Material surfaces that are thrombogenic can be modified to have more compatible material-tissue interactions for a variety of different surgical instrument and implant applications. Furthermore, inflammatory response can be controlled without systemic toxicity through localized release of therapeutic agents. Presented here are two examples illustrating the clinical needs to enhance material surface properties for increased biocompatible medical devices for implantation: endovascular stents and keratome blades. A discussion of materials for coating implantable medical devices will conclude this background.

Endovascular Stents

Percutaneous transluminal coronary angioplasty (PTCA) is a technique used for the treatment of coronary atherosclerosis and heart disease, where procedures for revascularization of coronary arteries involve flattening fatty plaques in the blood vessel against the vessel walls by a balloon catheter, see Figure 2.1.⁵ From 1987 to 2001, the number of PTCA procedures has increased 266% in the United States.⁶ In 2001, approximately 571,000 PTCA procedures were performed on 559,000 patients. Also,

475,000 of these procedures included cardiovascular stenting, which has been shown to significantly reduce restenosis as compared with balloon angioplasty alone.^{6,7}

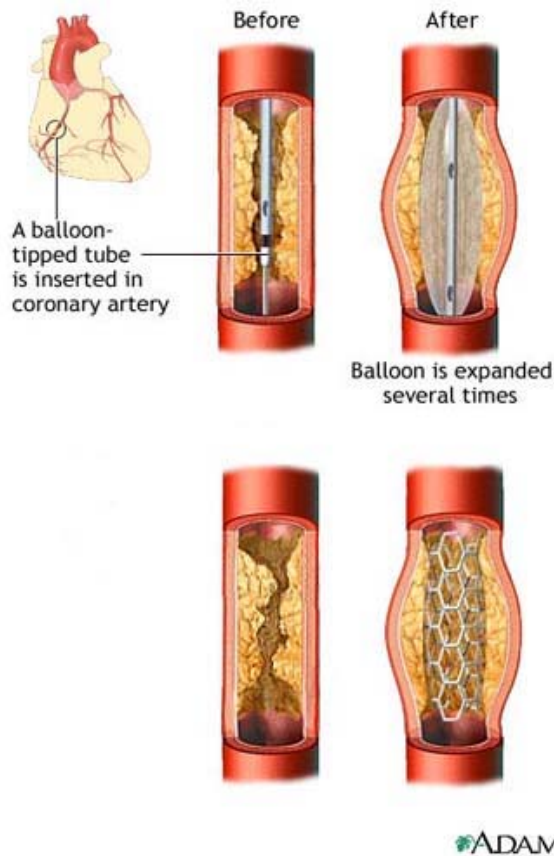


Figure 2.1 - Illustration of balloon angioplasty and stenting. Adapted from ADAM, Inc.

Restenosis is a phenomenon marked by an occluding lesion occurring after balloon angioplasty or stenting.⁵ Restenosis can require repeat surgeries and can lead to death. For patients undergoing percutaneous balloon angioplasty, 30-40% will develop restenosis in the first 6 months while stenting decreases the incidence to 20%.⁷ Although there have been vast stent technology improvements, the problem of in-stent restenosis has not been resolved and remains as relevant as the issue of restenosis after PTCA.

Recent studies suggest atherosclerosis, a disorder that causes fatty plaque to deposit along arterial and vessel walls, involves several factors including inflammation, vascular smooth muscle cell (VSMC) proliferation/migration, endothelial dysfunction and

extracellular matrix alteration.⁸ Similar factors are associated with the molecular mechanisms of restenosis and in-stent restenosis.⁹⁻¹¹

Restenosis after balloon angioplasty was found to be distinctively different from in-stent restenosis from a histological standpoint.¹⁰ Indolfi et al. suggests that the mechanism for restenosis after balloon angioplasty is predominantly due to negative vessel remodeling, while the proliferation of smooth muscle cells only accounts for 25% of the phenomenon, as illustrated in Figure 2.2.¹⁰ Indolfi et al. noted that there was no evidence of vessel remodeling with cardiovascular stenting; however, restenosis was still observed.

The in-stent restenosis mechanism appeared to be due entirely to the proliferation of smooth muscle cells. Consequently, it was found in swine coronary arteries that restenosis as a result of balloon angioplasty consisted of vessel remodeling and neointimal hyperplasia, while in-stent restenosis consisted of mostly neointimal hyperplasia.¹¹

Nakatani et al. concluded that neointimal proliferation of smooth muscle cells post-stenting persisted longer than the proliferation associated with balloon angioplasty. {Nakatani, 2003 #61} Likewise, Hofma et al. suggested stenting lead to longer wound healing cascades due to the permanency of stent placement leading to long-term endothelial dysfunction and inflammation. {Hofma, 2001 #194} These developments have lead to a focus in targeting cell cycle regulation as treatment against in-stent restenosis.

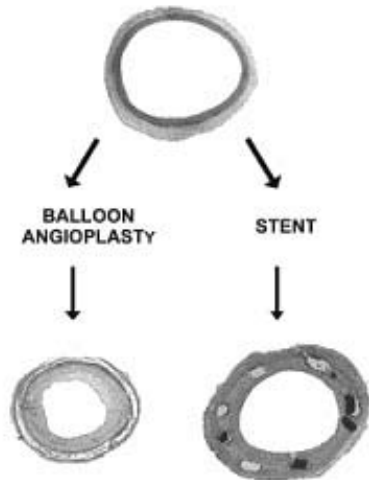


Figure 2.2 - Histological section of restenotic arteries following balloon angioplasty and stenting.¹⁰ Indolfi et al. 2003

Today, metallic vascular stents are available in several materials including various grades of stainless steel, cobalt-chromium, tantalum and nickel-titanium compounds.¹² However, when implanted without further surface treatment, many metallic formulations are thrombogenic and do not inhibit neointimal hyperplasia.¹³ Several coatings for enhanced biocompatibility of metallic stent materials have been investigated including inorganic/ceramic coatings (gold, carbon, iridium oxide and silicon carbide), synthetic and biological polymers (polyurethane, polylactic acid, phosphorylcholine, chondroitin sulfate, hyaluronic acid, fibrin, elastin and cellulose), and drugs (heparin, sirolimus and paclitaxel).¹⁴

Gold, carbon, and silicon carbide (SiC) inorganic/ceramic coatings on stents have been studied in human clinical trials.^{13, 14} In the first 30 days after intervention, gold coated stents were discovered to have no antithrombotic effects, and exhibited an increased incidence of neointimal hyperplasia within the first year.^{13, 14} Carbon coated stents, such as Carbostent (Sorin Biomedica Cardio), were found to yield low major adverse cardiac event (MACE) (12%) and binary restenosis (11%) rates at 6 months

follow-up with 112 intermediate risk patients.¹³ SiC coatings have been used without reports of biocompatibility issues, however high concentrations of SiC debris can be cytotoxic.¹⁴ SiC coatings did not have a considerable affect on rate of restenosis when compared with balloon angioplasty alone in a clinical trial.¹³

Synthetic and biological polymeric coatings have also been investigated in human clinical trials. Specifically, phosphorylcholine coatings have been evaluated in the SOPHOS (Study of Phosphorylcholine on Stents) trial with 425 patients. At 6 months, this study showed a MACE of 13.4% for Phosphorylcholine coated stents versus 15% for uncoated stents.¹⁴ The 6 month binary restenosis rate was 17.7% for the coated group. The researchers in this study concluded there was a less severe inflammatory response associated with phosphorylcholine coating as compared with several other polymers for the same application.

Immobilized drug coatings have been used in the clinical setting where drugs can be physically adsorbed or chemically tethered to the stent surface. Heparin coated Palmaz-Schatz stents exhibited comparable effectiveness in the prevention of restenosis when compared with uncoated stents combined with systemic abciximab treatments.¹⁴ Heparin coated stents did not demonstrate any significant differences in MACE and binary restenosis rates. The authors concluded that heparin coated stents did not have an effect on in-stent restenosis.¹³ Sirolimus and paclitaxel have also been examined in a clinical setting. Sirolimus coated stents when compared with uncoated stents (26.6%) had a 0% binary restenosis rate at 6 months post-intervention.¹³ The authors reported that no late thrombosis occurred with the sirolimus eluting treatment. ASPECT (Asian Paclitaxel-Eluting Stent Clinical Trial) examined a high and low dose condition for

paclitaxel coated stents with no polymer carrier.¹³ The 6 month binary restenosis rate was 4% versus 27% for the uncoated group. MACE rates are currently unpublished for this study.

Inert coatings alone on stents have not reduced restenosis rates or thrombosis to an acceptable level. Additionally, drug coatings alone did not yield satisfactory outcomes. Consequently, many vascular device companies have or are in the process of developing drug-eluting stents to combat in-stent restenosis.¹⁵ Some of the drugs involved in clinical trials of drug eluting stents include rapamycin (sirolimus), paclitaxel, tacrolimus, everolimus, 17 β -estradiol, and dexamethasone.^{8, 10, 15} The two most extensively evaluated drugs undergoing drug eluting stent clinical trials are paclitaxel and rapamycin (sirolimus). However, STRIDE (A Study of Antirestenosis with the BiodivYsio Dexamethasone-Eluting Stent), clinical trial launched in February 2003 and more recently the EASTER trial (Estrogen and Stents to Eliminate Restenosis), has yielded promising results in some patients.¹⁵

Sirolimus (Rapamycin) Eluting Stents

Sirolimus (Rapamycin) is an immunosuppressant antibiotic derived from *streptomyces hygroscopicus* from Easter Island soil samples.¹⁶ Sirolimus functions by binding to immunophilins inhibiting cell signal transduction thus targeting cell cycle progression.¹⁶⁻¹⁸ Sirolimus inhibits VSMC migration *in vitro* and proliferation *in vitro* and *in vivo*.

The results of several clinical trial investigations on the effects of sirolimus on restenosis rates have been remarkable with 1 year MACE as low as 0% and in-stent restenosis of 2.0%.^{13, 16} The Cordis CYPHER[®] stent is currently one of two drug eluting coronary stents approved for use in humans in the United States, Figure 2.3. The stent is

loaded with sirolimus to an effective surface concentration of approximately 150-180 $\mu\text{g}/\text{cm}^2$.^{14, 16} Despite the clinical benefits of sirolimus eluting stents, varying degrees of inflammation, delayed endothelialization and toxicity concerns remain.^{10, 15, 16, 18}

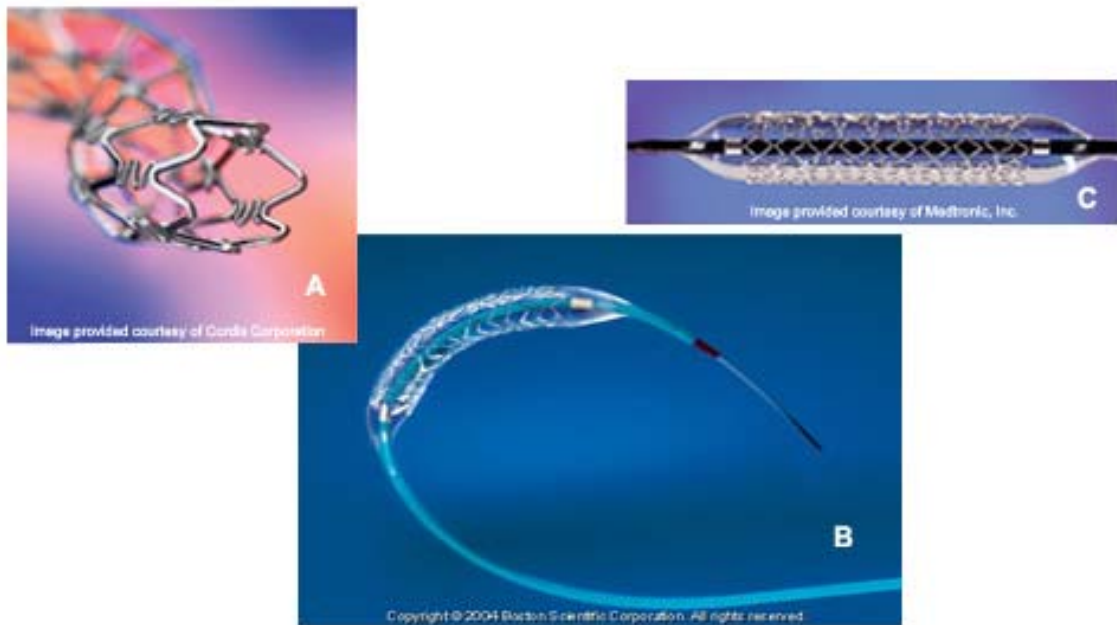


Figure 2.3 - Various stents. A) CYPHER[®] sirolimus-eluting coronary stent by Cordis Corporation, B) Stent by Boston Scientific Corporation, C) Stent by Medtronic, Inc

Paclitaxel Eluting Stents

Paclitaxel is an antineoplastic and chemotherapeutic agent derived from yew trees.¹⁶ Similar to sirolimus, paclitaxel interrupts signal transduction and has been shown to inhibit the proliferation and migration of VSMC. As in the ASPECT trial, the ELUTES (Evaluation of Paclitaxel Eluting Stents) also suggests a dose dependency for paclitaxel effectiveness in reducing restenosis and MACE.¹³ However, paclitaxel in the TAXUS I trial proved to be promising at 6 months with 0% binary restenosis for coated stents compared with 11% in the bare stent group. Additionally, no MACE was observed at 12 months.¹⁶

Like the Cordis CYPHER[®] stent, Boston Scientific's NIR poly(lactide-co- Σ -caprolactone) copolymer and paclitaxel stent is also approved for use in humans, see Figure 2.3. There are approximately 200 μg of paclitaxel loaded per stent.¹⁹ Problems associated with paclitaxel eluting stents include incomplete healing due to delayed endothelialization, persistence of macrophages, and deposition of fibrin. Furthermore, it was found that 80% of the loaded drug released within the first 3 days of deployment.^{10, 15, 16, 19}

17 β -estradiol Eluting Stents

The release of 17 β -estradiol has been investigated with phosphorylcholine coated stents. In 2002, Biocompatibles Ltd. filed a world patent titled "Stents with Drug-Containing Amphiphilic Polymer Coating".²⁰ The invention disclosed a shape memory alloy stent with a zwitterionic coating capable of releasing hydrophobic or hydrophilic drugs.

On March 17, 2004, an Estrogen And Stents To Eliminate Restenosis (EASTER) clinical trial report was released indicating that the release of 17 β -estradiol was safe and may be effective in inhibiting in-stent restenosis in humans.²¹ 17 β -estradiol was eluted from phosphorylcholine coatings on 316-L stainless steel balloon expandable stents during the EASTER clinical trials.²¹ However, a burst release profile was observed and the total release was completed within the first 24 hours of stent deployment.

The surface concentration used in this study was determined to be 2.52 $\mu\text{g}/\text{mm}^2$.²¹ Despite the rapid release, no in-stent thrombosis occurred and late-stent malapposition was not detected. Additionally, no edge restenosis was found at a 6 month follow-up. At 1-year, revascularization and low rates of restenosis were observed.²¹ In each follow-up, system toxicity was not evident. The EASTER trials indicate that 17 β -estradiol is a

viable alternative approach to other restenosis reducing agents. Although it has been reported that complete inhibition of restenosis was not observed, changing drug release properties, doses, and coating materials may improve efficacy.

The release properties of 17β -estradiol chemically incorporated into poly(acrylic acid) coated 316-L stainless steel plates by a hydrolysable covalent bond has been investigated in an *in vitro* model.²² The initial 17β -estradiol concentration in this study was determined to be $\sim 12 \pm 4.2 \mu\text{g}/\text{cm}^2$ and released for two weeks, with no initial burst effect. Currently, an *in vivo* investigation in a porcine coronary injury model has yielded promising preliminary results demonstrating a significantly lower incidence of restenosis at 8.58% when compared with non- 17β -estradiol treated stents (11.62%).²²

Dexamethasone Eluting Stents

Dexamethasone is a synthetic glucocorticosteroid that produces anti-inflammatory responses by interfering with macrophages and modifies protein synthesis.^{16, 23, 24} The release of dexamethasone from a biodegradable poly-L-lactic acid coating has been studied by Lincoff et al.²⁵ The investigation yielded intense inflammatory response by 28 days after implantation, which was attributed to the degradation mechanisms of the coating. It was also shown in this study that dexamethasone did not decrease neointimal hyperplasia in the porcine coronary artery after stent overexpansion trauma. Lincoff suggested the inflammatory responses that should have been suppressed by dexamethasone did not moderate a key pathway to restenosis in the porcine coronary model.

Dexamethasone release from liposome coatings composed of phosphatidylcholine and cholesterol have been investigated and are ongoing in the STRIDE trials.^{16, 23, 24} The STRIDE study has demonstrated a significant reduction of in-stent restenosis with a 6

month follow-up binary restenosis rate of 13.3%.^{16,23} From the STRIDE study, dexamethasone release from phosphorylcholine coating was found to be feasible and safe with no increases in thrombosis and low event rates. However, neointimal thickening was not found to decrease in this study. This observation was attributed to the low concentration of dexamethasone administered in the study. The authors suggested that further studies investigating higher dose treatment with dexamethasone would be necessary.²³

The use of dexamethasone impregnated in silicone coated stents was also briefly investigated in a porcine model. The results of these studies showed evidence of high anti-inflammatory and antifibrotic effects.¹⁶

Drug Release from Silicone

Hormone delivery from silastic vaginal rings has been widely available and accepted for hormone replacement therapy and contraception.²⁶⁻³³ Silastic vaginal rings have been shown to be effective for sustained and steady release of 17 β -estradiol (Estring[®]) and several other commercially available hormones.

Sustained release of these therapeutic agents from silicone has been attributed to the hydrophobicity of the material and lipophilic nature of the hormones.^{27-30, 34, 35} The successes of hormone replacement therapy and contraceptive silastic vaginal rings suggest that it is feasible to achieve steady state release of steroid hormones from silicone coatings. In addition to silastic vaginal rings, polydimethylsiloxane (PDMS), is currently used in several biomedical applications such as intraocular lenses, catheters, and various cosmetic implants.^{16, 31, 36-39}

Keratome Blades

Keratome blades are used in phacoemulsification procedures for cataract surgeries.⁴⁰ These blades are designed as single use devices, but can greatly affect the level of trauma associated with these surgeries. The sharpness, material composition, and geometries of these devices all contribute to this. As with stents, blade surface properties can greatly affect the degree of inflammation after tissue contact, which can result in complications such as astigmatism. Inflammation is also caused by the implant procedure, which requires a small incision with a width of ~3 mm, where blades have been reported to cause unpredictable incisions due to poor translation across the cornea.⁴¹ The surgery also includes the extraction of the cataract and natural vitreous and replacement with either a silicone oil or polysaccharide emulsion. If the implant is a foldable intraocular lens, then the incision can self-seal. Otherwise, the incision will require enlargement and must be sutured, glued or taped closed to heal.¹ Blade surface properties can greatly affect inflammation associated with both the cataract removal and intraocular lens placement procedure. Furthermore, infection at the incision site can prolong inflammation and associated complications.

Materials for Coatings and Implantable Medical Devices

316-L stainless steel has been used for several biomedical device applications including drug eluting stents. 316-L stainless steel has a composition in the range of <0.03% C, 16-18.5% Cr, 10-14% Ni, 2-3% Mo, <2% Mn, <1% Si, <0.045% P, <0.03% S, and Fe as the remaining constituent. Depth profiling studies of stainless steel films indicate high Cr₂O₃ surface content, which is a key component in corrosion resistance.¹² This Cr³⁺ rich layer has an approximate thickness of ~ 2 nm after electropolishing.¹² Additionally, trivalent chromium is an essential trace mineral, unlike hexavalent

chromium which has been shown to be toxic. Stainless steel has been used in permanent stent devices. It remains an ideal candidate for this application due to exhibiting relatively inert material behavior in most corrosive environments. However, 316L stainless steels do exhibit some unfavorable susceptibility to potential consequences of injury due to acute localized thrombus formation or neointimal hyperplasia.¹

Coupling agents are commonly used to enhance the binding of coatings to substrates. For 316-L stainless steel, silanes such as tetraethoxysilane (TEOS), hexamethyldisilane (HMDS), Bis(3-triethoxysilylpropyl) tetrasulfide, and SID-4612 (a silazane) are typically employed. Many silane coupling agents require more than a single step procedure for treatment. However, chromium (III) methacrylate and chromium (III) fatty acid coupling agents developed around 1942 that require only single step procedures for treatment (Figures 2.4, 2.5).^{42, 43}

As shown in Figure 2.4, Volan[®] is a chlorinated metal alkoxide with two Cl⁻ tethered to each Cr³⁺. The chlorine content is controlled by the percent of solids or salts in the mixture. The Volan[®] has more chlorine content than Volan[®] L making it more stable to hydrolysis. The scientists who developed this coupling agent claim the Cl⁻ remains tethered to the Cr³⁺ even after bonding. However, they have also suggested that the coupling action may be a slightly acidic reaction creating “some” chlorinated salt by-products.⁴³ Volan[®] L is designed to bind polyesters, epoxies, phenolics, vinyls, and acrylics to inorganic or polar surfaces such as glass, metals, polymer, silica, boron and some natural surfaces.

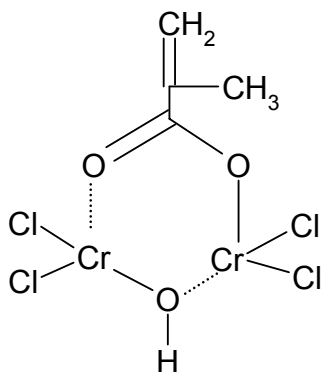


Figure 2.4 - Volan[®] and Volan[®] L bonding agent, chromium (III) methacrylate

Quilon[®] L is also a metal alkoxide coupling agent that is chromium (III) fatty acid based, see Figure 2.5. Fatty acid based systems can be useful for formation of carbonaceous surfaces that will undergo further treatments for binding organic coatings onto inorganic surfaces.

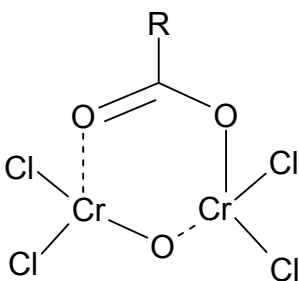


Figure 2.5 - Quilon[®] L bonding agent, chromium (III) fatty acid where R=C₁₄₋₁₈

The Cr³⁺ of Quilon[®] L, Volan[®], and Volan[®] L may interact favorably with the Cr₂O₃ surface protective films on 316L stainless steel. It is feasible to bind various monomers and vinyl addition silicones to this surface by reacting with the methacrylate and fatty acid groups of these metal alkoxides. Table 2.1 lists the chromium complex constituents of Volan[®], Volan[®] L and Quilon[®] L as provided by the manufacturer.

Table 2.1 - Metal alkoxide chromium complex constituents

	Volan [®]	Volan [®] L	Quilon [®] L
Chrome Complex, % (active ingredient)	19-21	17-18	61
% Chromium	6.0	6.0	9.2
% Chloride	8.2	3.2	12.7
% Methacrylic Acid or % Fatty Acid (C ₁₄₋₁₈)	5.1	5.1	21.2

Several hydrophilic polymers have been investigated for biomedical device applications such as poly(methacryloyloxyethyl phosphorylcholine), polyvinylpyrrolidone, polydimethylacrylamide, and poly(potassium sulfopropyl acrylate). These polymers have been shown to be biocompatible and have been investigated for ophthalmic and cardiovascular applications.^{13, 44-49} The monomer structures for these materials are illustrated in Figure 2.6.

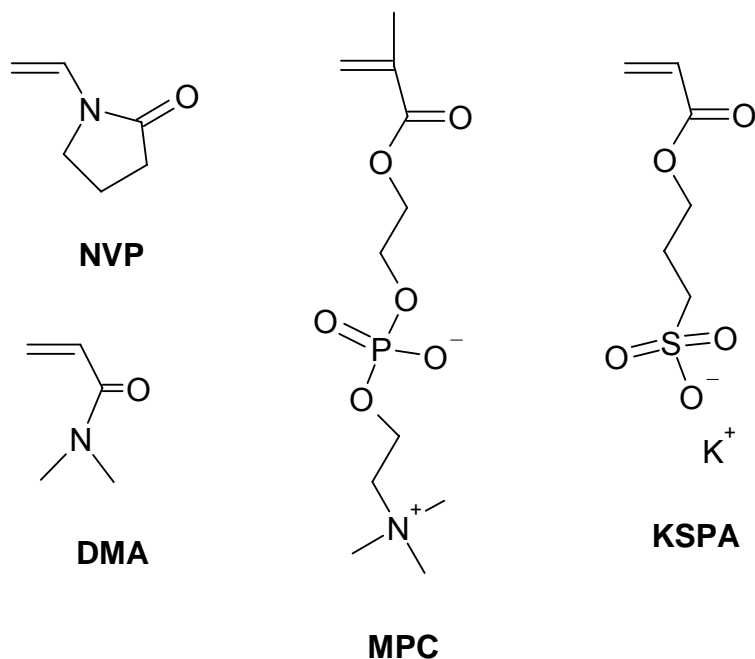


Figure 2.6 – Hydrophilic monomer structures: 2-methacryloyloxyethyl phosphorylcholine (MPC), N-vinyl pyrrolidone (NVP), N,N-dimethylacrylamide (DMA), and potassium 3-sulfopropyl acrylate (KSPA).

Table 2.2 - Silicone curing systems

Peroxide	$\begin{array}{c} \equiv \\ \text{Si} \end{array} + \begin{array}{c} \text{Si} \\ \equiv \\ \text{CH} \\ \text{CH}_2 \end{array} \xrightarrow{\text{Peroxide}} \begin{array}{c} \equiv \\ \text{Si} \end{array} \text{---} \text{CH}_2 \text{---} \text{CH}_2 \text{---} \begin{array}{c} \text{Si} \\ \equiv \\ \text{CH} \\ \text{CH}_2 \end{array}$
Condensation	$\begin{array}{c} \equiv \\ \text{Si} \end{array} \text{---} \text{OH} + \text{HO} \text{---} \begin{array}{c} \text{Si} \\ \equiv \\ \text{CH} \\ \text{CH}_2 \end{array} \xrightarrow{\text{H}^+} \begin{array}{c} \equiv \\ \text{Si} \end{array} \text{---} \text{O} \text{---} \begin{array}{c} \text{Si} \\ \equiv \\ \text{CH} \\ \text{CH}_2 \end{array} + \text{H}_2\text{O}$
Metal Salt	$\begin{array}{c} \equiv \\ \text{Si} \end{array} \text{---} \text{H} + \text{HO} \text{---} \begin{array}{c} \text{Si} \\ \equiv \\ \text{CH} \\ \text{CH}_2 \end{array} \xrightarrow{\text{Metal Salt}} \begin{array}{c} \equiv \\ \text{Si} \end{array} \text{---} \text{O} \text{---} \begin{array}{c} \text{Si} \\ \equiv \\ \text{CH} \\ \text{CH}_2 \end{array} + \text{H}_2$
Vinyl Addition	$\begin{array}{c} \equiv \\ \text{Si} \end{array} \text{---} \text{H} + \begin{array}{c} \text{Si} \\ \equiv \\ \text{CH} \\ \text{CH}_2 \end{array} \xrightarrow{\text{Pt}} \begin{array}{c} \equiv \\ \text{Si} \end{array} \text{---} \text{CH}_2 \text{---} \text{CH}_2 \text{---} \begin{array}{c} \text{Si} \\ \equiv \\ \text{CH} \\ \text{CH}_2 \end{array}$

Polydimethylsiloxane (PDMS) is a hydrophobic polymer that is currently used in biomedical applications.⁵⁰ As indicated in Table 2.2, there are four primary methods for curing silicone. Currently, the vinyl addition curing system is used predominantly.⁵¹ Many commercial formulations of silicone are available as two-component systems that cure through platinum catalyzed hydrosilylation.⁵¹ This reaction is illustrated in Figure 2.7. Part A consists of silicone oligomers with vinyl terminated silanes, resin reinforcing

fillers, and the platinum catalyst.⁵² Part B consists of hydride functional silicone oligomers and vinyl terminated silanes. To increase PDMS modulus, tensile strength, tear strength, and abrasion resistance, most silicones are reinforced with silica particulates.⁵¹ The silicone that will be used in this project is resin reinforced rather than particulate filled. The curing process is initiated when the components are combined. Heat is added to increase the curing rate and bring the process to completion.

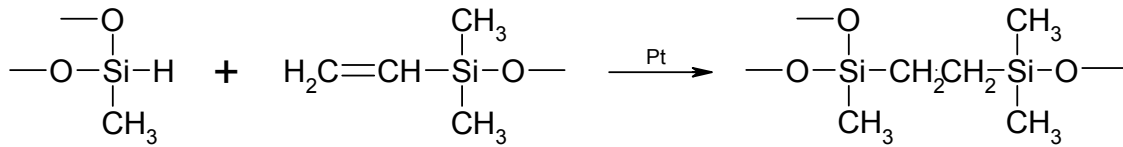


Figure 2.7 - Silicone vinyl addition curing system

Significance

Implantable medical devices often cause a cascade of responses due to trauma associated with implantation and material-tissue interfacial incompatibility. Furthermore, it has been demonstrated that drug therapy can reduce or control the host response to implants and possibly encourage wound healing. It is apparent that there is a need for enhancing the surface properties coupled with localized drug therapy for implant applications such as endovascular stents and surgical devices such as keratome blades. It is the goal of this research to develop new coating systems that are coupled by a one step coupling wash of 316L stainless steel to enhance coating stability and delivery of therapeutic agents, thus laying the groundwork for studies focused on biocompatibility testing of these promising surface modifications.

CHAPTER 3
METAL ALKOXIDE TREATMENTS AND LOW DOSE GAMMA SURFACE
MODIFICATION OF STAINLESS STEEL

Introduction

Stenosis of the coronary arteries is now often treated by percutaneous transluminal coronary angioplasty combined with endovascular stent implantation. Endovascular stents coated with hydrophilic polymers have been shown to exhibit reduced platelet reactivity and accumulation in-vivo compared to uncoated metal stents.^{44, 45} These coatings may decrease the risk of thrombosis and can potentially be loaded with therapeutic agents that reduce the incidence of post-intervention complications such as restenosis.^{53, 54}

Ongoing problems with coatings are drug release to inhibit restenosis and adhesion to the substrate metals. Poor coating adhesion can lead to delamination or otherwise make the coating unstable thus rendering the surface modification unacceptable. This research was devoted to metal alkoxide surface treatments that may enhance the adhesion and stability of coatings on metallic substrates. The two main objectives of this research were to develop new metal alkoxide treatments using trivalent chromium metal alkoxides for enhancing stability of subsequently applied polymeric coatings produced by gamma irradiation.

Metal Alkoxide Treatments

Silane coupling agents have been used extensively for applications such as aminosilanes used in the fiberglass industry, acryloxypropyltrimethoxysilanes used in

optical fiber coatings, and tetraethoxysilane in sol-gel processes for forming ceramic coatings and materials. The treatment process often requires several steps to complete, in addition to the procedures associated with the specific coating technology. Silane coupling systems often include a priming step in which agents such as bis[3-(triethoxysilyl)propyl]-tetrasulfide are applied metal surfaces. The agent is then hydrolyzed and converted to silanol. The coupling treatment is completed by condensing a silane coupling agent such as divinyltetramethyldisilazane to the pretreated substrate. The functionalized substrate is often heated to promote further condensation and formation of stable covalent bonds and driving off the organic species. The resulting porous gel can be sintered, or heated, under vacuum to remove the hydrolyzed organic species, promote further condensation and increase density. The approach taken here utilizes metal alkoxides with hydrolysable allylic organic species. The process used in this research deviates from conventional sol-gel processes because it does not involve the sintering step. This deviation preserves the porosity of the gel and presence of the allylic organic species within the porous structure. The unsaturated functionality of the hydrolyzates, such as with acrylates and methacrylates, is utilized to graft or enhance grafting of polymeric coating to inorganic materials such as stainless steel.

Medical grade 316L stainless steel develops a corrosion-inhibiting Cr_2O_3 coating of approximately 2 nm thick when the material is electropolished. The treatment of the protective layer by a chromium coupling system using new trivalent chromium based metal alkoxides binding agents to enhance the binding and stability of coatings is explored. Newer metal alkoxides such as chromium (III) methacrylates or chromium (III) fatty acids are used to functionalize surfaces by a simple solution dipping process.

Research aimed at development of chromium priming as an approach to improving various subsequent surface modifications is reported here.

Materials and Methods

Preparation of 316L stainless steel substrates

Substrates of 316L stainless steel (1 cm x 1 cm) were cut from a single stock of foil that had a thickness of approximately 0.1 mm. Substrate surfaces were cleaned by sequential sonication for 5 minutes at 47 KHz at room temperature in 30 mL each of 1,1,1-trichloroethane, chloroform, acetone, methanol, and Ultrapure™ water then dried under vacuum at 60°C. Fifty substrates were cleaned at a time. Substrates were not electropolished.

Treating 316L stainless steel with metal alkoxides

Clean substrates were placed in 25 mL aqueous solutions of 2%, 10% or 100% v/v chromium III fatty acid (Quilon® L, DuPont) for 1 single dip, 10 minutes rotating or 60 minutes while rotating. Ten substrates were treated for every 25 mL solution. Treated substrates were removed from solutions and allowed to either air dry or rinsed with Ultrapure™ water, then dried in air at room temperature. Silver acrylate (Gelest, Inc.) treatments were also explored. Silver acrylate was purchased in powder form and the chemical structure is given in Figure 3.1. Three silver acrylate treatment solutions were prepared in volumes of 25 mL with 2% w/v concentrations in isopropanol, acetone or a mixture similar in formulation to Volan® L, see Table 3.1.

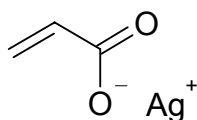


Figure 3.1 – Silver Acrylate (Gelest, Inc., Morrisville, PA).

Table 3.1 – Volan[®] L solution and Silver Acrylate mixed solvent solution composition.

Ingredient	Volan [®] L	Silver Acrylate
Complex, % (active ingredient)	17-18	17-18
% Isopropanol	56	56
% Acetone	10	10
% Water	16	16

Chromium alkoxide degradation study

Chromium complex degradation was studied to compare freshly opened stock solutions and solutions that had aged for approximately 12 months since their first use. The solutions studied were chromium III fatty acid (Quilon[®] L, DuPont) and chromium III methacrylate (Volan[®] and Volan[®] L, DuPont) at concentrations of 2% and 10% v/v solutions where 25 mL of each solution was prepared for treating 10 stainless steel substrates each. Cleaned substrates were placed in the solutions for 10 minutes while rotating, then removed and allowed to air dry.

Controls in all cases consisted of untreated 316L stainless steel specimens that were cleaned as previously described.

Analysis

Treatments were analyzed by x-ray photoelectron spectroscopy (XPS/ESCA) analysis using a Kratos Analytical Surface Analyzer XSAM 800. Analysis was performed using Mg and Al anodes for excitation. Survey scans were taken in low resolution with a dwell time of 150, 10 sweeps, and step size of 0.5 in FRR mode with both Al and Mg anodes. Elemental scans were taken in medium resolution with a dwell time of 60, 20 sweeps, and step size of 0.05 in FRR mode with only Al anode.

Results and Discussion

The Quilon[®] L, Volan[®] and Volan[®] L manufacturer, Dupont, suggests the optimal treating solution concentration for all substrate materials is 2% v/v with water and

buffered to $\text{pH} = 7.0$, a solution concentration optimization study was done to verify the this. It is important to point out that previous work in this laboratory by Dr. D. Urbaniak indicated that it is not necessary to buffer the metal alkoxide bonding agent solutions prior to application. This work showed that surface treatment with buffered solutions often resulted in uneven chrome complex deposition when examined by scanning electron microscopy (SEM), while buffered solutions yielded even, homogeneous surface treatments that were suitable for subsequent surface modification procedures.⁵⁵

For chromium alkoxide treatment optimization, XPS was used to examine surface concentrations of C1s, O1s, Fe2p₃, Cr2p₃, and Cl2p peaks on treated 316L stainless steel substrates. The C1s peak was examined for poly(ethylene terephthalate), a material used as an internal C1s and O1s reference. The theoretical relative concentrations of carbon and oxygen atoms are 71.4% and 28.6%, respectively. The experimental results were 73.1% C1s and 26.9% O1s, see Figure 3.3 for the survey scan. The difference was small and could be attributed to low molecular weight carbon deposition during the 24 hour vacuum cycle. The primary C1s peak corresponding to C-C bonding should be around 284.6 eV, but our analysis of PET yielded a primary C1s peak at 281.7 eV. This 3 eV shift to lower binding energy should be considered when examining all XPS data in this work. The raw XPS data are reported here without any post-processing such as signal normalization or shifting.

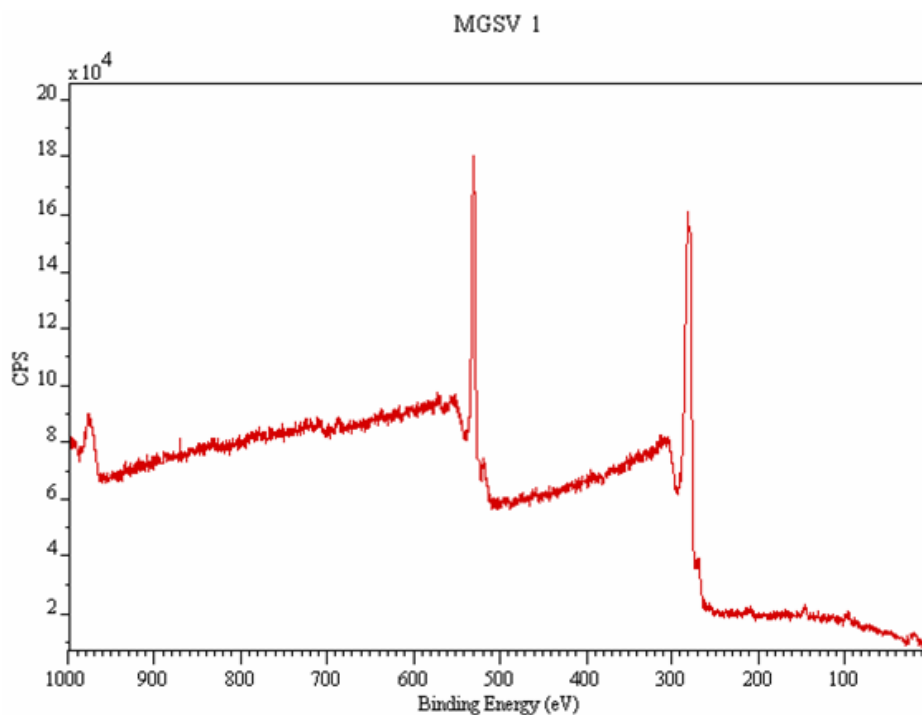


Figure 3.2 – XPS survey of PET.

It is significant that as the metal alkoxides are deposited from the solution the chromium moiety will bind to the chromium oxide on the surface of the substrate causing the methacrylate or fatty acid chains to be oriented away from the substrate. This orientation becomes important when discussing relative elemental concentrations since XPS has a surface sensitivity of 2-20 atomic layers.⁵⁶ For example, if the fatty acid chain is 18 carbons long and even folded on itself, the carbon signal detected by XPS would be much more efficient than the surface chromium, iron, etc.

Elemental analysis of Quilon[®] L treated substrates yielded no significant difference in peak location or surface concentrations for the C1s and Cr2p peaks of 2% and 10% v/v treating solutions for single dip, 10 minutes and 60 minutes tumble washing. This was true for air dry and rinse, then air dry conditions. There appeared to be no advantage in rinsing the treated substrates before drying. Additionally, increased Cr2p was observed for 10% v/v treating solutions that were rinsed and then air dried.

Substrates treated with 10% v/v solutions appeared to be spotty, while 100% v/v treatments resulted in scaly surfaces that easily peeled away from the substrate. This was not observed for any 2% v/v solution treated substrates. The relative iron content was lowest with the 100% v/v treatments, which was an expected outcome since the treatment is much denser. As listed in Table 3.2, the relative surface chromium content increased for all conditions when compared with untreated 316L stainless steel, which corresponded with the binding of chromium based metal alkoxides to the surface. Lastly, all conditions resulted in an increase in the C1s surface concentration, which corresponds to the fatty acid groups of Quilon[®] L, suggesting that the chrome complex was deposited during treatment.

Table 3.2 – XPS analysis for air dried samples without rinsing: % Cr2p3 and % C1s relative to % O1s, Fe2p3 and Cl2p. All conditions were examined on 316L stainless steel.

Condition	% Cr2p3	% C1s
Untreated 316L SS, Control	1.8	48.8
2 % Quilon [®] L, Single Dip	2.7	68.5
2 % Quilon [®] L, 10 Min	3.7	64.1
2 % Quilon [®] L, 60 Min	3.1	68.5
10 % Quilon [®] L, Single Dip	2.4	67.3
10 % Quilon [®] L, 10 Min	2.5	67.3
10 % Quilon [®] L, 60 Min	2.6	69.5
100 % Quilon [®] L, Single Dip	1.6	82.1
100 % Quilon [®] L, 10 Min	2.0	75.5
100 % Quilon [®] L, 60 Min	3.3	63.7

The use of silver acrylate was investigated to examine the feasibility of using other allyl metal alkoxide systems and was of particular interest because of potential antimicrobial properties that may arise from the silver moiety. Since silver acrylate is only available in powder form, attempts were made to develop a treatment solution to functionalize stainless steel. A 50% isopropanol and 50% acetone solution was used to

dissolve the metal alkoxide. The result was a 2% w/v solution. Next, acetone was used to dissolve the silver acrylate resulting in a 2% w/v solution. Finally, a solution was prepared similar to that of Volan[®] L for the silver acrylate treating solution. All three treatment groups were analyzed by XPS and elemental analysis focused on C1s, O1s, Fe2p3, Cr2p3 and Ag3d5. The isopropanol/acetone/water (like Volan[®] L) solution yielded the highest surface concentration of Ag3d5 at 3.5% compared with 0.9%, which was the same for both the isopropanol/acetone and acetone solutions, see Figure 3.3. The antimicrobial aspect of this treatment will be further analyzed in Chapter 6.

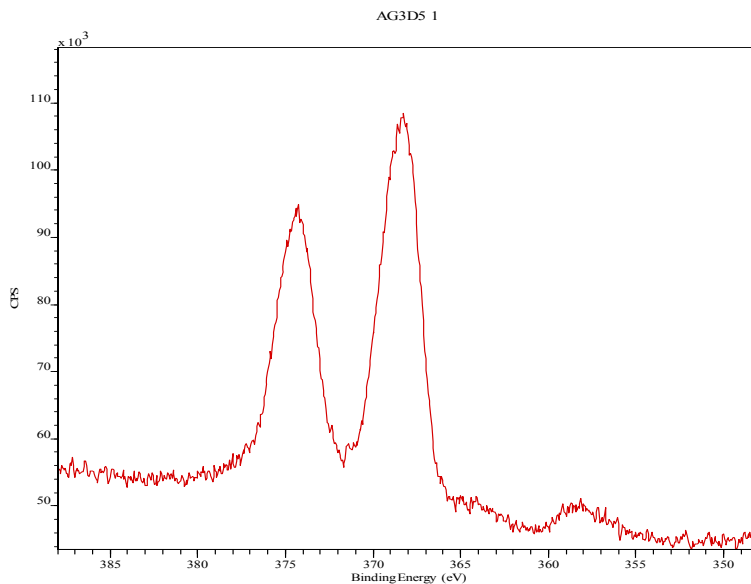


Figure 3.3 – XPS spectra of Ag3d5 of silver acrylate treatment on 316L stainless steel.

Fourier Transform Infrared-Attenuated Total Reflectance (FTIR-ATR) analysis was attempted, but no signal was achieved due to surface concentrations of the chrome complex being below the detectable limit of the instrument. The same was true for silver acrylate treated substrates.

Chromium alkoxide priming solution stability over time was investigated. Dupont suggests that these stock solutions remain highly stable over time. The stability of stock solutions was investigated by comparing the C1s and O1s oxidative states of surfaces

treated with freshly opened stock solutions and solutions that had aged for approximately 12 months since their first use. Evidence of oxidative degradation was seen as stock solutions of Quilon[®] L aged as shown by the shift to higher binding energies for both the O1s and C1s peaks corresponding to an increase in concentration of -C=O bonding when there should be an increased concentration of C-C corresponding to the complexed long aliphatic chains. The spectra are shown in Figure 3.4. Another interesting observation was a solution color change from dark green to dark blue-teal further supporting chemical changes in the priming solution 12 months after first use. For chromium (III) fatty acid coupling agent used in this study exhibited a change in surface composition of the functionalized stainless steel surfaces compared with untreated stainless steel when analyzed by XPS.

The changes in peak location and color were not observed for Volan[®] or Volan[®] L, see Figure 3.5. There was a 4 eV shift to higher binding energies seen for the C1s peak for Volan[®] L treatments when compared with Quilon[®] L, suggesting a greater quantity of surface carbon associated with the vinyl functionality of the methacrylate group. However, C1s in 316L stainless steel was observed to be at similar binding energies to Volan[®] and Volan[®] L treatment groups, which was higher than expected. The expected binding energy for C1s on 316L stainless steel was at a lower energy, closer to the primary C1s peak from the PET reference at 281.7 eV. XPS indicated that Volan[®] L surface functionalized stainless steel had 0% chlorine content, which was lowest when compared with other treatments used in this study. This is a favorable outcome since chlorine ions have been associated with stainless steel corrosion.

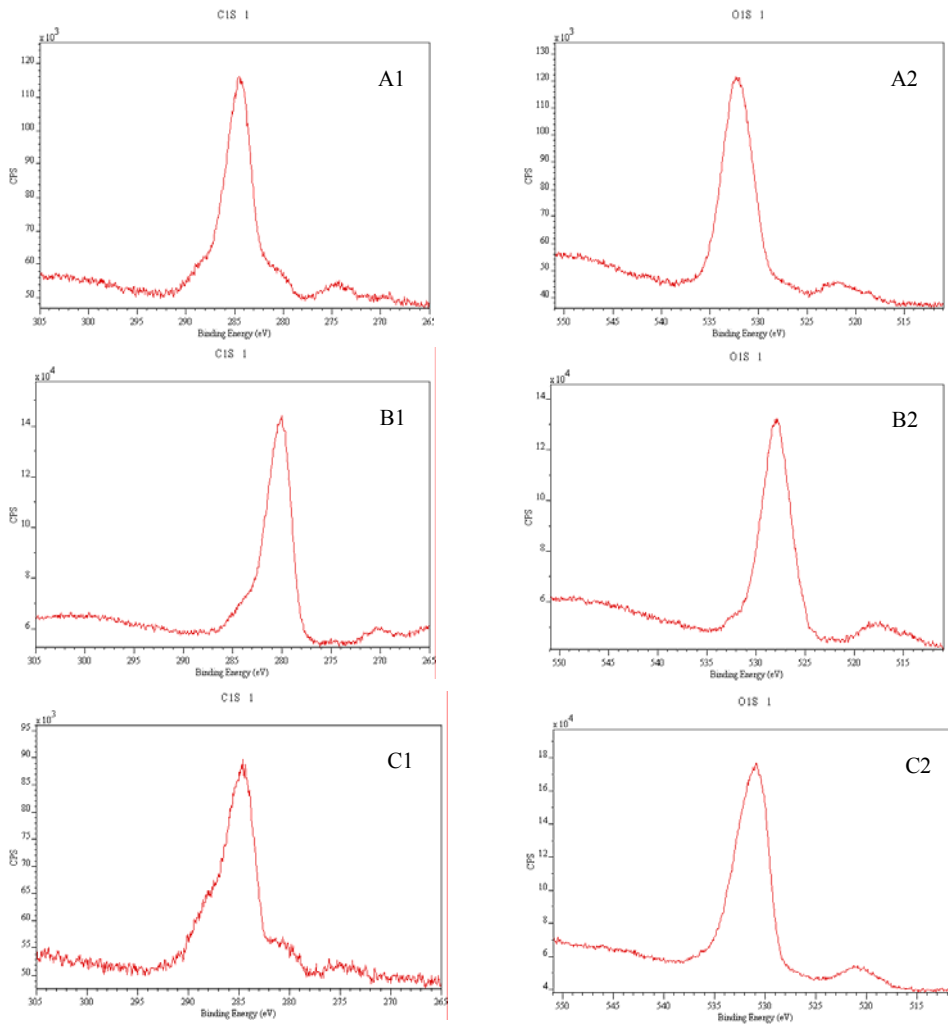


Figure 3.4 – XPS C1s and O1s spectra of: A) Previously-opened 2% Quilon[®] L treatment on 316 L stainless steel, B) Newly-opened 2% Quilon[®] L treatment on 316 L stainless steel, and C) 316L stainless steel control.

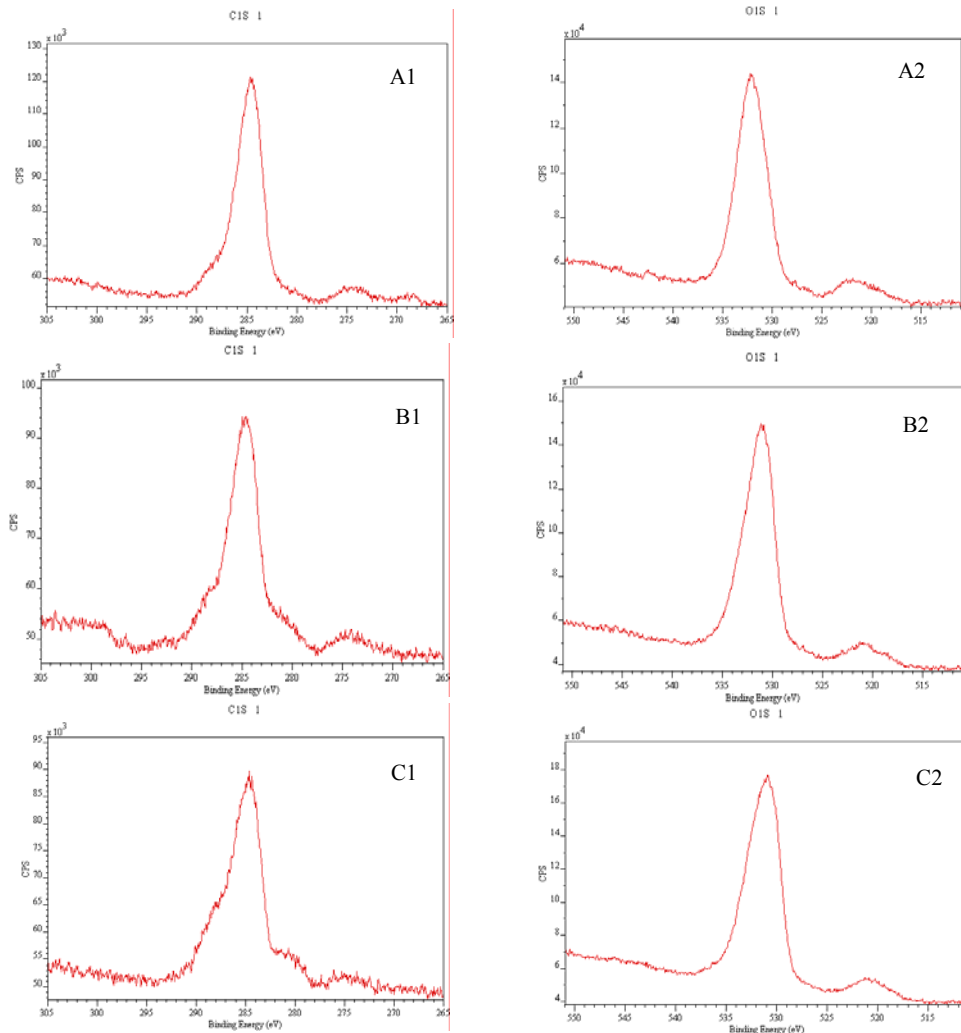


Figure 3.5 – XPS C1s and O1s spectra of: A) Previously-opened 2% Volan[®] treatment on 316 L stainless steel, B) Newly-opened 2% Volan[®] treatment on 316 L stainless steel, and C) 316L stainless steel control.

Summary

The results of the optimization study suggests a 2% v/v treating solution concentration is sufficient for priming the surface and exhibits reduced chlorine content at the stainless steel surface compared with 10% and 100% v/v concentrations. Rinsing the treated samples prior to drying in air was did not seem to effect to treatment outcome. As expected, using the solutions without further dilutions (100%) resulted in surfaces that were discolored and flaky. Although the treatments were not flaky, 10% v/v treatments were also discolored and appeared spotty. From this study, the best treatment was

determined to be 2% v/v solutions with 10 minute tumble washes and dried in air without rinsing, similar to the manufacturer's suggestion.

Silver acrylate seemed to deposit the most silver complex in mixtures similar in composition to Volan[®] L. These studies will be investigated further in later chapters.

Based on XPS data, degradation seems to only effect the Quilon[®] L treatment solutions even though solutions were backfilled with argon gas after each use. Volan[®] and Volan[®] L did not exhibit any binding energy shifts when comparing previously-opened to newly-opened stock solutions. An interesting observation was that Volan[®] L treated substrates had lower chlorine surface concentrations than other chromium alkoxide treatments.

Existing transition metals prevalent on the surface of a substrate can be used with metal alkoxides of the same transitions metals to enhance the binding and stability of coatings. This can easily reduced the number of steps associated with functionalizing 316L stainless steel.

Low Dose Gamma Irradiation Grafting of Polymers to Metal Alkoxide Treated Substrates

Gamma irradiation has been used to surface modify polymers by initiating polymerizations that result in grafting onto a material.^{55,57} Grafting by high energy radiation most often involves radical excitation of substrates and monomers. Gamma radiation is deeply penetrating, unlike other forms of high energy ionizing radiation such as electron beam accelerators. As a consequence, the effects of gamma irradiation are less dependent on substrate orientation and result in more uniform treatments to complex geometries.

Gamma radiation generates reactive sites in the monomer solution, as well as on the substrate. This is a unique advantage of radiation grafting with gamma irradiation in that fewer steps may be required to functionalize a substrate and to generate radicals at the surface compared with other techniques. Using this surface modification technique in conjunction with surfaces that have been functionalized by metal alkoxide treatments may enhance the adhesion and stability of metal surface modifications. Grafting can be achieved by polymer growth from tethered functional groups.

Gamma irradiation also lends itself to medical device modification since gamma radiation is often used for sterilization; although usually at significantly higher doses of ~2.5 MRads. No chemical or UV initiators are necessary, making gamma irradiation a relatively clean procedure without initiator residues. In this laboratory, low dose gamma irradiation (< 0.25 MRads total dose) has been shown to be effective for surface modification of a wide variety of substrate materials without inducing radiation damage to substrates. Reported here is the radiation grafting of hydrophilic polymers on stainless steel which has been surface treated with chromium alkoxide bonding agents. The resulting hydrophilic polymer surfaces were highly adherent and stable, as well as lubricious to the touch.

Materials and Methods

Preparation and treatment of 316L stainless steel substrates

Substrates of 316L stainless steel (1 cm x 1 cm) were cut from a single stock of foil with thicknesses of approximately 0.1 mm. Substrate surfaces were cleaned by sequential sonication for 5 minutes at 47 KHz and room temperature in 30 mL each of 1,1,1-trichloroethane, chloroform, acetone, methanol, and Ultrapure™ water then dried

under vacuum at 60°C. Fifty substrates were cleaned at a time. Stainless steel substrates were not electropolished.

For chromium alkoxide treatment, clean substrates were placed in 25 mL aqueous solutions of 2% v/v chromium III fatty acid (Quilon[®] L, DuPont) or chromium III methacrylate (Volan[®] and Volan[®] L, DuPont) for 10 minutes while rotating. 25 mL solutions were used to treat 10 samples at a time. Treated substrates were removed from solutions and allowed to air dry.

Controls consisted of untreated 316L stainless steel that undergoes irradiation treatment in monomer solutions and substrates that received no treatment and no irradiation with monomer solutions.

Preparation of monomer solutions

Monomer stock solutions of 10% v/v concentration with Ultrapure[™] water were prepared for all gamma irradiated experiments. The monomers investigated were 2-methacryloyloxyethyl phosphorylcholine (MPC; Dr. Ishihara, University of Tokyo), N-vinyl-2-pyrrolidone (NVP; Polysciences, Inc), n,n-dimethylacrylamide (DMA; Polysciences, Inc.), potassium 3-sulfopropyl acrylate (KSPA; Raschig GmbH). The co-monomer systems consisted of 9.5% monomer and 0.5% DMA with Ultrapure[™] water, where the monomer was MPC, NVP, or KSPA.

Gamma irradiation of substrates

316L stainless steel substrates were transferred to test tubes containing 3 mL aqueous solutions of either 10% v/v monomers with Ultrapure[™] water or 9.5% monomer and 0.5% DMA with Ultrapure[™] water. The solutions were degassed using vacuum generated by a mechanical pump, and subsequently backfilled with argon gas. The specimens were capped, placed in a ⁶⁰Co gamma irradiator and exposed to total doses of

0.1 or 0.15 Mrads at dose rates in the range of 569 - 536 rads/min. As shown in Figure 3.6, a rotating sample stage was used to account for uneven doses that may be caused by the asymmetrical shape of the gamma source. After irradiation, samples were placed into new test tubes and tumble washed for one week with 5 mL of Ultrapure™ water, which was decanted and replaced with 5 mL three times.

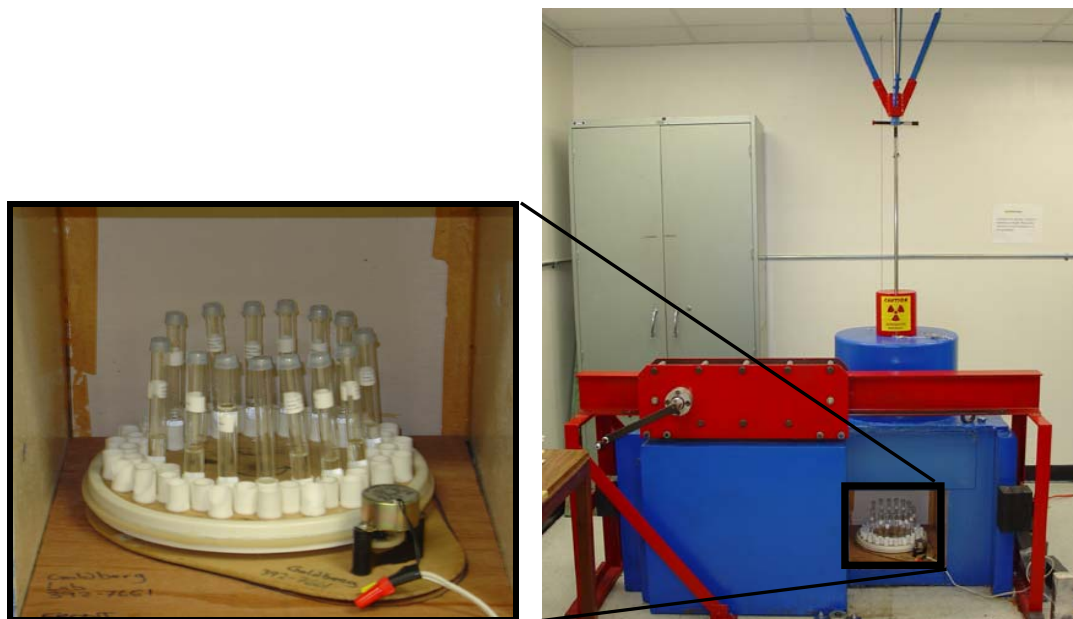


Figure 3.6 - ^{60}Co gamma irradiator and rotating sample stage.

Analysis

Surface modified 316L stainless steel substrates were characterized by captive air bubble contact angle with a Ramé-Hart A-100 goniometer, by scanning electron microscopy with a JEOL 6400 SEM, by fourier-transform infrared (FTIR) with a Nicolet Magna 706 (ZnSe crystal, 45°) and by x-ray photoelectron spectroscopy (XPS) analysis with Kratos Analytical Surface Analyzer XSAM 800 under the same conditions as previously described in the first portion of this chapter. SEM analysis was conducted with a working distance of 15 mm, 5 kV and condenser setting was at 10 with units in 6×10^{-6} Amps. The stability of grafted polymer coatings was evaluated by measuring contact

angles after initial hydration following irradiation and washing with Ultrapure™ water, dehydration in vacuum, and then again after rehydration.

Results and Discussion

Contact angle measurements for untreated substrates that underwent radiation grafting in monomer and co-monomer solutions yielded contact angles in the range of 22° - 40°. With the exception of hydrophobic recovery of the most hydrophilic surfaces, there was little difference in contact angle changes when tested for stability. This is illustrated graphically in Figures 3.7 - 3.13. After irradiation, DMA graft solutions were very viscous and to some extent stretchy. The substrates used in the DMA-only grafts were extremely difficult to remove from the crosslinked DMA surrounding them. For this reason DMA data was not included in all studies. These very high viscosities did not occur for co-monomer solutions with DMA.

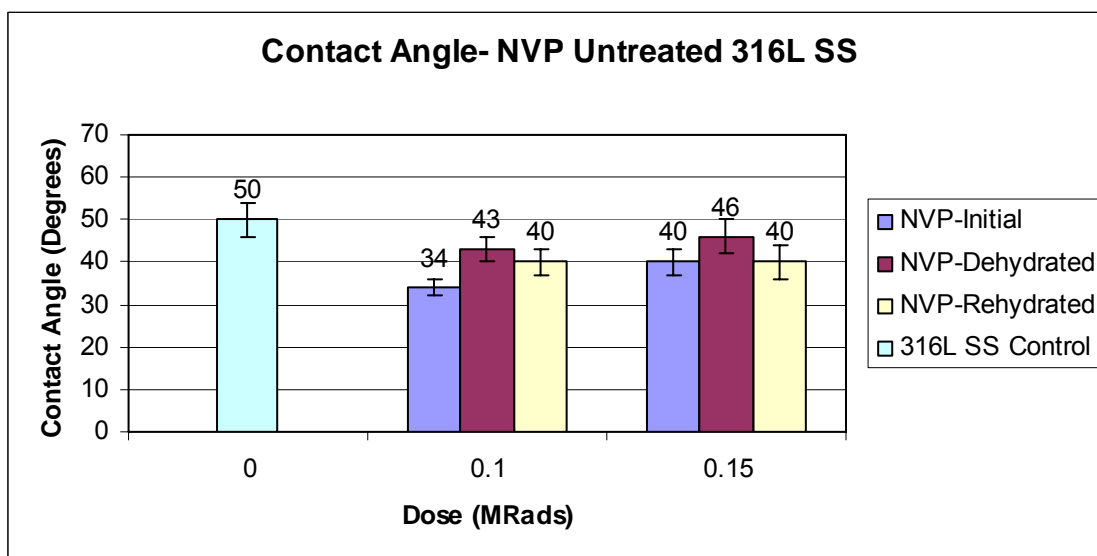


Figure 3.7 – Contact angle stability of untreated 316L stainless steel irradiated to 0.1 and 0.15 Mrads in 10% NVP / Ultrapure™ water solutions.

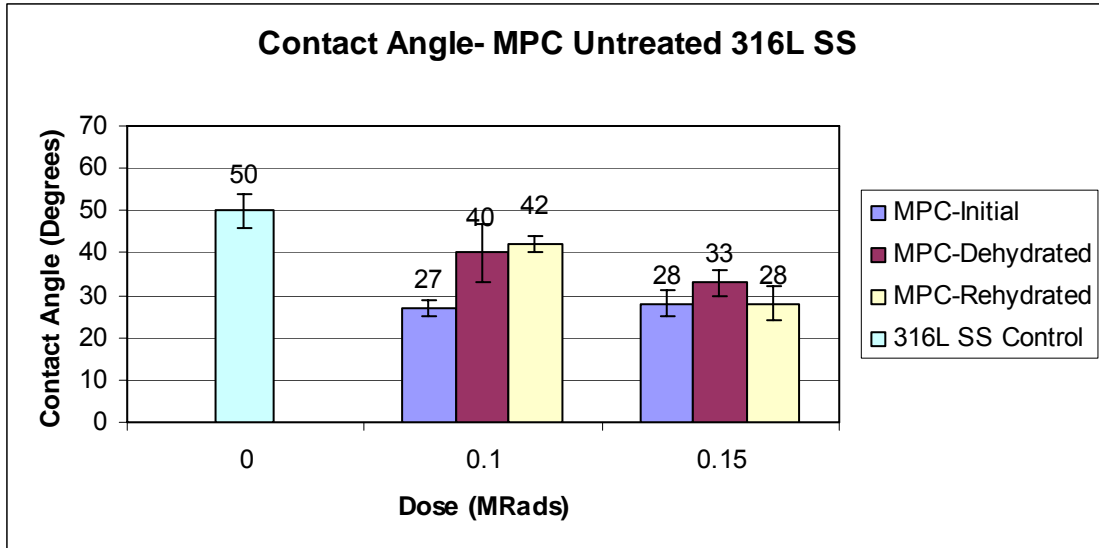


Figure 3.8 – Contact angle stability of untreated 316L stainless steel irradiated to 0.1 and 0.15 Mrads in 10% MPC / Ultrapure™ water solutions.

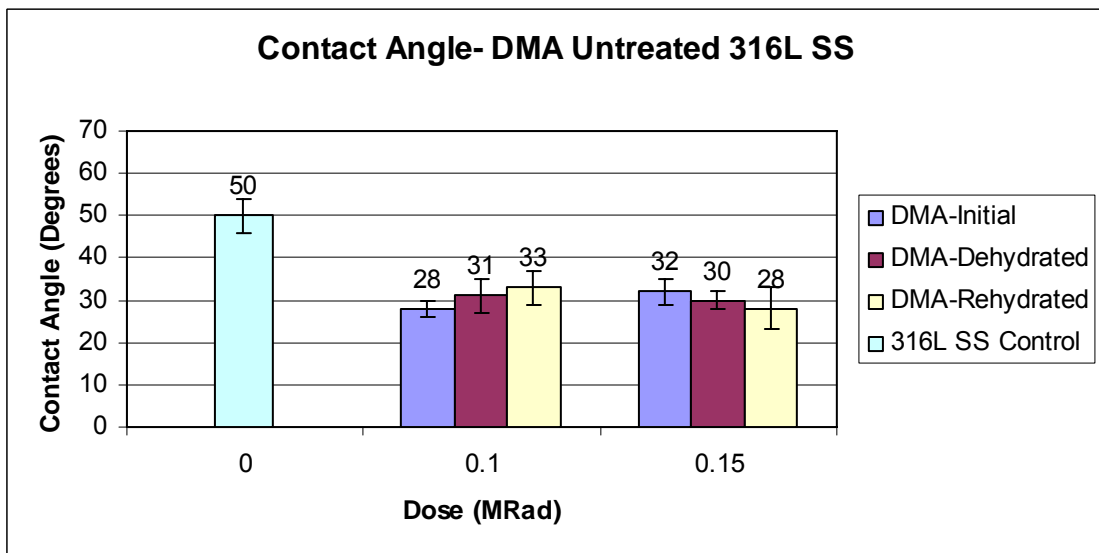


Figure 3.9 – Contact angle stability of untreated 316L stainless steel irradiated to 0.1 and 0.15 Mrads in 2.5% DMA / Ultrapure™ water solutions.

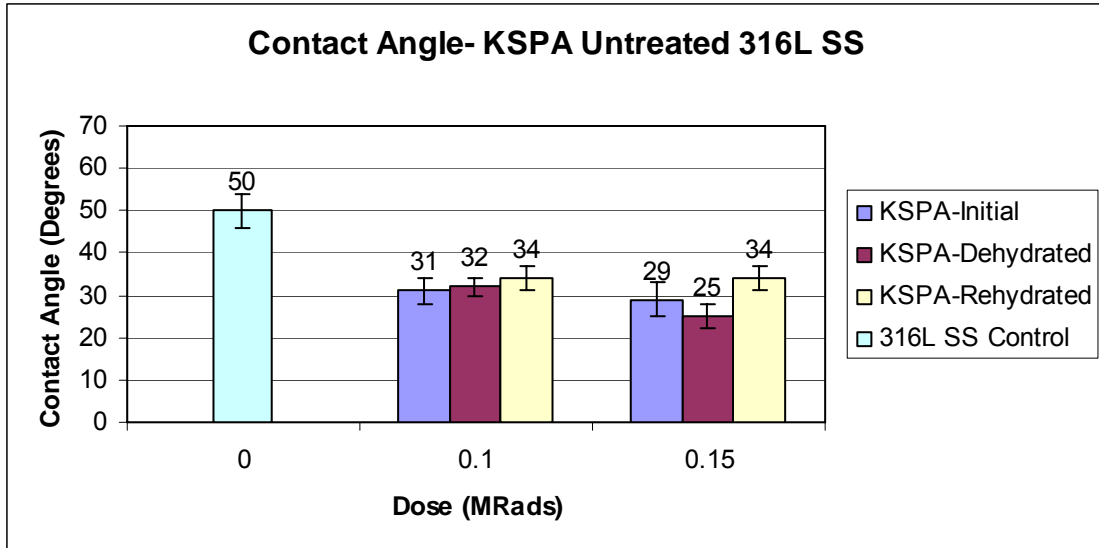


Figure 3.10 – Contact angle stability of untreated 316L stainless steel irradiated to 0.1 and 0.15 Mrads in 10% KSPA / Ultrapur™ water solutions.

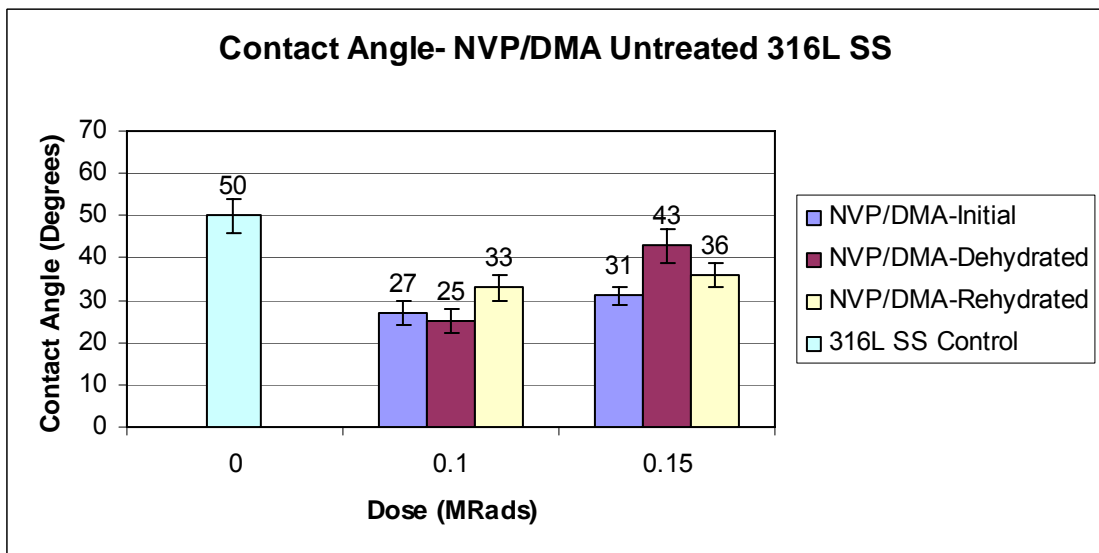


Figure 3.11 – Contact angle stability of untreated 316L stainless steel irradiated to 0.1 and 0.15 Mrads in 9.5% NVP / 0.5% DMA / Ultrapur™ water solutions.

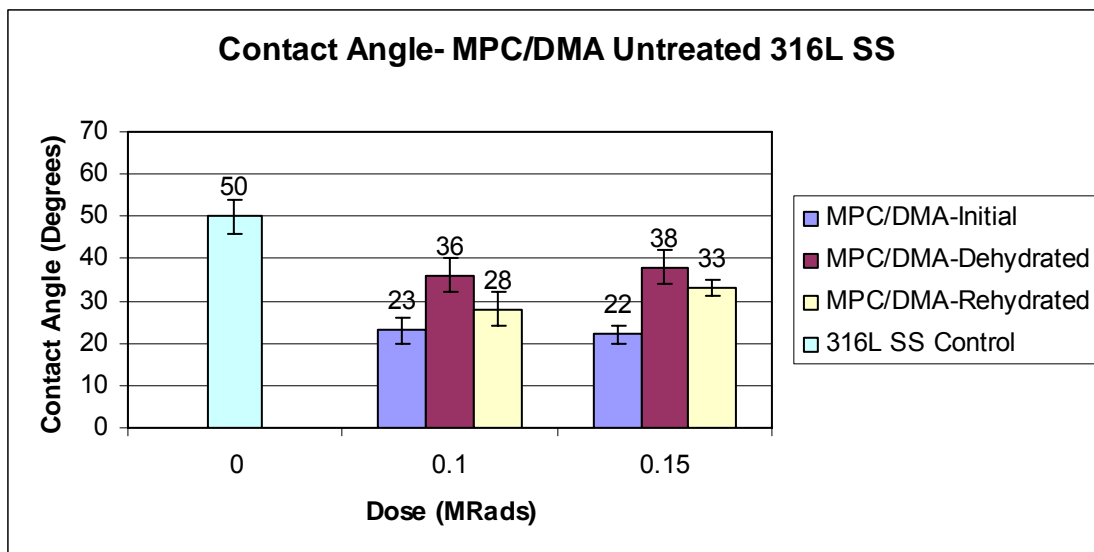


Figure 3.12 – Contact angle stability of untreated 316L stainless steel irradiated to 0.1 and 0.15 Mrads in 9.5% MPC / 0.5% DMA / Ultrapure™ water solutions.

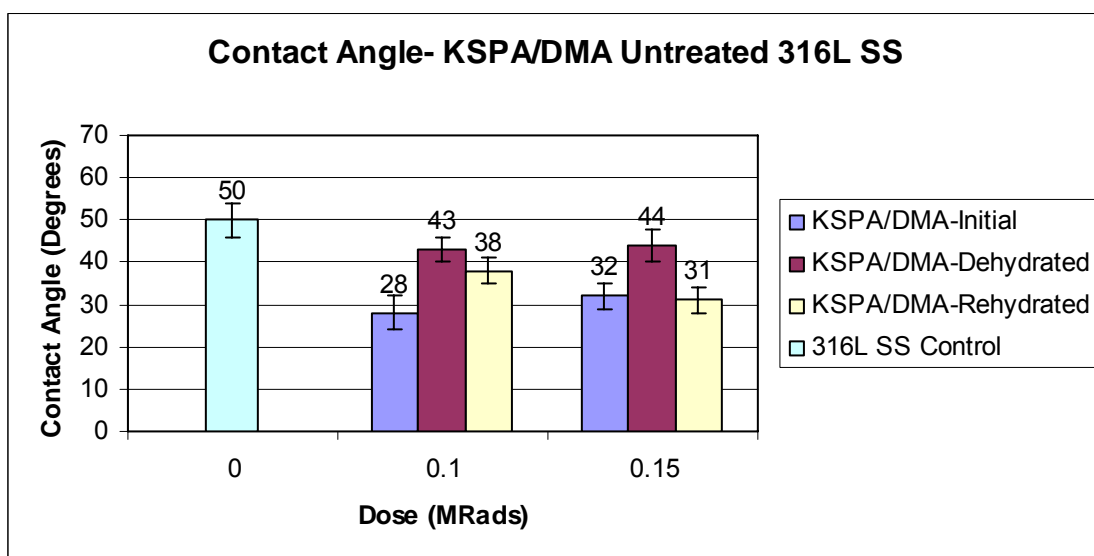


Figure 3.13 – Contact angle stability of untreated 316L stainless steel irradiated to 0.1 and 0.15 Mrads in 9.5% KSPA / 0.5% DMA / Ultrapure™ water solutions.

Contact angle results varied for NVP, KSPA and respective co-monomer grafting solutions with DMA on metal alkoxide functionalized substrates. With Quilon® L no significant change in contact angle was found compared with untreated 316L stainless steel irradiated in the same monomer solutions. Volan® treatment result in contact angles of ~20° for all NVP and KSPA grafting solutions with no hydrophobic recovery. This

stability was not observed for co-monomer systems where there was hydrophobic recovery for some conditions. Volan[®] L consistently reduced the contact angles to ~20° for NVP and KSPA grafts. Additionally, contact angles as low as 18° were found for co-monomer systems with no hydrophobic recovery. Hydrophilicity of these coatings was stable. This data is shown in Figures 3.14 - 3.25.

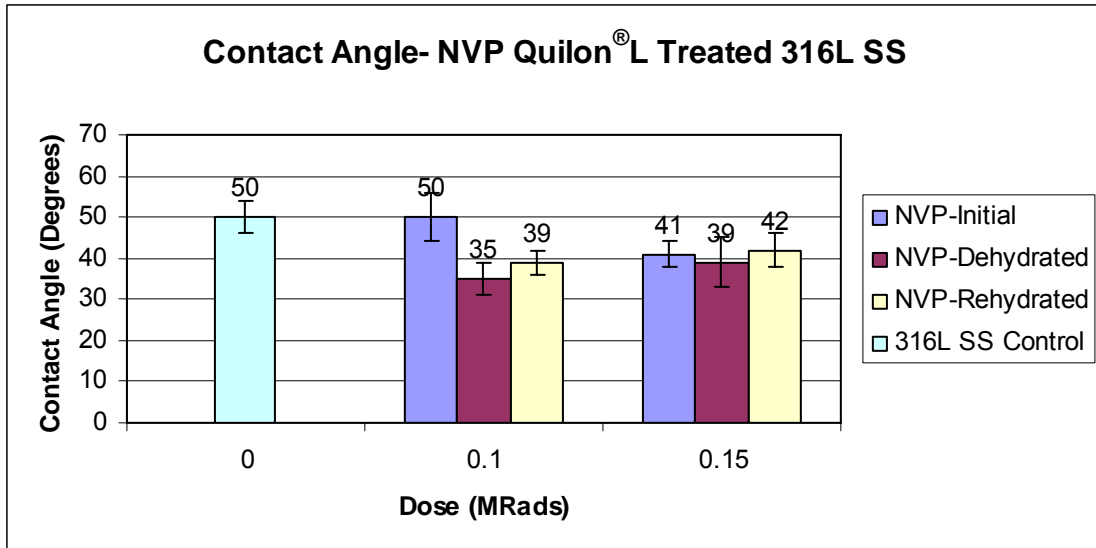


Figure 3.14 – Contact angle stability of Quilon[®] L treated 316L stainless steel irradiated to 0.1 and 0.15 Mrads in 10% NVP / Ultrapure[™] water solutions.

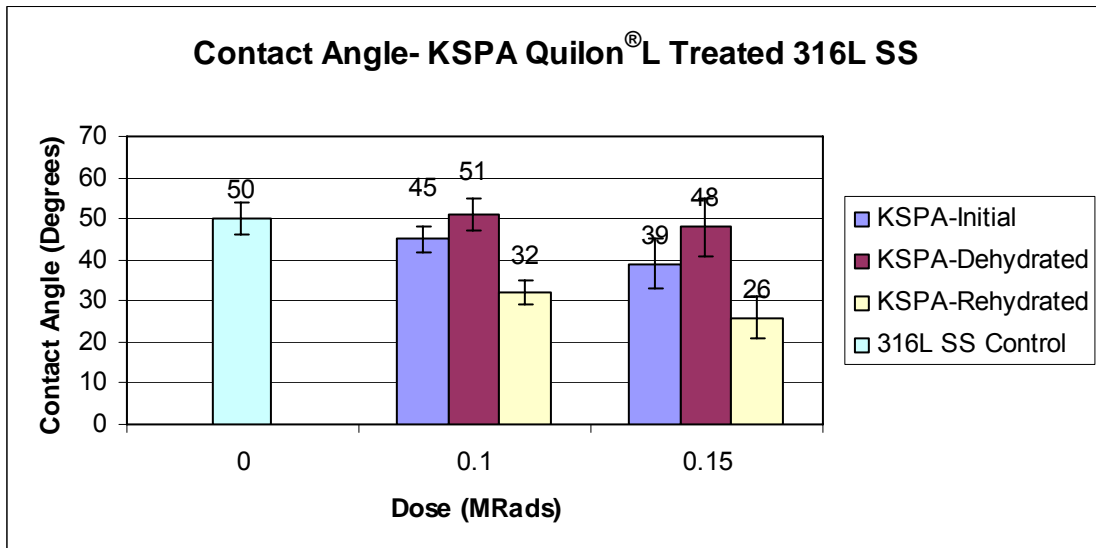


Figure 3.15 – Contact angle stability of Quilon[®] L treated 316L stainless steel irradiated to 0.1 and 0.15 Mrads in 10% KSPA / Ultrapure[™] water solutions.

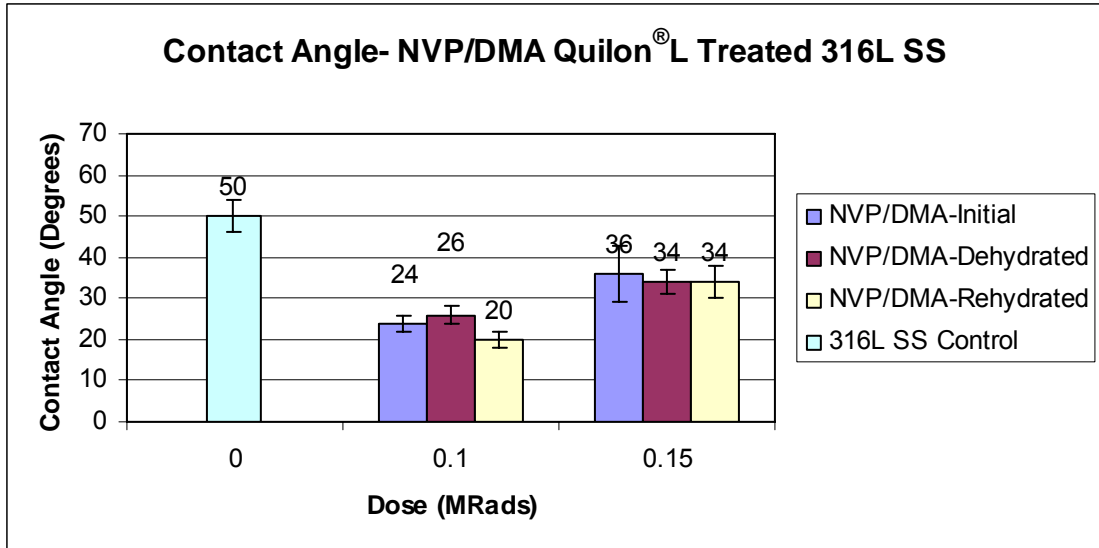


Figure 3.16 – Contact angle stability of Quilon[®] L treated 316L stainless steel irradiated to 0.1 and 0.15 Mrads in 9.5% NVP / 0.5% DMA / Ultrapure[™] water solutions.

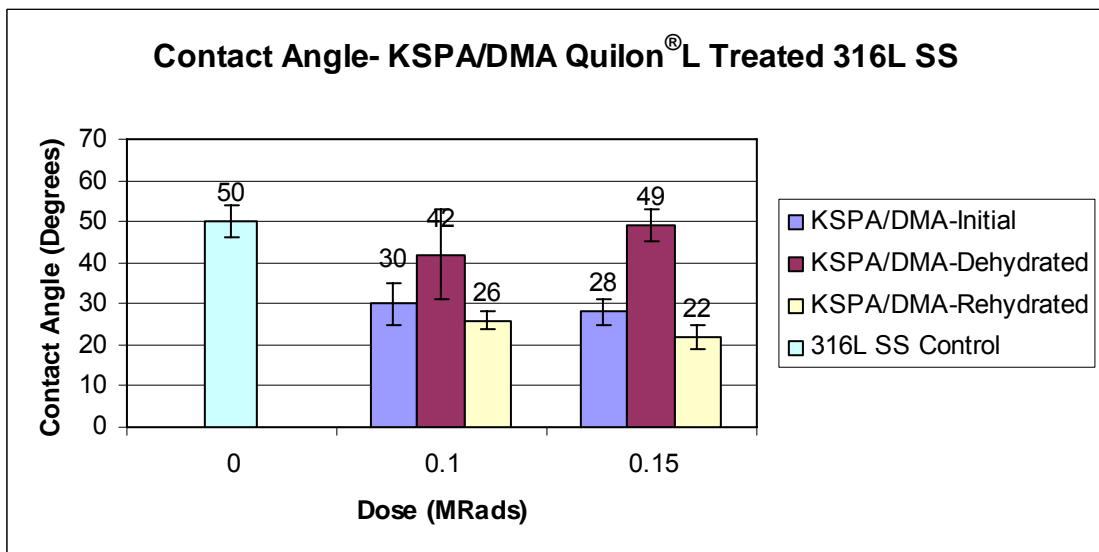


Figure 3.17 – Contact angle stability of Quilon[®] L treated 316L stainless steel irradiated to 0.1 and 0.15 Mrads in 9.5% KSPA / 0.5% DMA / Ultrapure[™] water solutions.

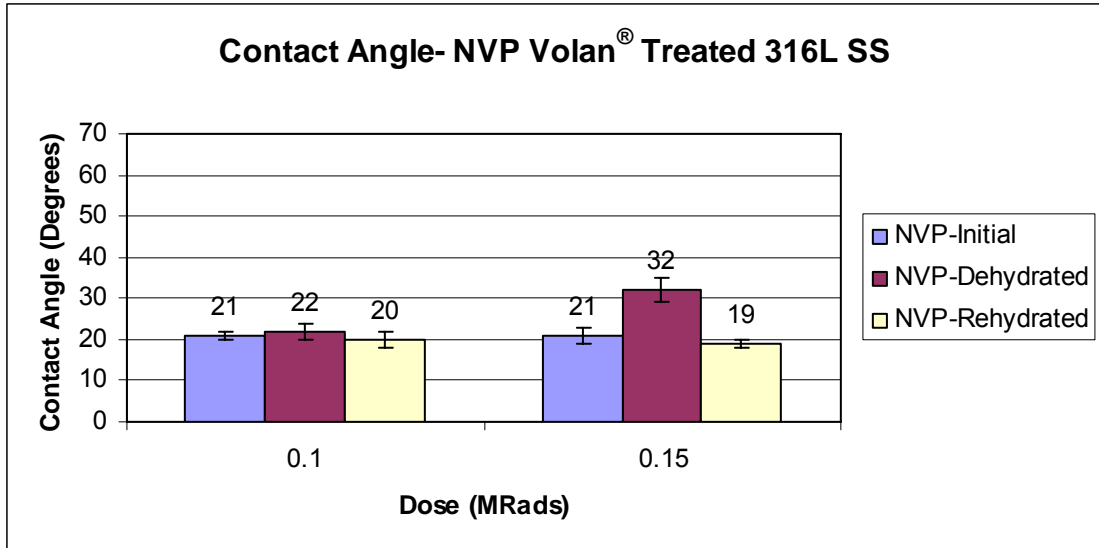


Figure 3.18 – Contact angle stability of Volan[®] treated 316L stainless steel irradiated to 0.1 and 0.15 Mrads in 10% NVP / Ultrapure[™] water solutions.

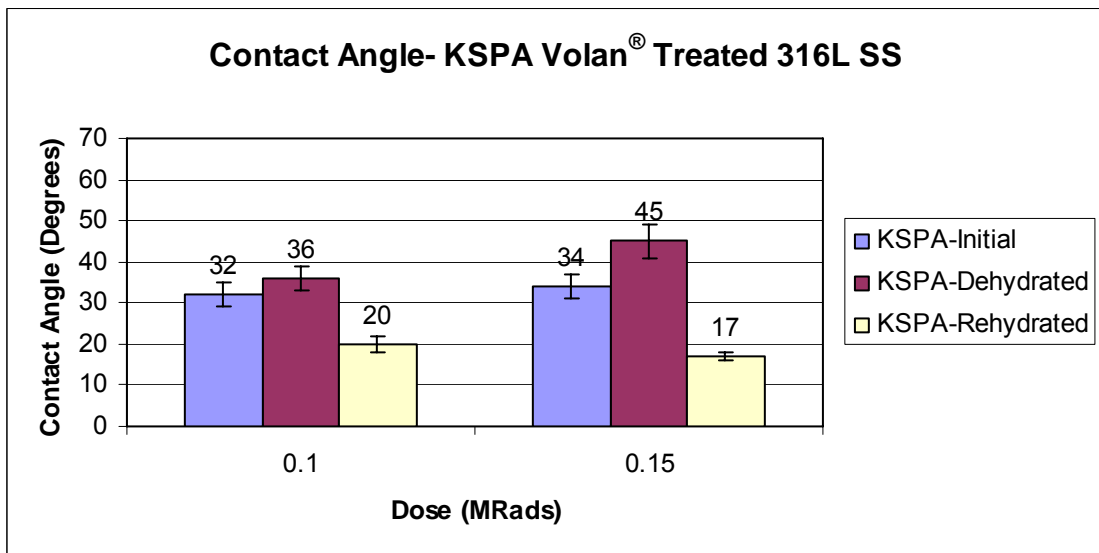


Figure 3.19 – Contact angle stability of Volan[®] treated 316L stainless steel irradiated to 0.1 and 0.15 Mrads in 10% KSPA / Ultrapure[™] water solutions.

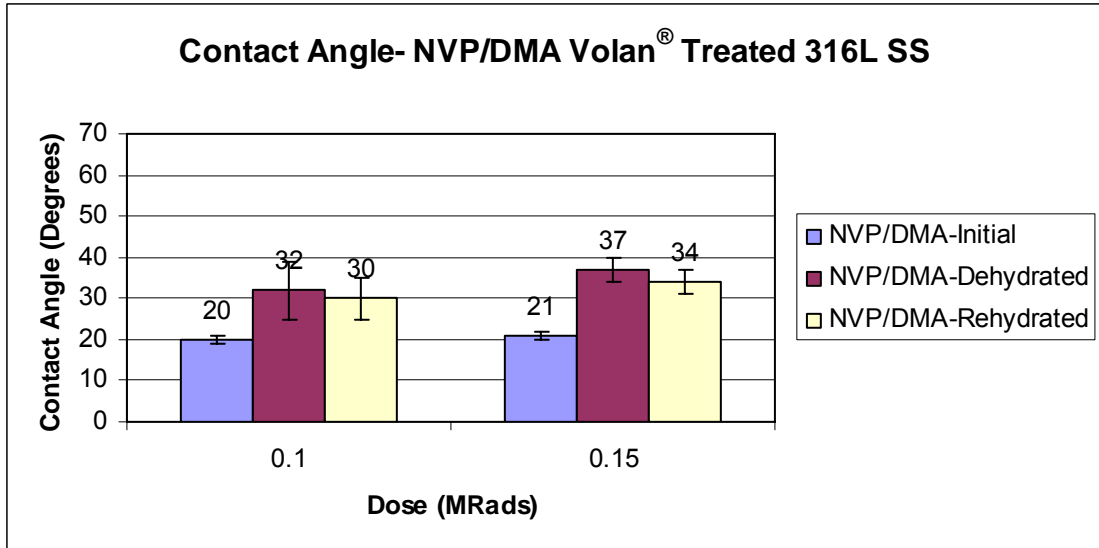


Figure 3.20 – Contact angle stability of Volan[®] treated 316L stainless steel irradiated to 0.1 and 0.15 Mrads in 9.5% NVP / 0.5% DMA / Ultrapure[™] water solutions.

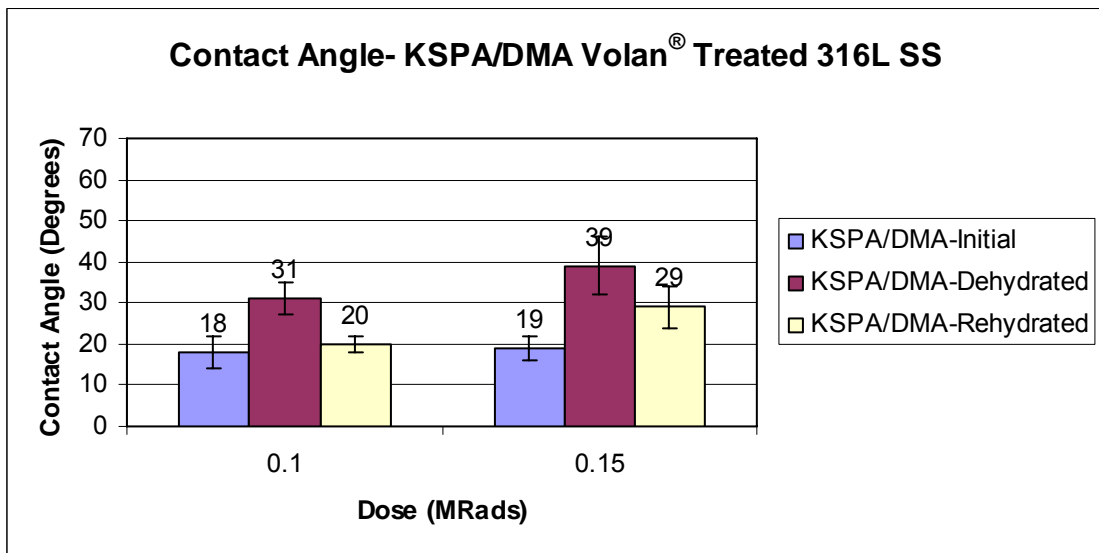


Figure 3.21 – Contact angle stability of Volan[®] treated 316L stainless steel irradiated to 0.1 and 0.15 Mrads in 9.5% KSPA / 0.5% DMA / Ultrapure[™] water solutions.

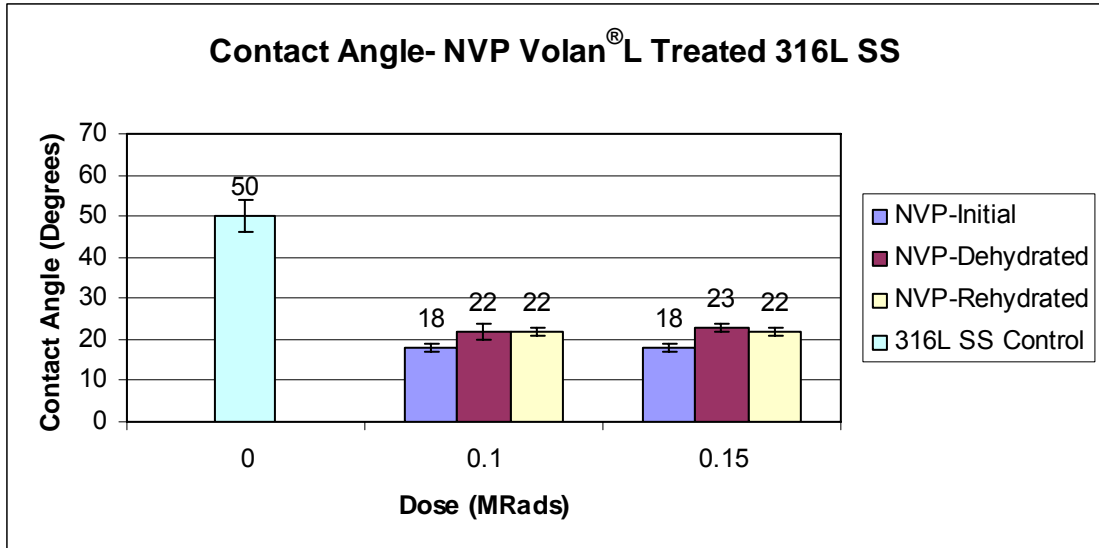


Figure 3.22 – Contact angle stability of Volan[®] L treated 316L stainless steel irradiated to 0.1 and 0.15 Mrads in 10% NVP / Ultrapure[™] water solutions.

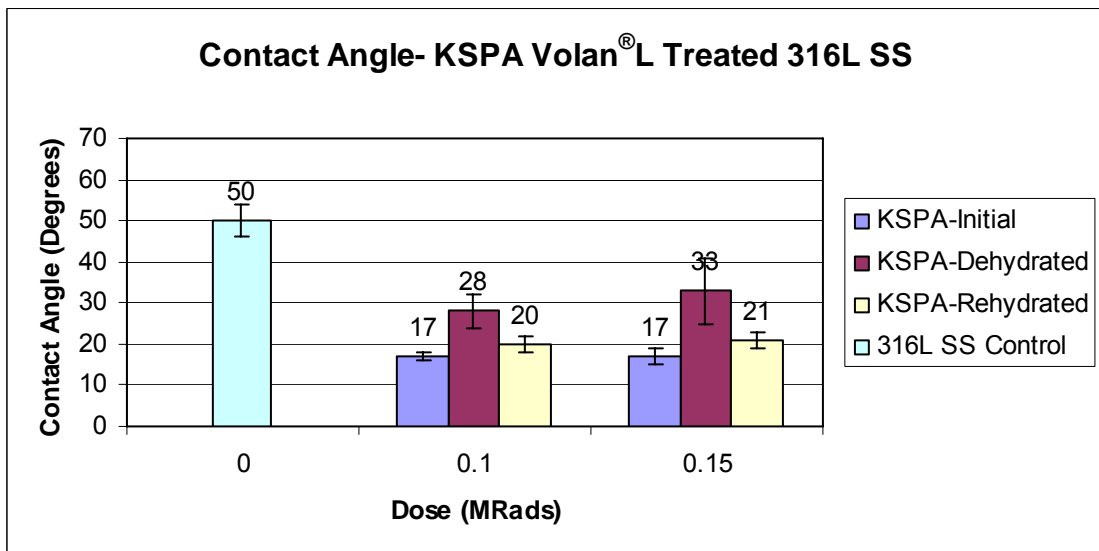


Figure 3.23 – Contact angle stability of Volan[®] L treated 316L stainless steel irradiated to 0.1 and 0.15 Mrads in 10% KSPA / Ultrapure[™] water solutions.

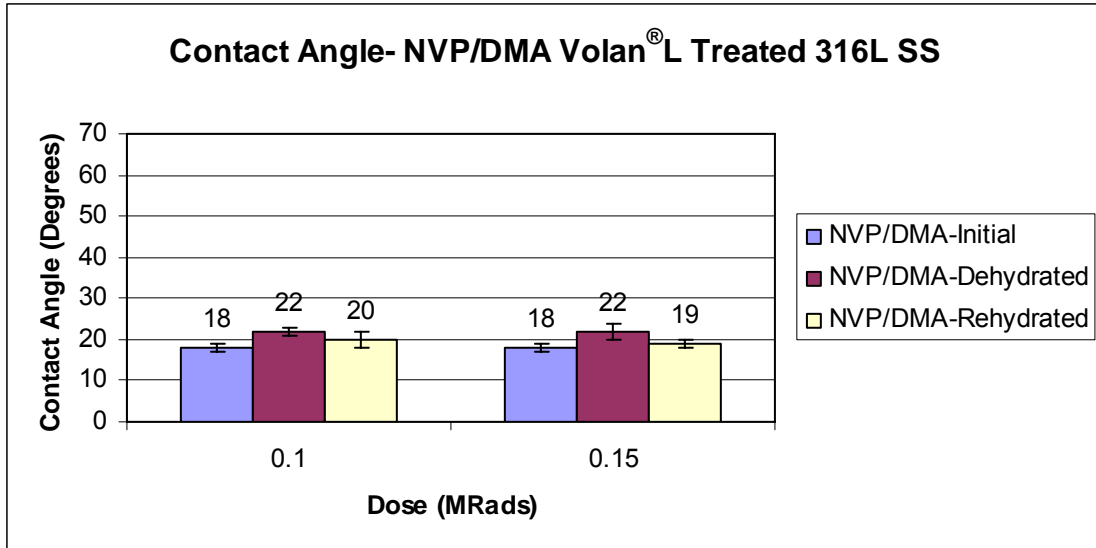


Figure 3.24 – Contact angle stability of Volan[®] L treated 316L stainless steel irradiated to 0.1 and 0.15 Mrads in 9.5% NVP / 0.5% DMA / Ultrapure[™] water solutions.

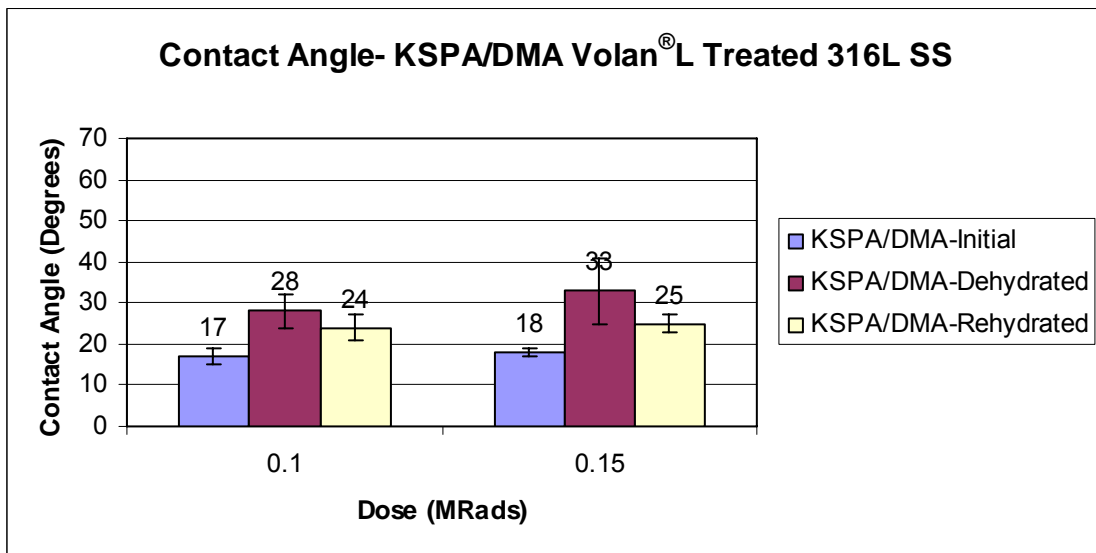


Figure 3.25 – Contact angle stability of Volan[®] L treated 316L stainless steel irradiated to 0.1 and 0.15 Mrads in 9.5% KSPA / 0.5% DMA / Ultrapure[™] water solutions.

Contact angle measurements of MPC coatings on metal alkoxide functionalized surfaces were significantly lower than both 316L stainless steel and MPC coated stainless steel with no pre-treatment; see Figures 3.26 - 3.31 and Table 3.3. These results were observed for all MPC and metal alkoxide treatment combinations explored in this study. Additionally, MPC and MPC/DMA coated functionalized substrates were similarly

hydrophilic. After dehydration, MPC and MPC/DMA coatings on functionalized stainless steel exhibited similar hydrophilicity with no evidence of hydrophobic recovery as well as very little hydration time.

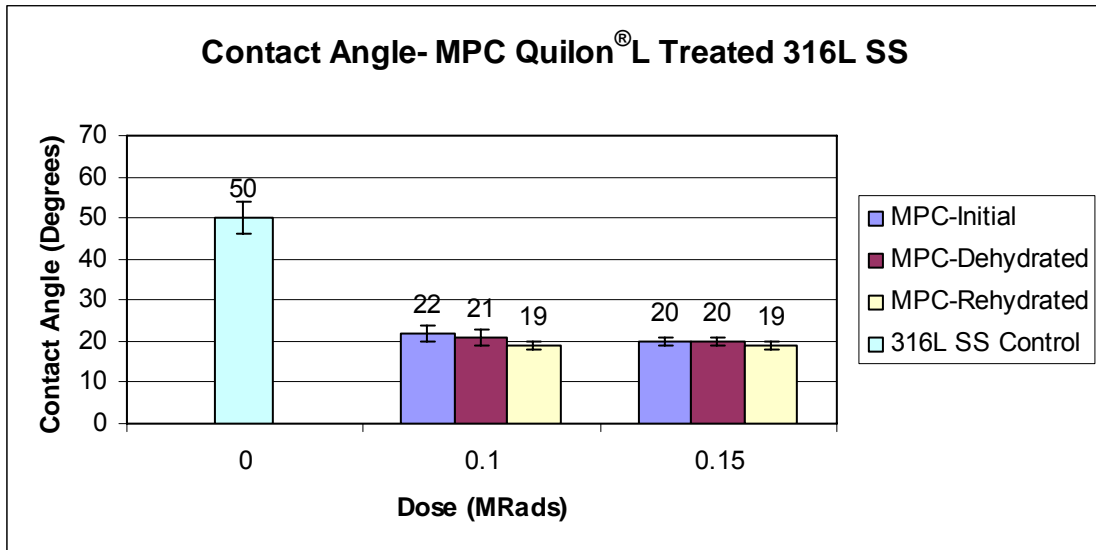


Figure 3.26 – Contact angle stability of Quilon[®] L treated 316L stainless steel irradiated to 0.1 and 0.15 Mrads in 10% MPC / Ultrapure[™] water solutions.

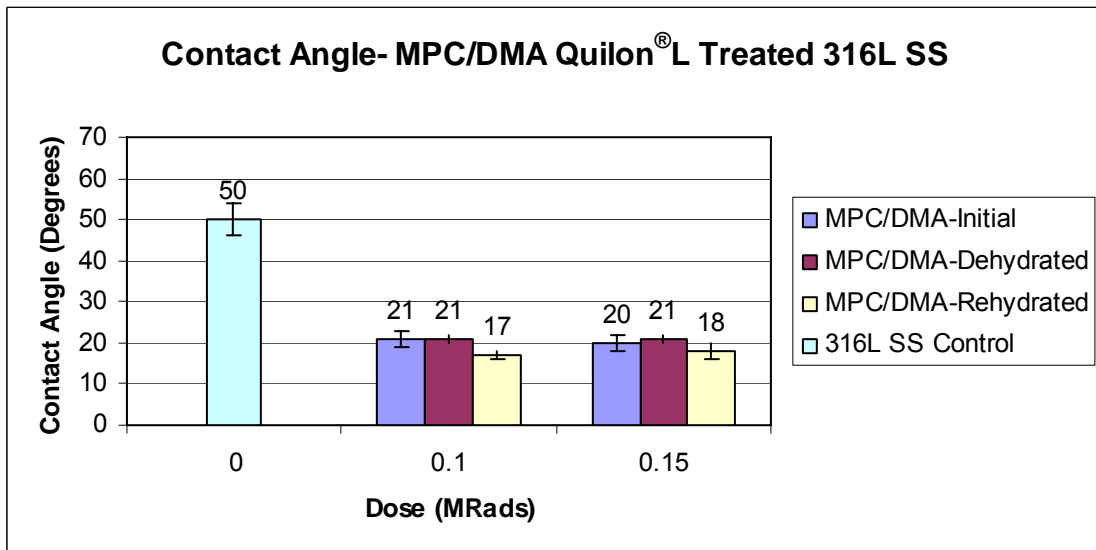


Figure 3.27 – Contact angle stability of Quilon[®] L treated 316L stainless steel irradiated to 0.1 and 0.15 Mrads in 9.5% MPC / 0.5% DMA / Ultrapure[™] water solutions.

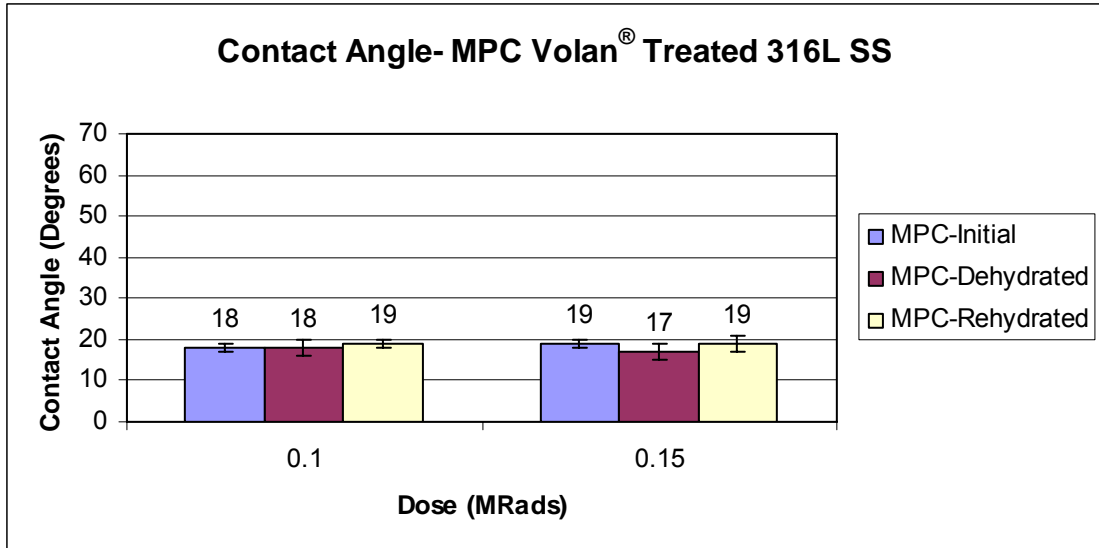


Figure 3.28 – Contact angle stability of Volan[®] treated 316L stainless steel irradiated to 0.1 and 0.15 Mrads in 10% MPC / Ultrapure[™] water solutions.

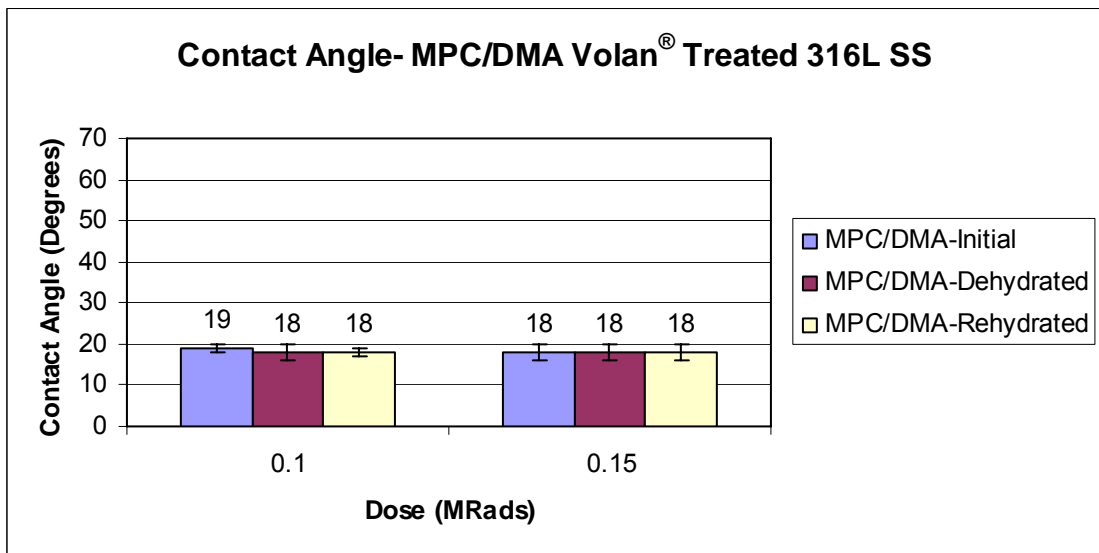


Figure 3.29 – Contact angle stability of Volan[®] treated 316L stainless steel irradiated to 0.1 and 0.15 Mrads in 9.5% MPC / 0.5% DMA / Ultrapure[™] water solutions.

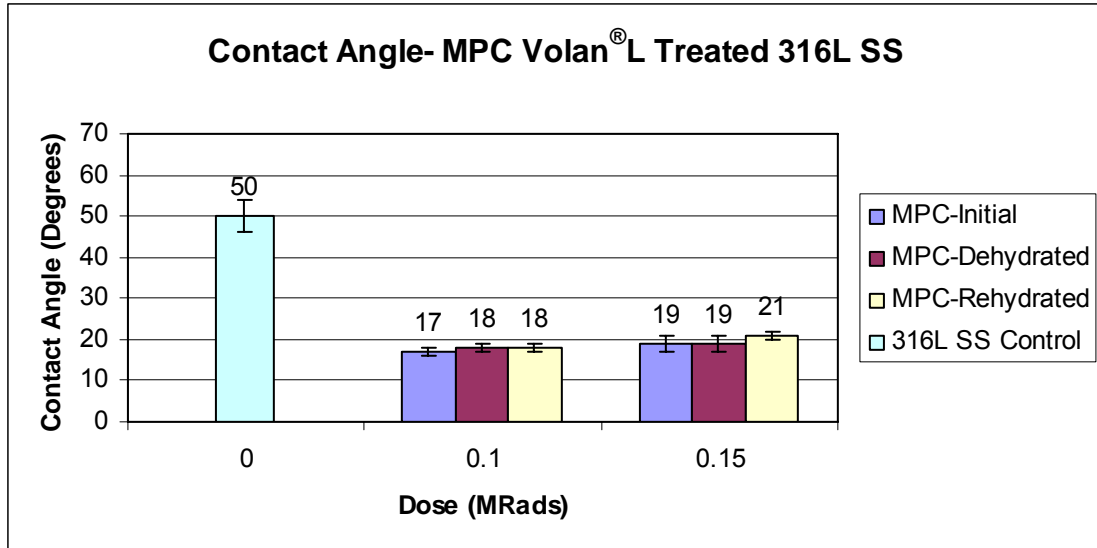


Figure 3.30 – Contact angle stability of Volan[®] L treated 316L stainless steel irradiated to 0.1 and 0.15 Mrads in 10% MPC / Ultrapure[™] water solutions.

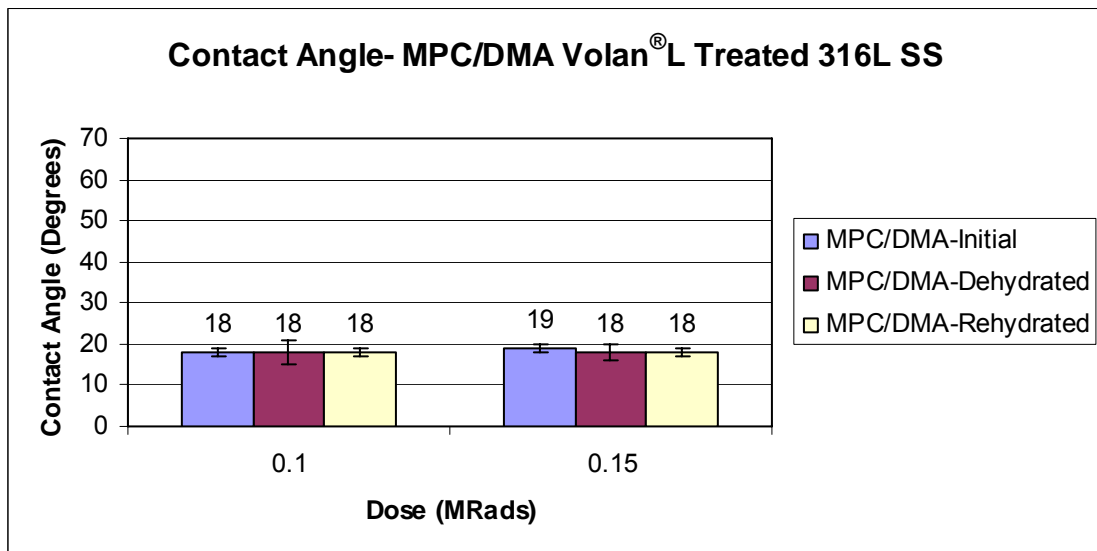


Figure 3.31 – Contact angle stability of Volan[®] L treated 316L stainless steel irradiated to 0.1 and 0.15 Mrads in 9.5% MPC / 0.5% DMA / Ultrapure[™] water solutions.

As shown by XPS analysis, NVP coatings on Volan[®] L treated stainless steel specimens exhibited the highest N1s concentrations, whereas Quilon[®] L treatments yielded the lowest N1s concentrations as shown in Table 3.4. Additionally, chromium (III) methacrylate pretreatments resulted in stable hydrophilic surfaces. The P2p and N1s from MPC coated surfaces were analyzed and exhibited a ratio closest to 1:1 when coated

on Volan[®] L treated stainless steel. These data are summarized in Table 3.3 and Figure 3.32. All MPC coatings on metal alkoxide treated substrates resulted in hydrophilic surfaces.

Table 3.3 – MPC XPS elemental surface composition (%) and rehydrated contact angle of surfaces for dose of 0.1 Mrads. MPC* refers to theoretical concentrations of elemental composition.

Treatment	C1s	O1s	N1s	P2p	Fe2p3	Cr2p3	P2p/N1s	Contact Angle (°)
316L Control	48.2	42.3	< 0.1	0.0	7.9	1.2	0.0	50 ±4
None/MPC	42.5	36.6	4.3	1.1	7.5	7.8	0.3	42 ±2
Quilon [®] L/MPC	55.0	33.6	3.6	2.2	2.0	3.6	0.6	19 ±1
Volan [®] /MPC	46.0	37.7	4.8	2.8	4.3	4.5	0.6	19 ±1
Volan [®] L/MPC	45.6	39.1	4.6	4.0	3.3	3.5	0.9	18 ±1
MPC*	57.8	31.6	5.3	5.3	0.0	0.0	1.0	—

Table 3.4 – NVP XPS elemental surface composition (%) and rehydrated contact angle of surfaces for dose of 0.1 Mrads. NVP* refers to theoretical concentrations of elemental composition.

Treatment	C1s	O1s	N1s	Fe2p3	Cr2p3	Cl2p	Contact Angle (°)
316L Control	48.2	42.3	< 0.1	7.9	1.2	0.0	50 ±4
None/NVP	62.5	27.4	3.7	1.9	3.3	1.3	40 ±3
Quilon [®] L/NVP	75.6	19.3	2.2	0.3	1.5	1.0	39 ±3
Volan [®] /NVP	67.1	23.9	4.0	0.9	2.6	1.6	20 ±2
Volan [®] L/NVP	64.6	26.2	5.6	1.5	2.0	0.1	22 ±1
NVP*	75	12.5	12.5	0.0	0.0	0.0	—

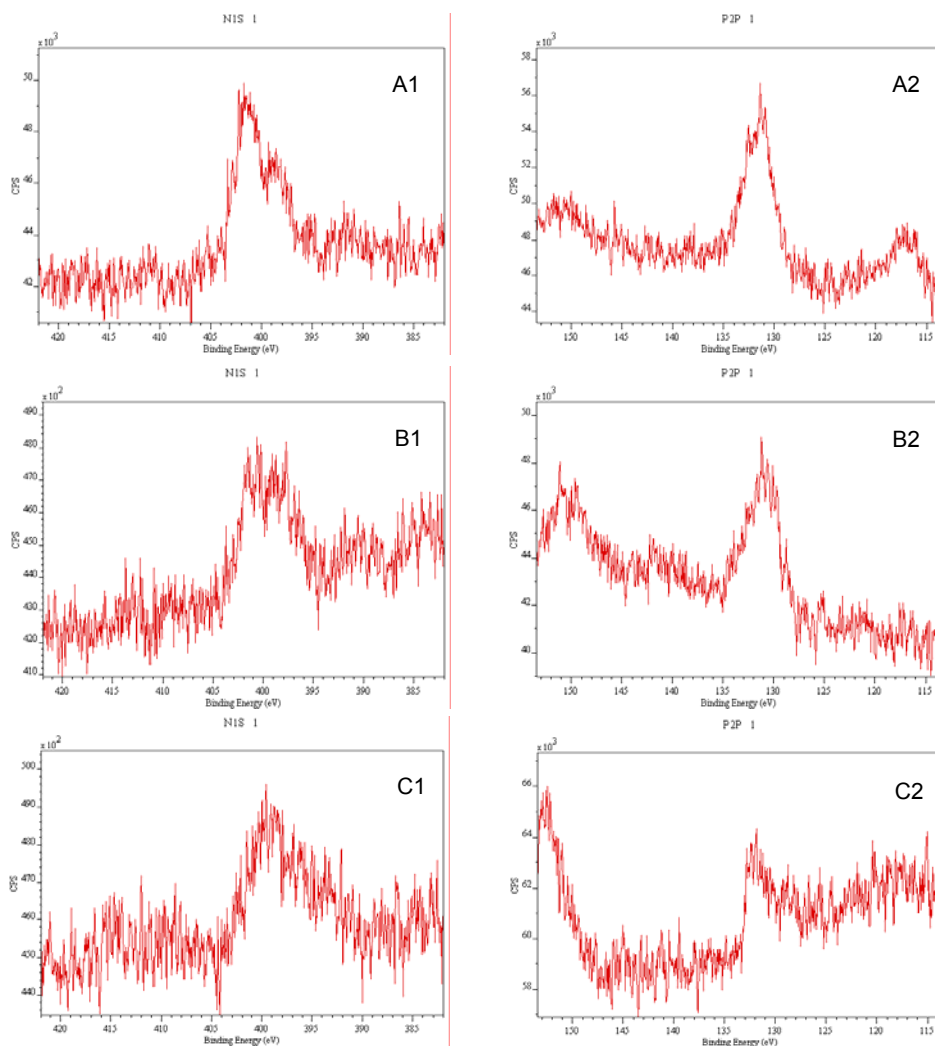


Figure 3.32 – MPC grafted on treated and untreated 316L SS. XPS elemental spectra for N1s and P2p. A) 2% Volan[®] L treated, B) 2% Quilon[®] L treated, and C) untreated.

As shown in Table 3.5, XPS analysis of KSPA treatments showed there was little to no signal from potassium ions. This could be due to dissociation of the potassium salt from sulfopropyl acrylate. This is likely to happen during the irradiation process due to the presence of the electron withdrawing sulfopropyl head which can facilitate dissociation in an irradiated environment. With KSPA, stable hydrophilic surfaces were produced with Volan[®] and Volan[®] L treated substrates.

Table 3.5 – KSPA XPS elemental surface composition (%) and rehydrated contact angle of surfaces for dose of 0.1 Mrads. KSPA* refers to theoretical concentrations of elemental composition.

Treatment	C1s	O1s	N1s	Fe2p3	Cr2p3	K2p3	S2p3	Cl2p	Contact Angle (°)
316L Control	48.2	42.3	< 0.1	7.9	1.2	0.0	0.0	0.0	50 ±4
None/KSPA	56.5	34.4	0.0	2.8	4.4	0.0	3.9	0.0	34 ±3
Quilon [®] L/ KSPA	76.7	20.5	0.0	0.4	1.3	0.0	1.1	0.0	32 ±3
Volan [®] /KSPA	62.3	31.8	0.0	1.4	3.1	0.0	1.4	0.0	20 ±2
Volan [®] L/ KSPA	57.7	33.8	0.0	1.0	5.8	0.0	1.8	0.0	20 ±2
KSPA*	46.1	38.5	0.0	0.0	0.0	7.7	7.7	0.0	—

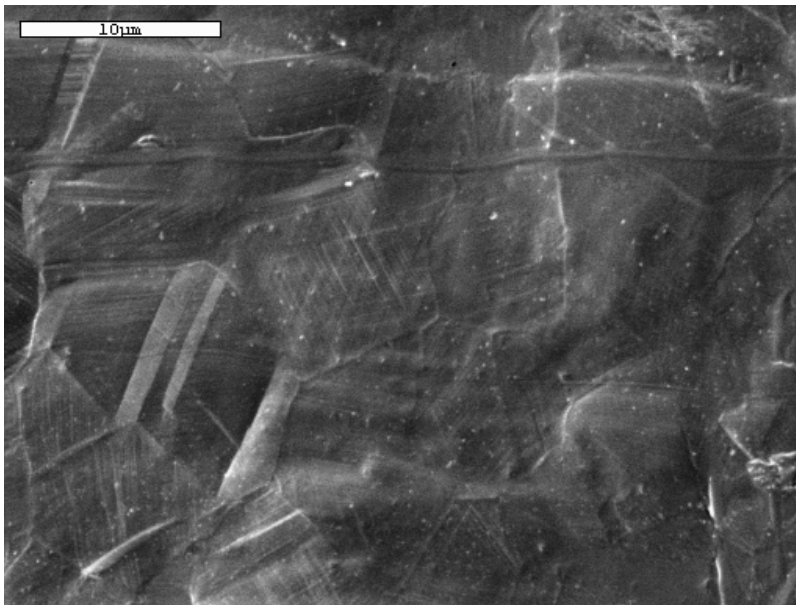


Figure 3.33 – SEM of cleaned 316L stainless steel at 5000x.

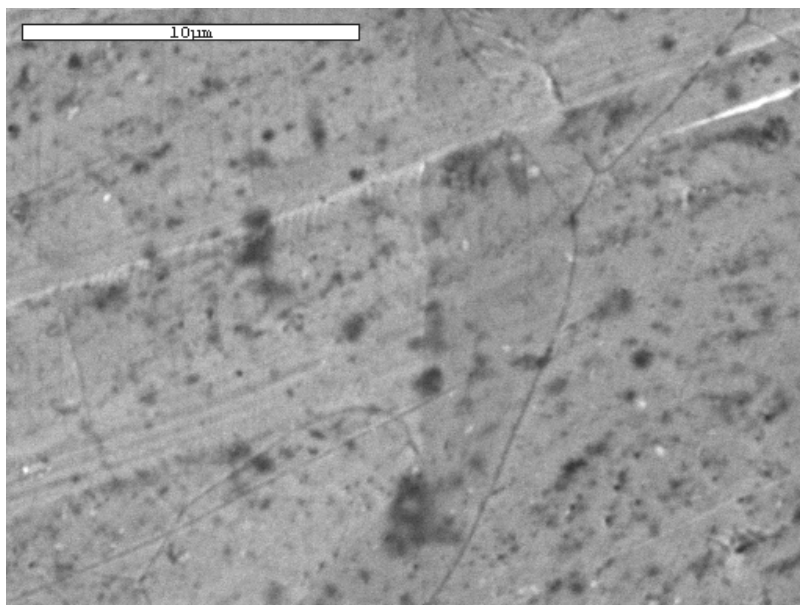


Figure 3.34 – SEM of 10% v/v MPC gamma irradiation grafted (0.1 MRads) coating on Volan[®] L activated 316L stainless steel at 5000x.

From Tables 3.3 - 3.5, Fe_{2p3} and Cr_{2p3} peaks were present even for the most hydrophilic conditions. This suggests that coatings are either very thin or are not homogeneously coated on the substrate, which could be the result of uneven chromium alkoxide binding. SEM micrographs confirmed surface modifications were very thin since much of the 316L topography was discernable in all micrographs of gamma irradiation grafted coatings as shown in Figures 3.33-34. Based on XPS analysis, surface modifications is likely to be ~2 - 20 atomic layers in depth. SEM micrographs did not show any evidence of corrosion for gamma irradiated modifications.

Summary

The results of this study indicate that chromium functionalized stainless steel surfaces on which hydrophilic vinyl functional monomers were polymerized results in coatings with improved stability and increased hydrophilicity in contrast to non-surface functionalized stainless steel.

It should be noted that the stainless steel used in this study had a surface composition somewhat lower in Cr_2O_3 content than electropolished stainless steel which is most often used for endovascular stents. Because the stainless steel used in these and subsequent studies were not electropolished, surface elemental compositions will be different from reported values for electropolished 316L stainless steel. Also, decreased surface roughness may result from electropolishing. Due to increased surface chromium concentrations as a result of electropolishing, increase bonding agent concentrations may result when treating these specimens, which could result in further improved coating stability.

Volan[®] L, which resulted in the lowest chlorine surface content, is an ideal metal alkoxide for functionalizing 316L stainless steel surfaces, since chlorine ions have been associated with pitting corrosion on stainless steels. Evidence of corrosion was not seen in SEM micrographs for any of the conditions investigated in this study. Due to highly efficient crosslinking, DMA was satisfactory as a co-monomer component. However, no significant advantage was seen for using the co-monomer compared to NVP, MPC and KSPA monomer formulations used here.

Stable hydrophilic coatings were prepared by gamma irradiation of monomer solutions on chromium alkoxide functionalized 316L stainless steel. MPC coatings on all chromium alkoxide treated substrates resulted in stable hydrophilic surfaces. Additionally, Volan[®] and Volan[®] L treatments consistently produced stable hydrophilic surfaces with all monomer and co-monomer systems investigated. Quilon[®] L, which is a trivalent chromium fatty acid, only produced stable hydrophilic coatings with MPC and MPC/DMA formulations. Overall, stainless steel surface modification was enhanced by

the use of the chromium alkoxide bonding agents and has been shown to be of value to enhance adhesion of polymer coatings to metallic medical devices such as endovascular stents or keratome blades.

CHAPTER 4
PULSED LASER ABLATION DEPOSITION (PLAD) AND RF PLASMA
POLYMERIZATION DEPOSITION

Introduction

As discussed in Chapter 3, high energy ionizing radiation has been used for surface modifying various materials under normal ambient conditions of temperature and pressure with the advantages of substrate geometry flexibility and absence of chemical or UV initiators for “clean” modifications. Surface modifications involving high energy sources and which employ vacuum conditions can be used to enhance surface binding by ablation etching and deposition. Two examples of such systems are radio frequency glow discharge plasmas (RF plasma), and pulse laser ablation deposition (PLAD). For both, sample orientation can affect coating uniformity as a result of the directional nature of the depositions.

This chapter discusses research aimed at exploring the potentially unique effectiveness of trivalent chromium metal alkoxide treatments for enhancing the stability of RF plasma and PLAD surface modifications on 316L stainless steel.

Pulsed Laser Ablation Deposition (PLAD)

Pulsed laser ablation deposition (PLAD) modification has been reported for many polymers and semiconductor materials. For example, PLAD has been used for modifying fiber surface properties and curing the resin material.⁵⁸ Of particular, PLAD offers a solvent free method for polymerization and surface modification.

Coating stainless steel with polymers by pulsed laser ablation/deposition (PLAD) for medical devices is a relatively new concept. We have pioneered the use of PLAD for the deposition of cross-linked polymer thin films in this laboratory.⁵⁹

In that research, PLAD was shown to be a feasible technique for coating medical implants.⁵⁹⁻⁶¹ Following the work of Rau et al, silicone elastomer targets were ablated with a pulsed 248 nm KrF excimer laser to form silicone plasma and deposited onto the substrate. Previous research with silica filled silicone indicated increasing surface hydrophilicity of PLAD deposits with increasing fluence (mJ/cm^2 , energy density), especially above a fluence of $200 \text{ mJ}/\text{cm}^2$.⁶⁰ Furthermore, Rau et al observed that smooth low fluence depositions resulted in hydrophobic surfaces similar to that of the target material. Whereas, higher fluences deposited somewhat granular surfaces that were hydrophilic. These experiments were conducted in vacuum environments with higher oxygen contents than the studies presented here.

Pulsed laser ablation deposition is carried out at vacuum pressures at most of 1 Torr with a target mounted on a rotating base. The substrate to be coated is mounted on a stationary fixture. The target absorbs photons emitted from a UV laser source at 248 nm. Atoms at the target surface rise to an electronically excited state. Due to various degrees of excitation, bond rupture and ionization occurs, various species from the target material are emitted forming a plume consisting of the excited ionic and radical fragments. This plume of excited species contacts the substrate, which is positioned as illustrated in Figure 4.1. As the excited plume species contact the substrate, recombination reactions occur with the silicone species and the substrate. The degree to which the coatings are mechanically and chemically bound to the substrate remain unclear.⁶⁰

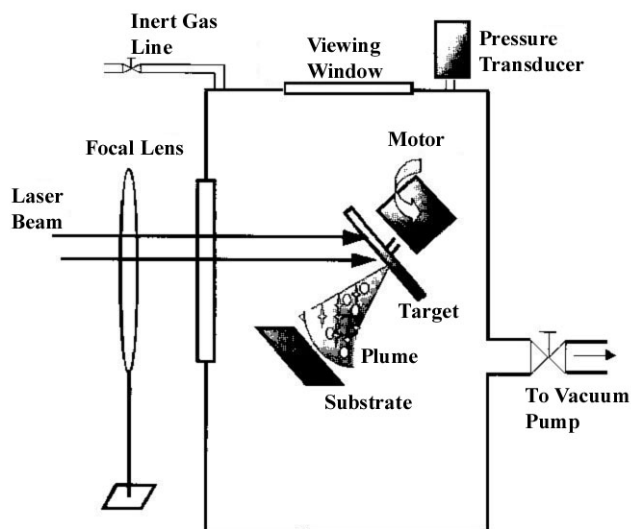


Figure 4.1 – Illustration of PLAD system setup.⁶⁰

In the research reported here, we extended the initial work of Rau et al and investigated PLAD deposition using a biomedical grade poly (dimethylsiloxane), PDMS, containing a nanostructured resin filler (Nusil, MED 6820 A, B). Additionally, these investigations were carried out in a vacuum environment that was more oxygen free than the previous studies. The interesting and different results are reported here.

Materials and Methods

Preparation of silicone targets and substrates

PDMS targets were made from a two part resin system (Nusil, MED 6820 A, B and MED 6210 A, B), where MED 6820 silicone is an FDA approved materials for long-term implants beyond 90 days. 5 mL volumes of each resin component (A and B) were measured and placed into separate syringes. Both syringes were concurrently unloaded into a large container, such as a 600 mL Pyrex beaker, and hand-mixed with a spatula. The beaker containing the uncured silicone was subsequently degassed by vacuum to allow entrapped air to escape the mixture. The uncured silicone mixture was determined to be sufficiently degassed when no visible bubbles were apparent. The mixture was

removed from the vacuum environment and poured onto square acetate sheets that were placed on square glass plates (5" x 5") and degassed a second time, after which glass slides of 1mm thickness were placed on each of the four corners of the square acetate sheets. A second acetate sheet was placed on top of the glass slides followed by another glass plate. The glass slides were slowly pushed toward the center to remove trapped air and control the casting thickness. Finally, the mixture was cured at 60°C for 12 hours resulting in cast silicone sheets of 1 mm thicknesses. Plaques of 1 cm diameter were punched from the sheets and washed in methanol for 2 hours to clean the target surface. The washed plaques were dried under vacuum for 12 hours and mounted on 1 inch diameter aluminum stubs for use as targets. This procedure was used for the silicone formulations, MED 6820 and MED 6210.

Silicon wafers and 316L stainless steel (1 cm x 1 cm x 0.1 mm) were used as substrates for all depositions. Silicon wafers were sequentially sonicated in acetone and methanol then dried under vacuum. Stainless steel substrates were cleaned by sequential sonication in 1,1,1-trichloroethane, chloroform, acetone, methanol, and Ultrapure™ water then dried under vacuum at 60°C for 12 hours. 316L Stainless was used in two ways, untreated and treated with 2% v/v Volan®, which is low chlorine chromium (III) methacrylate metal alkoxide. These procedures are described in detail in Chapter 3.

Pulsed laser ablation deposition chamber

The PLAD system consisted of a vacuum chamber housing both the target and substrate, see Figure 4.1. To ensure uniform ablation, the target was rotated with a motor for every deposition. A KrF excimer laser (Lambda Physik 301x) operating at 248 nm with a pulse width of 25 ns was used in all experiments. The laser beam was directed into the chamber with a pair of plane mirrors and a collimating lens. A 250 mm lens

focused the laser beam onto the target. With all depositions, a base pressure of at least 5.0×10^{-5} mTorr was reached except where noted, after which the chamber was backfilled with helium until a pressure of 100 mTorr was achieved.

The energy density (mJ/cm^2 , fluence) was controlled by adjusting the energy constant of the laser and the focusing lens to get the desired spot size incident on the target. Fluence is calculated by multiplying the energy constant (mJ) with the measured attenuation error, which is then divided by the measured spot size (cm^2). The energy constant is a value that is programmed into the operating system. The attenuation error corresponds to the amount of decreased laser energy due to the lens sequence. Finally, the spot size is obtained by visually measuring the burned spot the laser leaves on thermal sensitive paper. The fluences used in this investigation were in the range of 50-400 mJ/cm^2 . The laser operated at a repetition rate of 5 Hz. The deposition time was 30 minutes, thus the number of laser pulses for each deposition was 9000.

Analysis

Surfaces were characterized by captive air bubble and sessile drop methods with a Ramé-Hart A-100 goniometer, scanning electron microscopy with a JEOL 6400 SEM, fourier-transform infrared (FTIR) with a Nicolet Magna 706 (ZnSe crystal, 45°) and x-ray photoelectron spectroscopy (XPS) analysis with Kratos Analytical Surface Analyzer XSAM 800. The analysis conditions used are described in Chapter 3.

Results and Discussion

Contact angle data are shown in Table 4.1. In contrast to previous PLAD deposition of silica filled PDMS in a chamber containing higher concentrations of oxygen species⁶⁰, the data here indicate that higher fluences result in higher contact angles or decreasing hydrophilicity when resin filled silicone was deposited on untreated 316L

stainless steel. Depositions on chromium (III) methacrylate treated 316L stainless steel resulted in contact angles of $\sim 25^\circ$ for fluences of 125 mJ/cm^2 . Compared to the hydrophobic depositions on untreated 316L stainless steel at fluences of 200 and 400 mJ/cm^2 , coatings on Volan[®] treated 316L stainless steel swelled with water on contact distorting the topography of the deposition. Thus, contact angles were not measurable for these conditions. This is a departure from previous studies conducted in our laboratory, since coating swelling with water has not previously been observed for PLAD treatments.

A difference from the earlier work is that in previous studies the chamber was evacuated to a base pressure of 30 mTorr, whereas the current studies used base pressures of at least 5.0×10^{-5} mTorr, which results in depositions in a more oxygen free environment. In both studies, the chamber was backfilled with helium to 100 mTorr. Contact angles for MED 6820 and MED 6210, which are different from the silica-filled silicones used by Rau et al, depositions on untreated stainless steel using a base pressure of 30 mTorr was conducted to compare the two resin filled materials and verify the hydrophilic results of previously reported studies. The hydrophilicity of MED 6820 and MED 6210 depositions were similar to depositions by Rau et al, where contact angles were $\sim 20^\circ$ at fluences over 200 mJ/cm^2 .

Table 4.1 – Contact angle of MED 6820 depositions at various fluences on untreated 316L stainless steel.

Fluence (mJ/cm^2)	50	75	100	125	200	300	400
Contact Angle	40- 50°	16- 21°	16- 21°	>170°	>170°	>170°	>170°

Analysis of nanosurface modified silicon and untreated 316L stainless steel by FTIR-ATR did not yield measurable peaks for MED 6820 depositions on silicon wafers

at 50-300 mJ/cm². As illustrated in Figure 4.2, small peaks at 1260, 1215-930, and 900-730 cm⁻¹ corresponding to SiMe_x deformation, SiOSi asymmetric stretching (main chain), and Si(CH₂)₃ and Si(CH₂)₂ rocking (chain ends), were evident for depositions at 400 mJ/cm² fluence on silicon wafer. Spectra for depositions on untreated 316L stainless steel did not result in any detectable peaks. FTIR-ATR of MED 6820 depositions on 2% v/v Volan[®] treated 316L stainless steel yielded spectra for fluences of 125, 200 and 400 mJ/cm², which were the fluences investigated for the chromium III methacrylate treatment. Although different in magnitude, the spectras shown in Figures 4.3-4.5 reflect similar peaks compared with 400 mJ/cm² depositions on silicon wafers. While the peak locations are similar to that of MED 6820, the shapes of the peaks are grossly different as a result of shifts in concentrations of bonding structures. This difference could be due to higher concentrations of specific bonding structures deposited such as SiOSi asymmetric stretching as well as sharp increases in rocking chain ends, Si(CH₂)₃ and Si(CH₂)₂. This increase can be attributed to scrambling of the molecular structure in the plume that is then recombined. Recombination is not controlled resulting in a deviation of PLAD deposited silicone compared with unablated silicone.

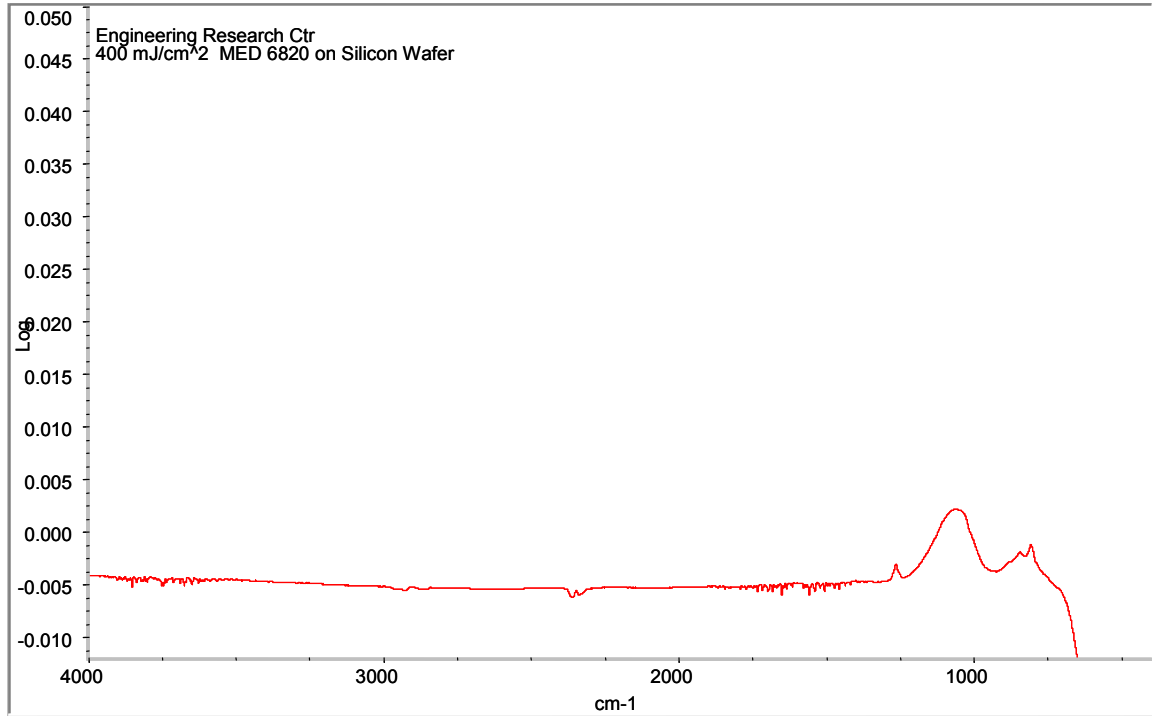


Figure 4.2 – FTIR-ATR spectra of MED 6820 deposited at a fluence of 400 mJ/cm² on silicon wafer.

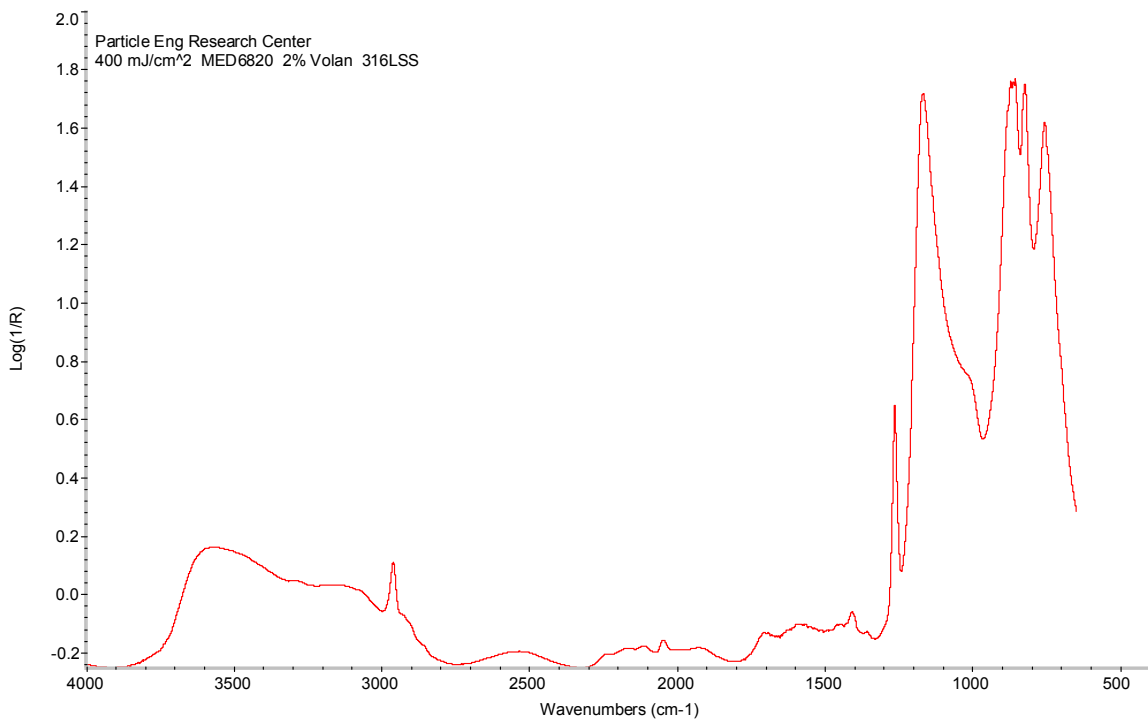


Figure 4.3 – FTIR-ATR spectra of MED 6820 deposited at a fluence of 400 mJ/cm² on 2% Volan treated 316L stainless steel.

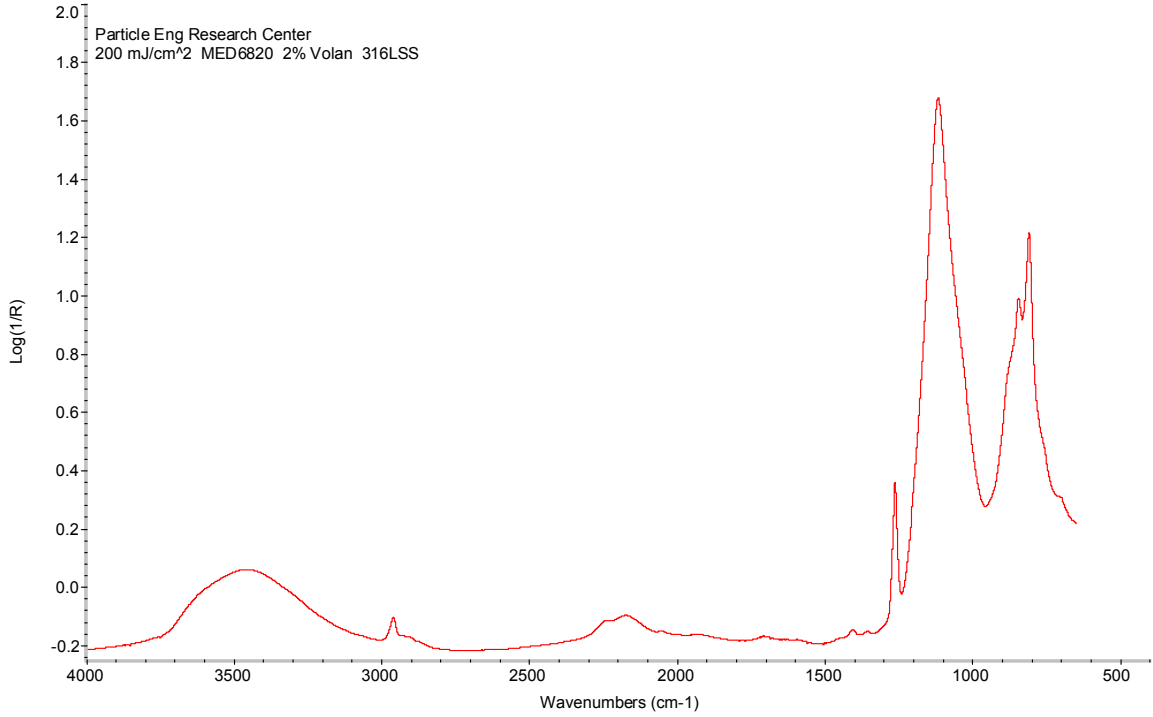


Figure 4.4 – FTIR-ATR spectra of MED 6820 deposited at a fluence of 200 mJ/cm² on 2% Volan treated 316L stainless steel.

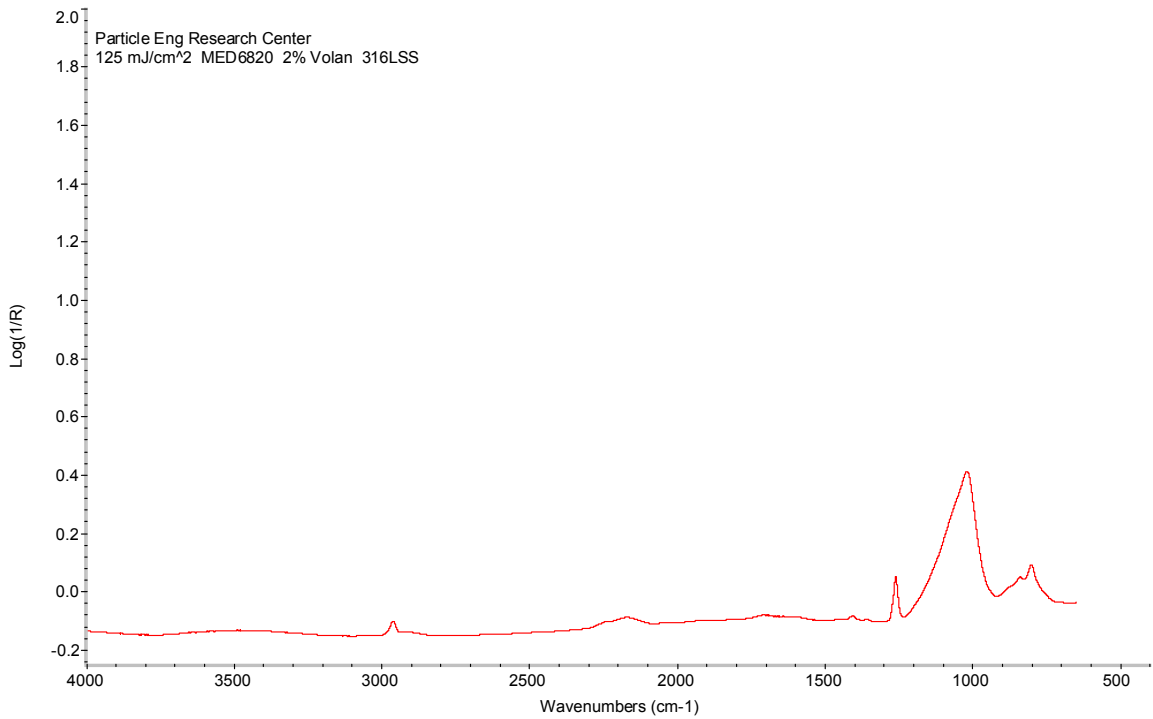


Figure 4.5 – FTIR-ATR spectra of MED 6820 deposited at a fluence of 125 mJ/cm² on 2% Volan treated 316L stainless steel.

Changes in elemental composition of depositions at varying fluences were examined by XPS analysis (Table 4.2 - 4.3). For MED 6820 coated untreated 316L stainless steel, overall oxygen content decreased with increasing fluence levels, while the silicon content increased. The O:Si ratio at low fluences decreased from approximately 2 to 1 at higher fluences. This may indicate that a more silica-like film is deposited at lower fluence, while a more PDMS-like film is deposited at higher fluences on untreated 316L stainless steel.

Table 4.2 – XPS elemental analysis (%) of PLAD coated samples on untreated 316L stainless steel.

Fluence (mJ/cm ²)	Fe2p3	O1s	C1s	Cr2p3	Si2p	O:Si Ratio
PDMS	0.0	25.0	50.0	0.0	25.0	1.0
400	0.0	27.9	41.1	0.1	25.9	1.1
300	0.1	27.2	46.2	0.2	26.3	1.0
200	0.0	29.1	41.2	0.0	29.8	1.0
125	0.0	32.3	38.8	0.0	28.5	1.1
100	0.3	38.8	33.6	0.1	27.2	1.4
75	0.2	39.7	32.2	0.0	27.8	1.4
50	0.8	35.6	43.8	0.8	18.9	1.9
316L SS Control	5.5	36.1	53.2	1.8	3.5	10.4

At 400 mJ/cm² fluences, elemental analysis showed that deposited MED 6820 resin-filled silicone coatings on Volan[®] treated 316L stainless steel exhibited similar elemental concentrations as coatings on untreated stainless steel. However, at lower fluence deposition compositions on Volan[®] treated substrates had higher Si2p and lower O1s concentrations when compared with the untreated 316L stainless steel group. This difference could be due to several factors. While the chamber is under high vacuum, low molecular weight species still exist. The vacuum pump forces these particles to be pushed against the wall of the chamber decreasing the number of particles freely floating in the system. As the target is ablated, reactive fragments are emitted as a plume and

could react with other particles in the system. These reactions may be the source of the reduced O:Si ratio seen for lower fluence deposition conditions on Volan[®] treated 316L stainless steel. The electron withdrawing vinyl groups on the 316L stainless steel surface could preferentially bind with the silicone fragments in the plume, which may be another explanation. It is likely that a combination of both explanations is the reason for this reduced O:Si ratio.

Table 4.3 – XPS elemental analysis (%) of PLAD coated samples on Volan[®] treated 316L stainless steel.

Fluence (mJ/cm ²)	Fe2p3	O1s	C1s	Cr2p3	Si2p	O:Si Ratio
PDMS	0.0	25.0	50.0	0.0	25.0	1.0
400	0.0	25.8	44.6	0.0	29.6	0.9
200	0.0	25.7	35.9	0.0	38.4	0.7
125	0.0	24.0	37.7	0.0	38.2	0.6
316L SS Control	5.5	36.1	53.2	1.8	3.5	10.4

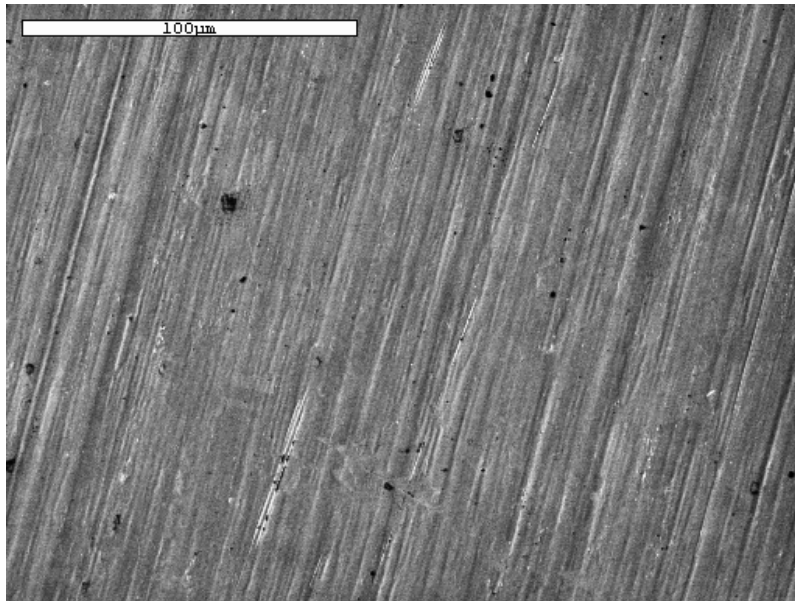


Figure 4.5 – SEM of 316L stainless steel at 500x.

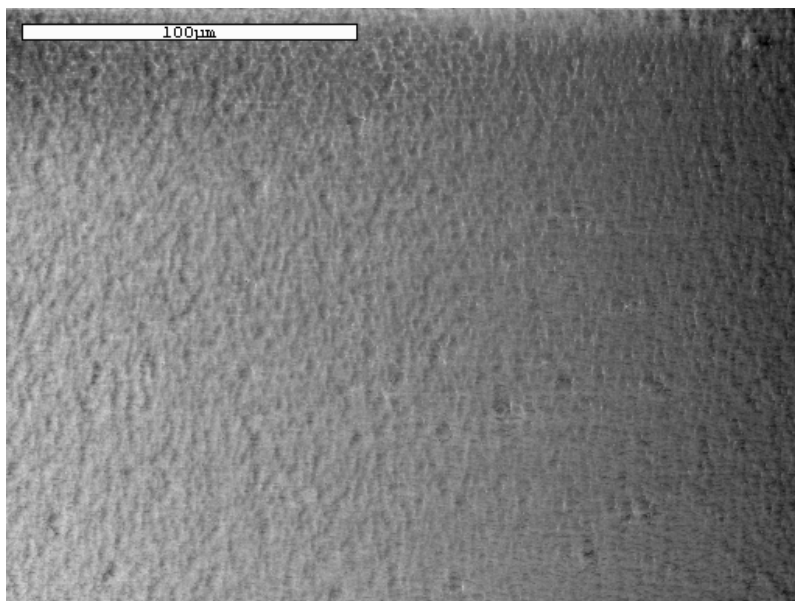


Figure 4.6 – SEM of MED6820 PLAD coated at fluence of 300 mJ/cm^2 onto untreated 316L stainless steel at 500x.

As shown in Figures 4.5-6, analysis with SEM at 500x showed that coatings on untreated 316L stainless steel exhibited granular surface texture at fluences higher than 125 mJ/cm^2 . For coatings deposited at lower fluences, surfaces were fairly smooth in comparison. Depositions on Volan[®] treated 316L stainless steel appeared very smooth. These observations suggest that texture may be an important factor in the wettability of PLAD deposited silicone coatings.

Summary

The results of this investigation indicate a departure from previously published data utilizing the PLAD technique for surface modifying of 316L stainless steel with PDMS. Biomedical grade poly(dimethylsiloxane), (PDMS), containing a nanostructured resin filler (MED 6820), was used here to form stable, uniform silicone-like coatings on chromium III methacrylate (Volan[®]) treated and untreated 316L stainless steel. The coatings exhibited characteristics that were different from previous results with silica reinforced PDMS in that different elemental ratios of O:Si for depositions on Volan[®]

treated and untreated 316L stainless steel at low fluences were achieved. Differences were seen in contact angles from fluences of 125-400 mJ/cm^2 , where silicone depositions on chromium alkoxide treated stainless steel were hydrophilic and depositions on untreated stainless steel were hydrophobic. Furthermore, the silicone depositions on untreated stainless steel from previous studies yielded hydrophilic surfaces at higher fluences such as 200-600 mJ/cm^2 , which was not observed in this study where coatings on untreated stainless steel deposited at high fluences were hydrophobic indicating that surface bonding characteristics are related to laser fluence and chamber oxygen content. This is further supported by FTIR and XPS data. These experiments were conducted in a more rigorously controlled oxygen free system than previously published work. From Table 4.2, the %O decrease with increasing fluence may correspond with a more PDMS-like film that is deposited at higher fluences for coatings on untreated 316L stainless steel. At 400 mJ/cm^2 fluences, depositions on Volan[®] treated 316L stainless steel resulted in PDMS-like thin films. Such PDMS thin films may be useful for drug delivery from surfaces and/or for drug grafting.

RF Plasma Surface Modification

Radio frequency glow discharge plasma (RF plasma) is a surface modification technique involving high energy and vacuum to achieve surface ablation etching and deposition of RF plasma polymerized monomers. This technique is commonly used in industry for surface modification. The technology involves the RF field excitation of gases such as argon, oxygen, solvents, or monomer vapors. The RF field excitation causes the gaseous mass to dissociate creating the plasma of excited species, i.e. radicals, ions, ion radicals. The surface binding and recombination of excited species results in

modification of the substrate surfaces. Typically, substrates are treated one side at a time due to the directional nature of this treatment.

RF plasma has been used successfully in our laboratory to pretreat polymeric and metallic substrates with hexane plasma for subsequent gamma irradiation polymerization.^{57, 62, 63} The hexane plasma deposits a crosslinked carbonaceous layer on the substrate surface. The substrate is then submerged in a monomer solution and irradiated immersed in a monomer solution, thus depositing polymer on the RF plasma/hexane coating. Initial contact angles reported were lower than those of samples treated with either RF Plasma or gamma alone.

Presented here is an investigation of monomer RF plasma polymerization deposition with monomers, NVP, DMA and comonomer, NVP/DMA. The objective was to evaluate Quilon[®] L (chromium III fatty acid) and Volan[®] L (chromium III methacrylate) treated 316L stainless steel substrates. Additionally, a new substrate stage was developed for the purpose of treating both sides of the substrate at the same time by orienting the samples vertically. The results of these studies are reported here.

Materials and Methods

Preparation of substrate, monomers, and comonomer

Substrates of 316L stainless steel (1 cm x 1 cm x 0.1 mm) were cut from a single stock of foil. Stainless steel substrates were cleaned by sequential sonication in 1,1,1-trichloroethane, chloroform, acetone, methanol, and Ultrapure[™] water then dried under vacuum at 60°C for 12 hours. 316L Stainless was used in three ways, untreated and treated with 2% v/v Volan[®] L or Quilon[®] L, which are low chlorine chromium (III) methacrylate and low chlorine chromium (III) fatty acid metal alkoxide. These procedures are described in Chapter 3.

A quantity of 1 ml of each monomer, NVP and DMA, was poured into separate 25 ml long neck round bottom flasks. For comonomer, NVP/DMA, 500 μ L of each monomer was poured into one 25 ml long neck round bottom flask. Before each RF plasma treatment, the monomers and comonomer flasks were degassed by vacuum and attached to the RF plasma apparatus.

Monomer RF plasma

To clean the bell-jar vacuum chamber, it was evacuated to 50 mTorr and purged with argon gas to 1 Torr. This procedure was repeated five times, after which the flow rate of argon gas was reduced and the RF plasma controller was turned on with a power of 50 Watts (incident) and 0 Watts (reflected). The RF plasma was allowed to run for 5 minutes thoroughly clean the bell-jar and components. Once this was finished, the flow of argon gas was closed and the bell-jar pressure was returned to ambient conditions.

Treated substrates were oriented vertically on a custom designed sample stage. Three treatment groups were included with each run, untreated, Quilon[®] L, and Volan[®] L treated 316L stainless steel. For each experimental run, one flask containing 1 mL of either monomer or comonomer of NVP and DMA were attached to the RF plasma apparatus. The treatment followed the same procedure as described above, except after the last evacuation to 50 mTorr, the bell-jar was backfilled by leaking in volatized monomer or comonomer to 100 mTorr. After this operating pressure was reached, the RF plasma controller was turned on at the same power as previously described and operated for either 5 or 10 minutes. After the RF plasma was turned off, the chamber was further purged with monomer for 2 minutes to allow for further polymer conversion and reaction with surface radicals. Finally, the chamber was purged with argon gas to 1 Torr two times before returning the bell-jar pressure to ambient pressure of 760 Torr.

Following treatment, substrates were submerged in Ultrapure™ water to wash and await analysis.

Analysis

RF plasma treated surfaces were characterized by captive air bubble and sessile drop methods with a Ramé-Hart A-100 goniometer, SEM with a JEOL 6400, FTIR with a Nicolet Magna 706 (ZnSe crystal, 45°) and XPS analysis with Kratos Analytical Surface Analyzer XSAM 800 under the same operating conditions as described in Chapter 3.

Results and Discussion

As shown in Figures 4.7- 4.9, initial contact angles measured prior to drying, were hydrophilic and approximately 20° in all cases. Additionally, both sides of the flat substrates were measured indicating uniform modifications substrate surfaces. No differences were seen between 5 and 10 minute monomer RF plasma treatments. To determine treatment stability, modified substrates were dehydrated under vacuum, then rehydrated for 24 hours in Ultrapure™ water and rehydrated contact angles were recorded for both sides of each sample. As the data shows in Figures 4.10- 4.12, initial hydrophilicity of monomer RF plasma modifications was not reflected in measurements after rehydration. However, some samples only lost a fraction of hydrophilicity as shown by the rehydrated DMA RF plasma on Quilon® L treated 316L stainless steel of the 10 minute treatment and on Volan® L treated 316L stainless steel of the 5 minute treatment. Once again, measurements were consistent for both sides of the sample. The differences seen in initial and rehydrated contact angle data are likely due to condensation of surface species when dehydrated.

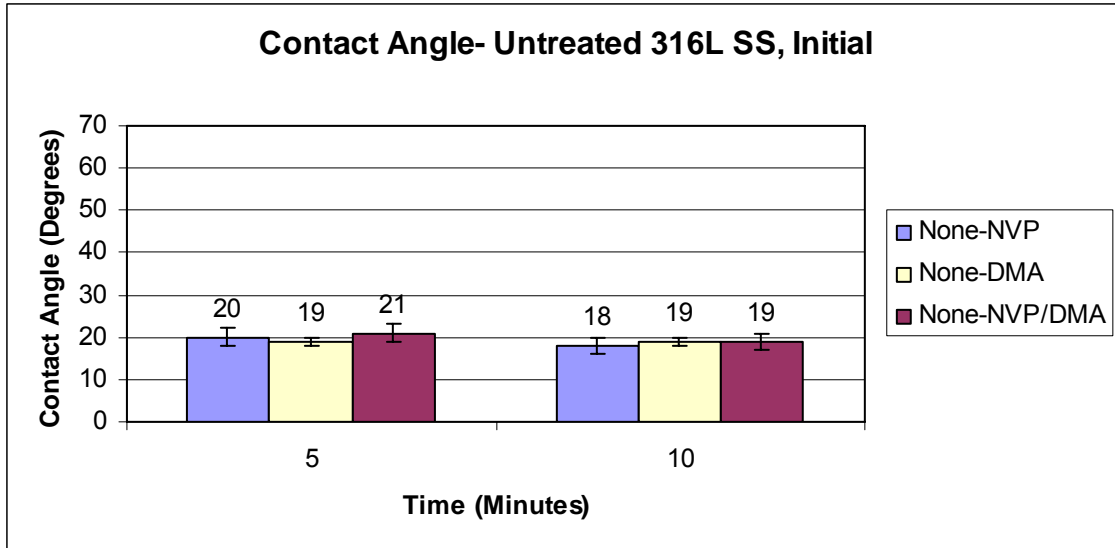


Figure 4.7 – Initial contact angle measurements for NVP, DMA and NVP/DMA RF plasma surface modifications on untreated 316L stainless steel.

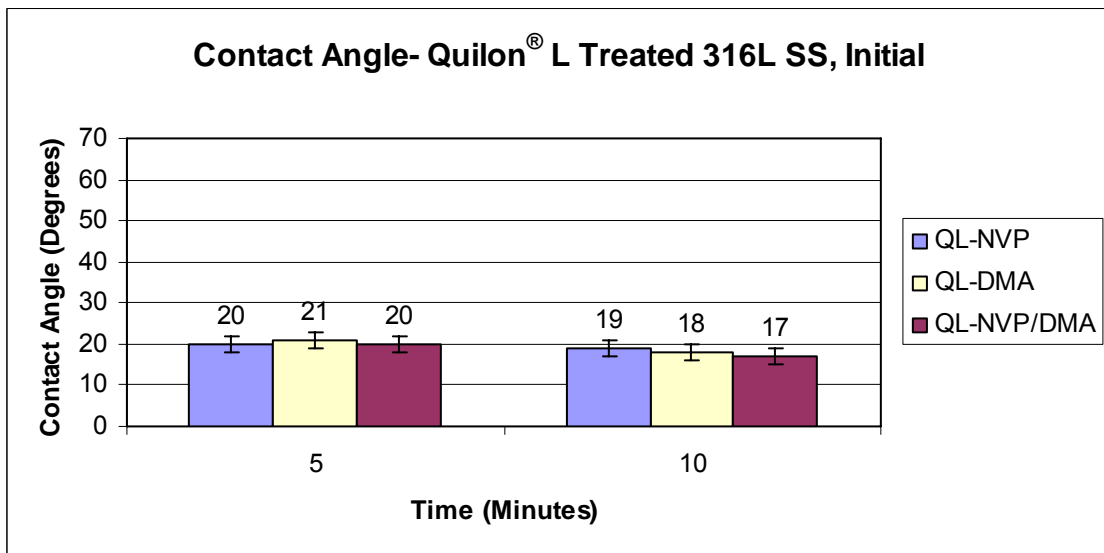


Figure 4.8 – Initial contact angle measurements for NVP, DMA and NVP/DMA RF plasma surface modifications on 2% v/v Quilon[®] L treated 316L stainless steel.

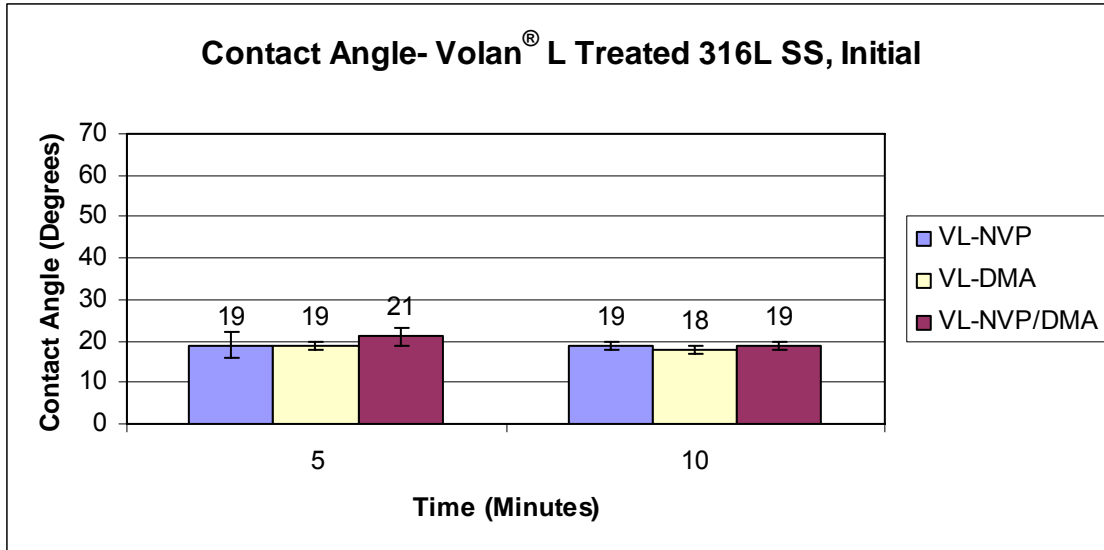


Figure 4.9 – Initial contact angle measurements for NVP, DMA and NVP/DMA RF plasma surface modifications on 2% v/v Volan[®] L treated 316L stainless steel.

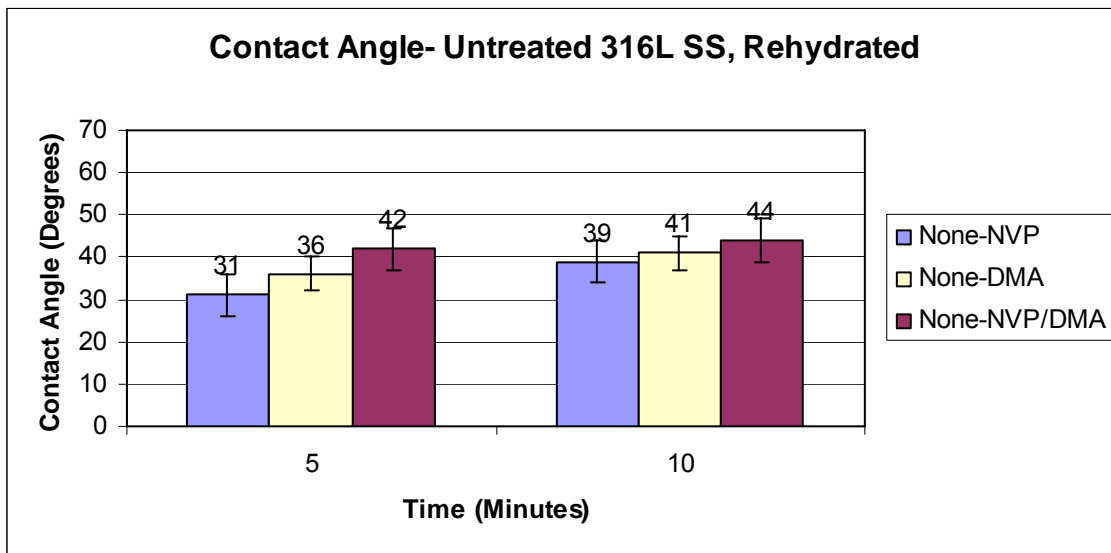


Figure 4.10 – Rehydrated contact angle measurements for NVP, DMA and NVP/DMA RF plasma surface modifications on untreated 316L stainless steel.

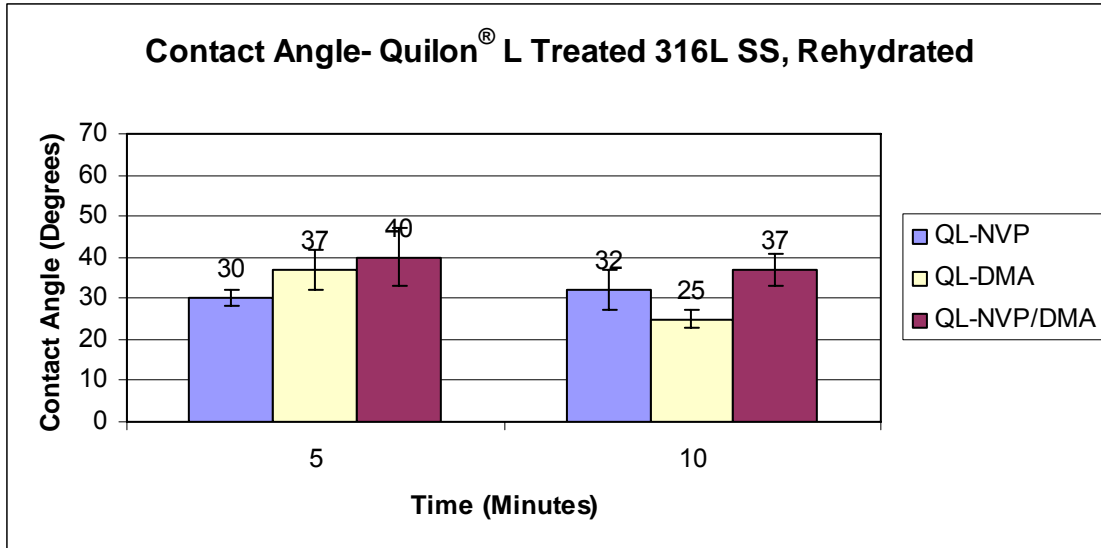


Figure 4.11 – Rehydrated contact angle measurements for NVP, DMA and NVP/DMA RF plasma surface modifications on 2% v/v Quilon[®] L treated 316L stainless steel.

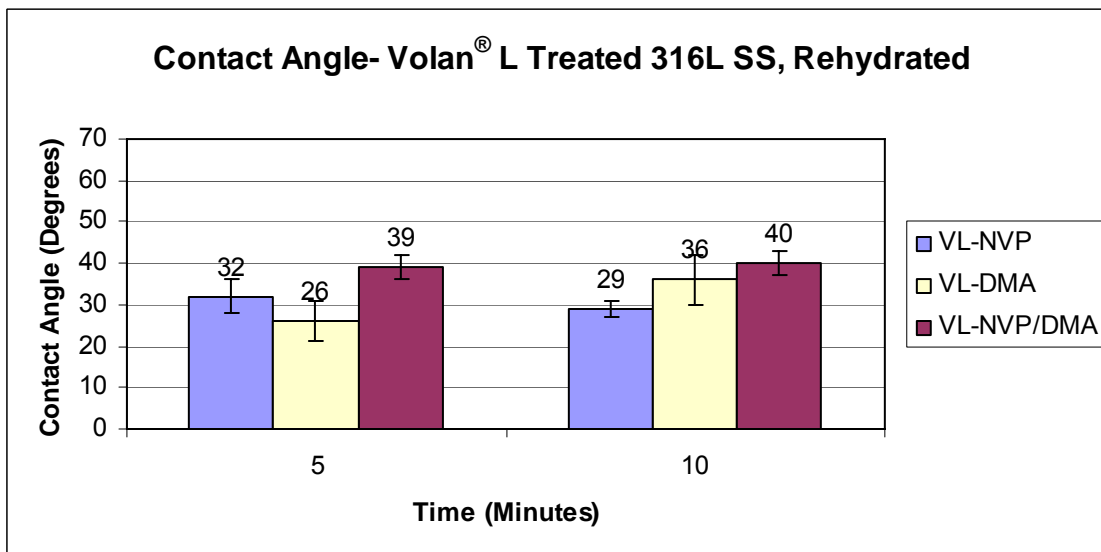


Figure 4.12 – Rehydrated contact angle measurements for NVP, DMA and NVP/DMA RF plasma surface modifications on 2% v/v Volan[®] L treated 316L stainless steel.

FTIR-ATR analysis did not yield discernable peaks for any conditions examined in this study. This is likely due to low surface concentrations of treatment since RF plasma modifications typically result in thin treatments.

XPS analysis of monomer RF plasma treated substrates showed N1s peaks for all conditions in the range of 1.8 to 3.6% when evaluated with C1s, O1s, Fe2p3, Cr2p3 and Cl2p elemental concentrations. The detected N1s peaks correspond to the nitrogen atoms of NVP, DMA, or NVP/DMA depositions. Unmodified untreated 316L stainless steel did not exhibit discernable N1s peaks. Increase in C1s was seen for all Quilon[®] L treated 316L stainless steel. This is likely due to polymerization or crosslinking of the fatty acid pendant groups on the chromium alkoxide treatment. The only difference seen by this analysis between the 5 and 10 minute RF Plasma modifications are reduced Cl2p concentrations for 10 minute treatments.

Table 4.4 – XPS elemental analysis (%) of 5 minute monomer RF plasma modification of untreated, Volan[®] L and Quilon[®] L treated 316L stainless steel.

	C1s	O1s	N1s	Fe2p3	Cr2p3	Cl2p
Unmodified, Untreated 316L SS	48.2	42.3	< 0.1	7.9	1.2	0.0
NVP - Untreated 316L SS	48.9	37.8	3.5	3.5	4.0	2.3
NVP – Volan [®] L Treated 316L SS	52.0	36.0	3.4	2.9	3.5	2.2
NVP – Quilon [®] L Treated 316L SS	60.9	30.0	3.2	1.2	2.8	1.8
DMA – Untreated 316L SS	51.5	37.6	3.3	3.7	1.9	1.9
DMA – Volan [®] L Treated 316L SS	50.8	39.1	2.2	2.9	2.4	2.9
DMA - Quilon [®] L Treated 316L SS	60.5	32.2	2.3	1.6	0.4	2.7
NVP/DMA - Untreated 316L SS	49.1	41.4	1.9	3.9	1.8	1.9
NVP/DMA – Volan [®] L Treated 316L SS	53.2	28.4	2.7	2.4	3.9	2.9
NVP/DMA – Quilon [®] L Treated 316L SS	63.3	34.9	1.8	0.9	2.5	3.2

Topography changes due to surface modifications were not evident in SEM micrographs. Surface modifications may be ~2 - 20 atomic layers in depth based on elemental analysis depth of penetration limitations. SEM micrographs did not show any evidence of corrosion these surface modifications.

Summary

In the current studies, elemental analysis showed the presence of nitrogen species that correspond to the monomer species from RF plasma treatments. Yet, these surface

modifications did not yield stable hydrophilic coatings after drying and rehydration. Orienting the samples vertically with a new substrate stage was shown to consistently treat both sides of the substrates.

While the use of chromium based metal alkoxides did not appear to enhance the stability of monomer RF plasma surface modifications, initial contact angle measurements were very hydrophilic and surfaces appeared lubricious prior to drying. This technology may be useful for single use applications that do not require drying.

In our laboratory, hexane RF plasma treatments on metals have been used as a primer for gamma initiated surface modifications by creating a carbonaceous surface layer. Functionalizing 316L stainless steel with metal alkoxide treatments will prime the surface in a simplified one step process. These functionalized metals can be further modified in a variety of ways including gamma initiated grafting and solution coating.

CHAPTER 5 SOLUTION POLYMERIZATION COATING SURFACE MODIFICATION

Introduction

A number of common coating techniques with polymer solutions are used extensively for industrial applications, i.e. dip coating, spray coating, and film casting. These techniques are also used with polymers that are solubilized in a solvent or melt coated above their melting temperature.⁶⁴ Dip coating, spray coating and film casting techniques do not ensure bonding at the coating-substrate interface and typically result in coatings that are merely adsorbed to the substrate unless coupling agents or other priming systems are employed. The focus of this chapter will be polymerizations of monomers in the presence of a solvent and the substrate surface. This research evaluates the effectiveness of trivalent chromium methacrylate, Volan[®] L, to enhance the binding and stability of hydrophilic and hydrophobic polymers onto 316L stainless steel by solution polymerization coating.

In Chapter 3, substrates were soaked in monomer-solvent solutions that were subsequently treated with high energy ionizing radiation to initiate the polymerization and grafting of chains to functionalized surfaces. In the solution polymerization coating studies discussed here, polymerization was initiated by the addition of azobisisobutyronitrile (AIBN) initiator and controlling the temperature of the reaction environment. Medical grade silicone was also evaluated with this coating technique. The addition of AIBN to these silicone solution studies was not necessary, due to the presence of a catalyst for the two component silicone system.

Materials and Methods

Preparation and Treatment of 316L Stainless Steel Substrates

Stainless steel substrates (1 cm x 1 cm 0.1 mm) were cleaned by sequential sonication with 1,1,1-trichloroethane, chloroform, acetone, methanol, and Ultrapure™ water, after which the substrates. After which, the samples were placed in a vacuum oven at 60°C. Cleaned substrates were washed in a 2 % (v/v) solution of Volan® L, which is a chromium (III) methacrylate, with water at room temperature for 10 minutes while agitating. After washing, treated substrates were removed from the solution and air dried for 2 hours. These procedures are described in detail in Chapter 3. Substrates were coated as described below.

Controls consisted of untreated 316L stainless steel that underwent solution polymerization coating and substrates that received no chromium alkoxide treatment or solution polymerization coating.

Preparation of Monomer Solutions

The monomers used in this study were 2-methacryloyloxyethyl phosphorylcholine (MPC; Dr. Ishihara, University of Tokyo), N-vinyl-2-pyrrolidone (NVP; Polysciences, Inc), and potassium 3-sulfopropyl acrylate (KSPA; Raschig GmbH). MPC, NVP and KSPA monomer stock solutions of 10% v/v concentrations were prepared with 0.125% v/v AIBN initiator and Ultrapure™ water. A higher MPC and NVP monomer solution concentration of 25% v/v was also evaluated with the same concentration of initiator. A solution volume of 3 ml was used for each substrate.

Preparation of Silicone Component Solutions

Solutions of 45% v/v Nusil Med 6820 silicone oligomers components A and B with chloroform were prepared of the same volume. A 0.75 ml volume of each solution of

components A and B were placed in glass test tubes for each condition and mixed thoroughly resulting in 1.5 ml of both components A and B with chloroform to treat each substrate. A single cleaned and Volan[®] L treated 316L stainless steel substrate was placed into each test tube and soaked in the silicone solution for 2 hours while rotating, after which the samples were transferred to clean test tubes and cured at 60°C for 12 hours.

Solution Polymerization (SP) Coating of Substrates

Chromium (III) methacrylate treated 316L stainless steel substrates were transferred to test tubes containing aqueous solutions of either 10% v/v, 25% v/v of NVP, MPC, or KSPA monomer with Ultrapure[™] water or 45% MED 6820 oligomers with chloroform. The solutions were then bubbled and backfilled with argon gas. The specimens in monomer solutions were placed in an oven that was heated to a minimum of 70°C and a maximum of 76°C for ~6 hours. After coating, samples were placed in new test tubes and tumble washed for one week with 5 mL of Ultrapure[™] water, which was decanted and replaced three times with 5 mL. Specimens in MED 6820 silicone oligomers solutions were treated as described in the previous section of this chapter. In short, functionalized substrates were dipped into diluted solutions of uncured silicone components and subsequently heated to cure, which has been shown to be effective for coating silane coupling agent treated stainless steel with silicone.³⁹

Analysis

Wettability of coatings was characterized by sessile drop and captive air bubble contact angle goniometry data using a Ramé-Hart A-100 Goniometer. Surface chemistry of modified substrates was characterized with Fourier Transform Infrared - Attenuated Total Reflectance Spectroscopy (FTIR-ATR) using a Nicolet Magna[™] 706 FTIR, and

elemental composition was analyzed by X-ray photoelectron spectroscopy (XPS) with a Kratos XSAM 800, all under the same conditions as described in Chapter 3. The contact angles for unmodified 316L stainless steel and unmodified resin-cast MED 6820 silicone are approximately 50° and 90°, respectively.

Results and Discussion

From initial contact angle data shown in Figures 5.1 – 5.2, differences in wettability were seen for 25% v/v NVP solution polymerization (SP) coatings when comparing untreated and Volan[®] L treated 316L stainless steel, in that Volan[®] L treated 316L stainless steel exhibited increased wettability. This was not observed for the 10% v/v NVP solution concentrations possibly due to kinetics associated with the reduction in the amount of reactive species in solution. In contrast, contact angles of ~ 20° were observed for MPC solution coating on untreated and Volan[®] L treated 316L stainless steel for both concentrations, which can be attributed to the amphoteric structure of MPC causing increased adsorption onto the substrate.

As shown in Figures 5.3 – 5.4, contact angle measurements taken immediately after dehydration under vacuum for 24 hours indicated that Volan[®] L treatments maintained the hydrophilicity of coatings with little recovery time. Furthermore, these specimens were lubricious to the touch. Surfaces treated with Volan[®] L and SP coated in NVP and KSPA retained contact angles less than 26° following dehydration. The dehydration process affected coated surfaces that were not treated with Volan[®] L such that contact angles increased beyond 30°, which was a similar observation to gamma irradiation grafting studies. While exhibiting increased wettability compared with other solution coatings and unmodified 316L stainless steel, MPC coatings did not yield measurable differences for the concentrations and substrate treatment conditions investigated here.

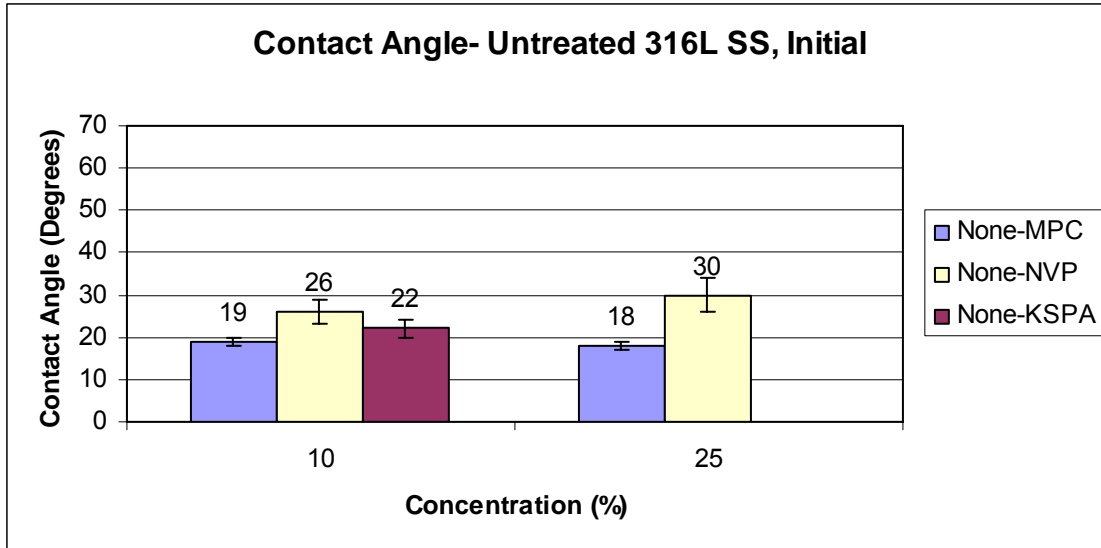


Figure 5.1 – Initial contact angle measurements for 10% and 25% v/v monomer SP coated untreated 316L stainless steel.

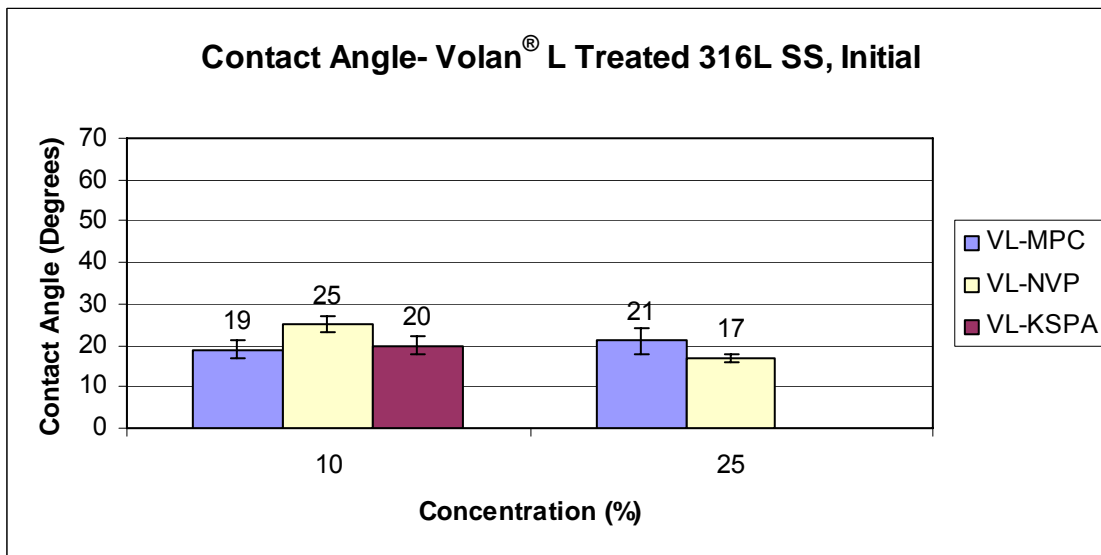


Figure 5.2 – Initial contact angle measurements for 10% and 25% v/v monomer SP coated Volan[®] L treated 316L stainless steel.

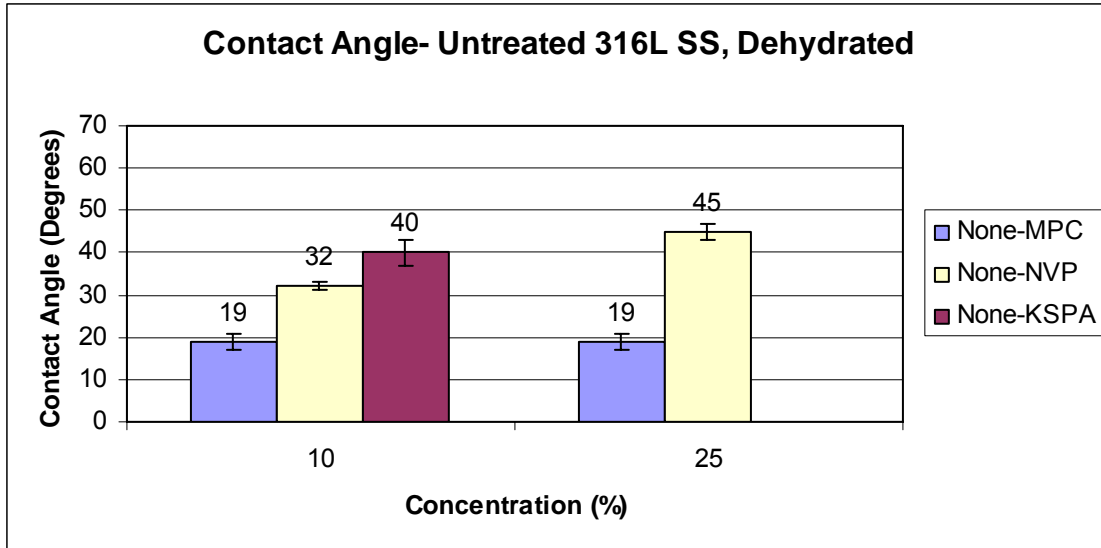


Figure 5.3 – Contact angle measurements immediately after dehydration for 10% and 25% v/v monomer SP coated untreated 316L stainless steel.

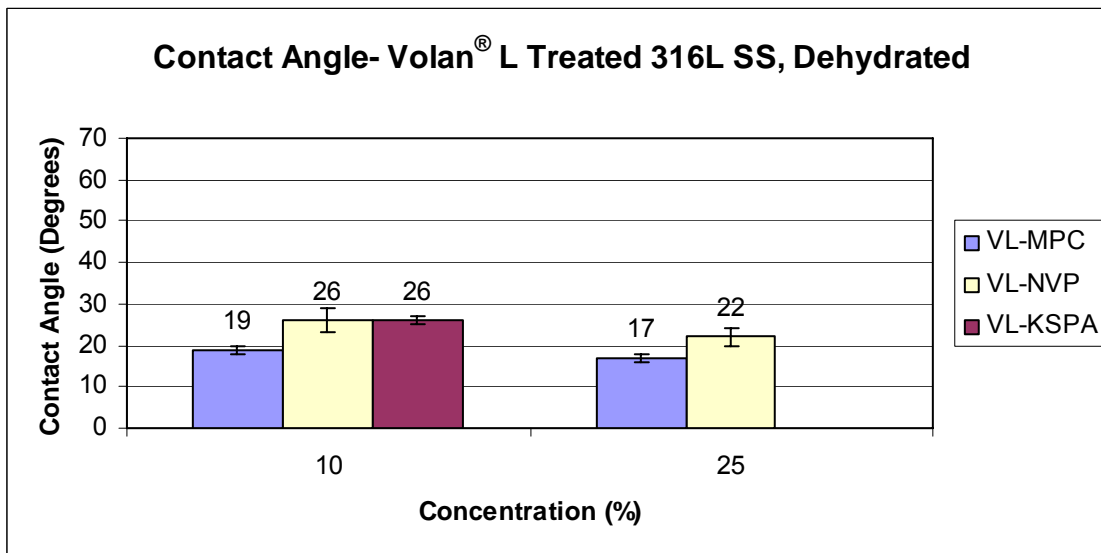


Figure 5.4 – Contact angle measurements immediately after dehydration for 10% and 25% v/v monomer SP coated Volan[®] L treated 316L stainless steel.

After rehydration, NVP and KSPA SP coatings on untreated 316L stainless steel did not recover initial wettability, see Figures 5.5 - 5.6. With the Volan[®] L treatment, hydrophilicity was recovered for 25% v/v NVP SP coatings, but not for the 10% v/v concentrations (Figures 5.7 5.8). Once again, this is believed to be associated with reduced quantity of reactive species for the 10% v/v NVP solution. MPC SP coatings

maintained initial wettability throughout these stability tests for all conditions as presented in Figures 5.9 - 5.10. As shown in Figures 5.11 - 5.12, KSPA SP coatings on Volan[®] L treated 316L stainless steel resulted in consistently low contact angles, which was not observed for the untreated stainless steel group.

MED 6820 SP coatings on untreated 316L stainless steel exhibited contact angle measurements of $\sim 104^\circ$. Measurements of these silicone coatings on Volan[®] L treated substrates were $\sim 94^\circ$, which was similar to unmodified MED 6820 substrates of $\sim 90^\circ$.

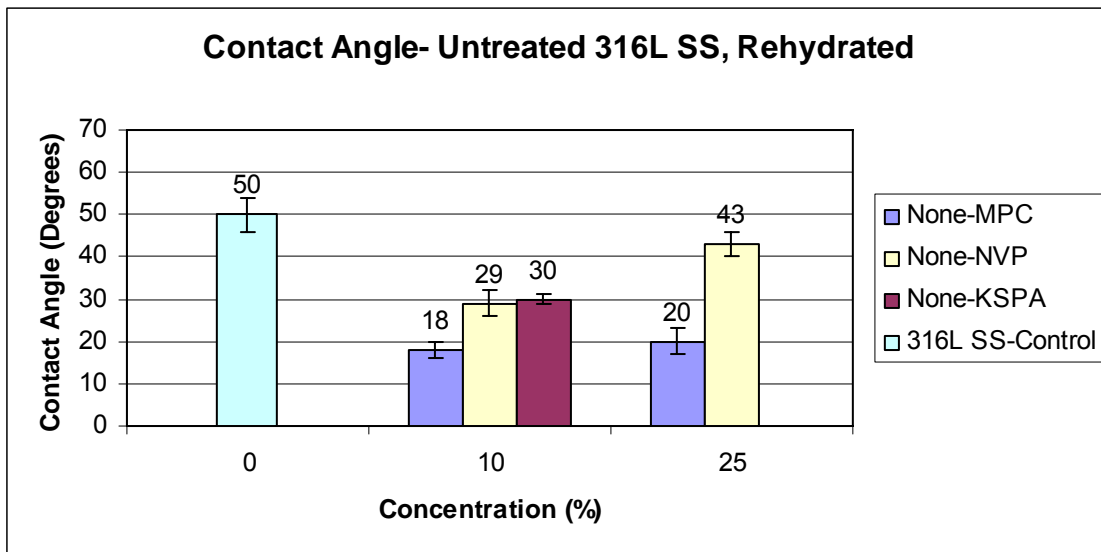


Figure 5.5 – Rehydrated contact angle measurements for 10% and 25% v/v monomer SP coated untreated 316L stainless steel.

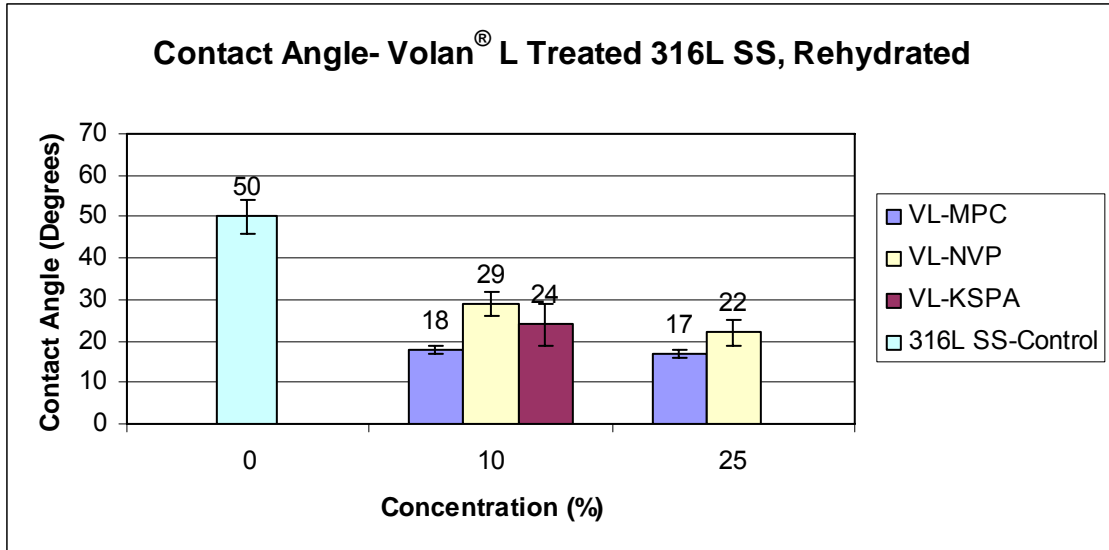


Figure 5.6 – Rehydrated contact angle measurements for 10% and 25% v/v monomer solution coated Volan[®] L treated 316L stainless steel.

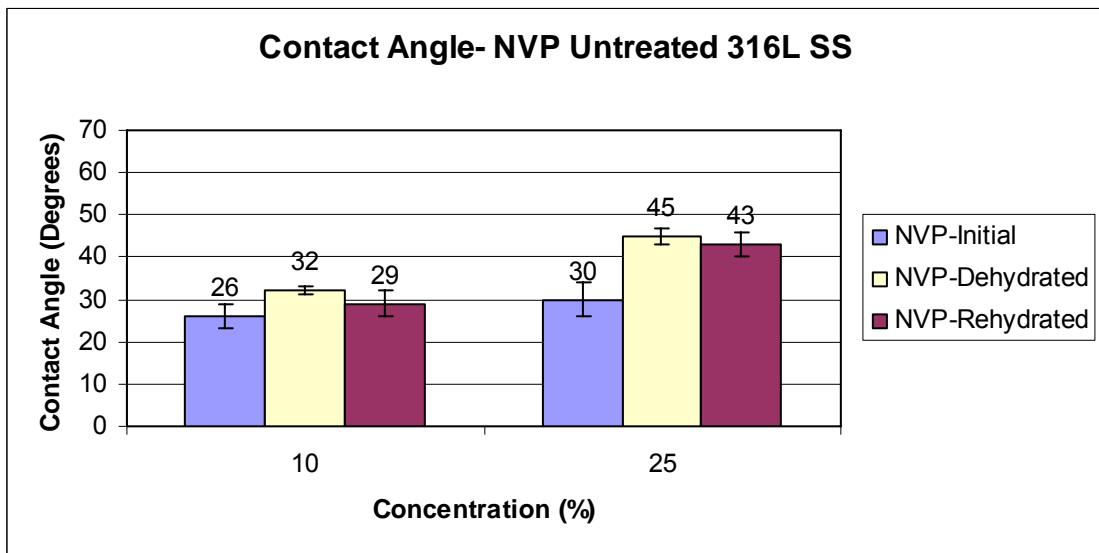


Figure 5.7 – Contact angle measurements for 10% and 25% v/v NVP SP coated untreated 316L stainless steel.

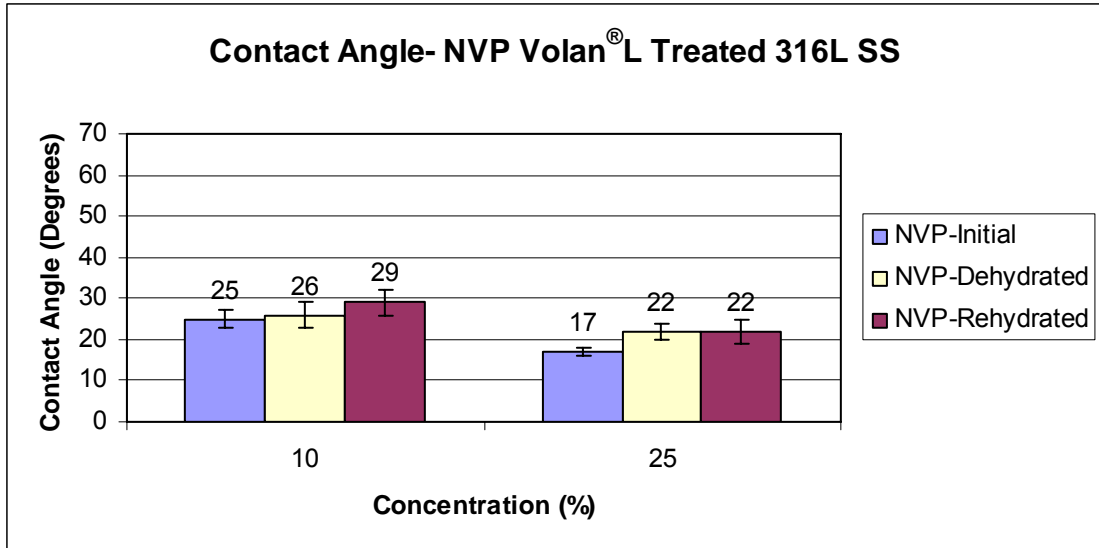


Figure 5.8 – Contact angle measurements for 10% and 25% v/v NVP SP coated Volan[®] L treated 316L stainless steel.

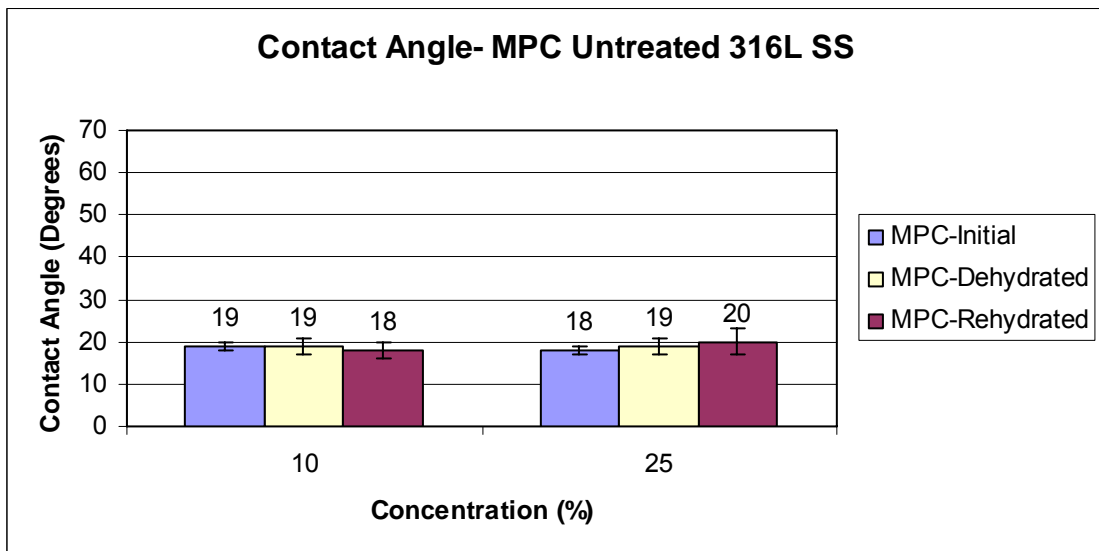


Figure 5.9 – Contact angle measurements for 10% and 25% v/v MPC SP coated untreated 316L stainless steel.

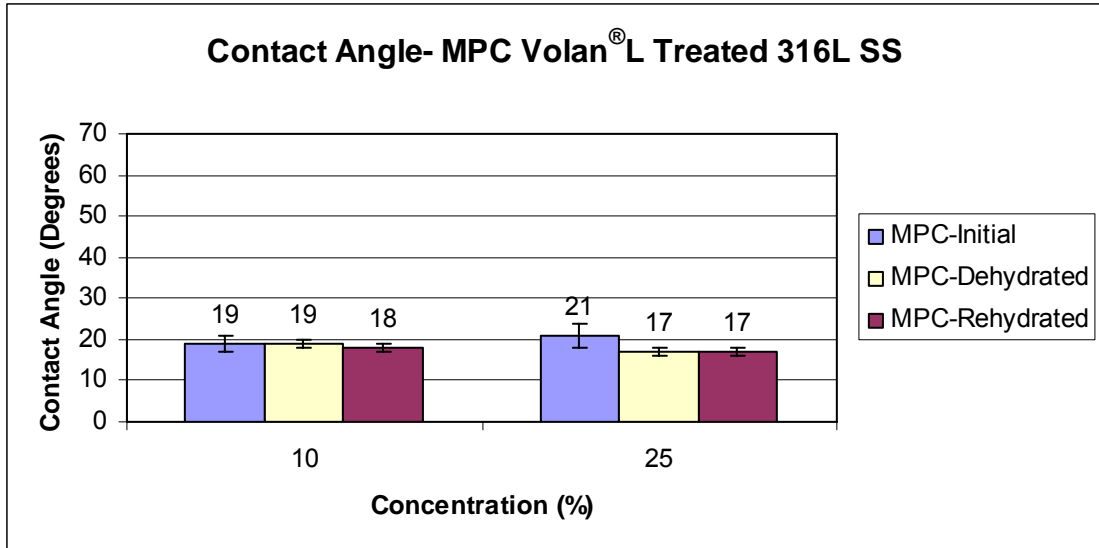


Figure 5.10 – Contact angle measurements for 10% and 25% v/v MPC SP coated Volan[®] L treated 316L stainless steel.

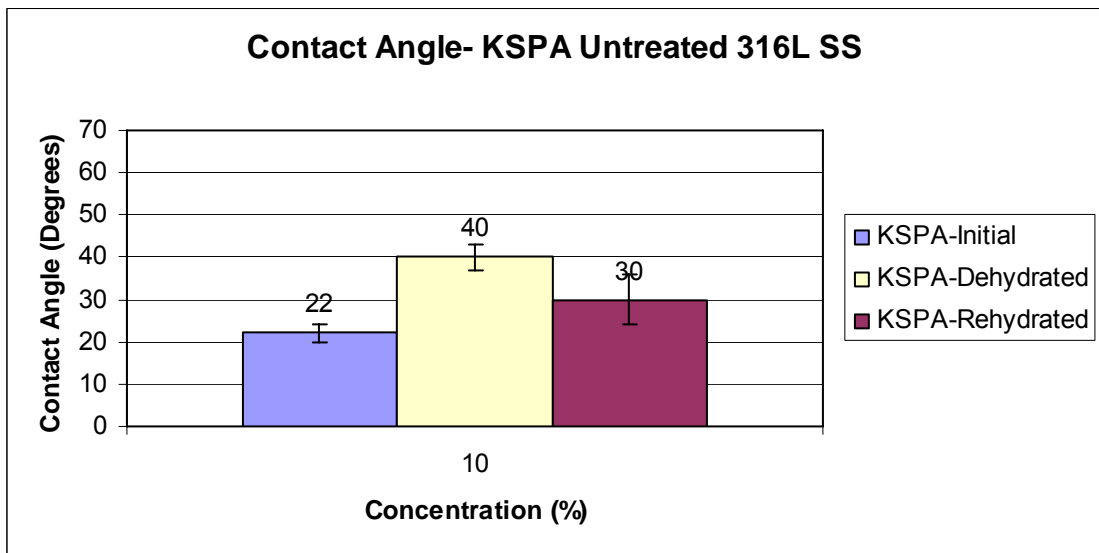


Figure 5.11 – Contact angle measurements for 10% v/v KSPA SP coated untreated 316L stainless steel.

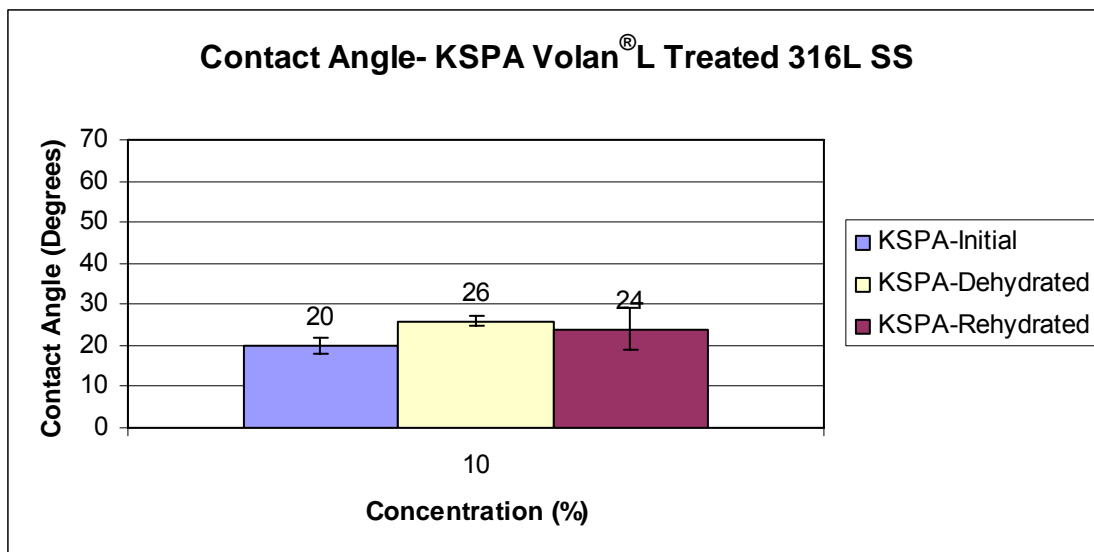


Figure 5.12 – Contact angle measurements for 10% v/v KSPA SP coated Volan[®] L treated 316L stainless steel.

FTIR measurements were carried out on all samples and controls. The polymer coatings did not yield detectable peaks. FTIR-ATR analysis was useful for evaluation of silicone coatings. The spectra of these SP coated samples compared to spectra of cast silicone slabs may exhibit some spectral differences. Since the MED 6820 silicone has resin reinforced filler; SP coating may change the resin content due to possible dissolution. Compared against unmodified cast silicone substrates, shifts were detected in chain end ($\text{Si}(\text{CH}_2)_3$ and $\text{Si}(\text{CH}_2)_2$ rocking) and main chain (SiOSi asymmetric stretching) peaks ($1215\text{-}930$ and $900\text{-}730\text{ cm}^{-1}$, respectively) for both stainless steel coatings. No differences between MED 6820 solution coatings were observed comparing untreated and Volan[®] L treated 316L stainless steel.

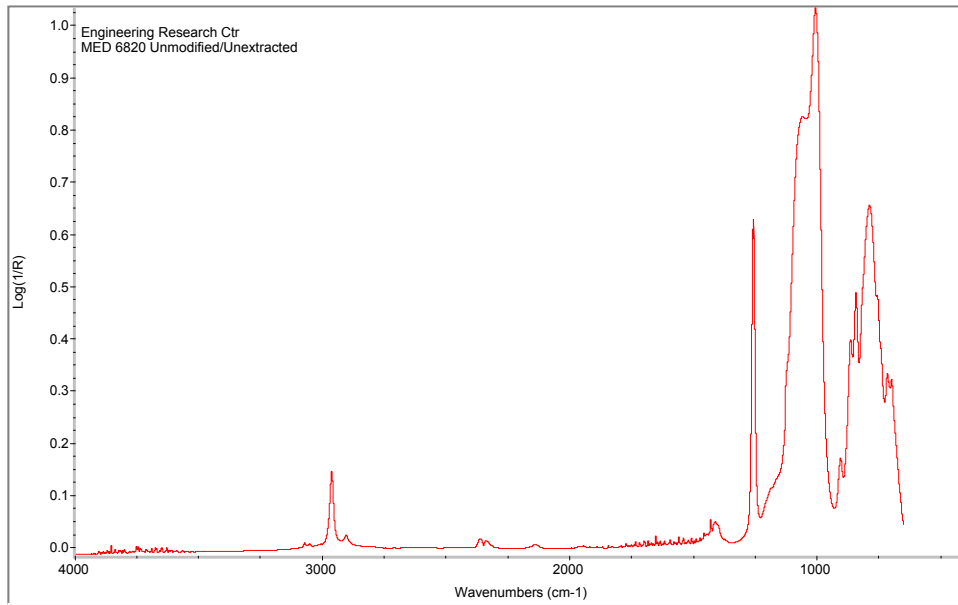


Figure 5.13 – FTIR-ATR spectra of MED 6820 medical grade silicone.

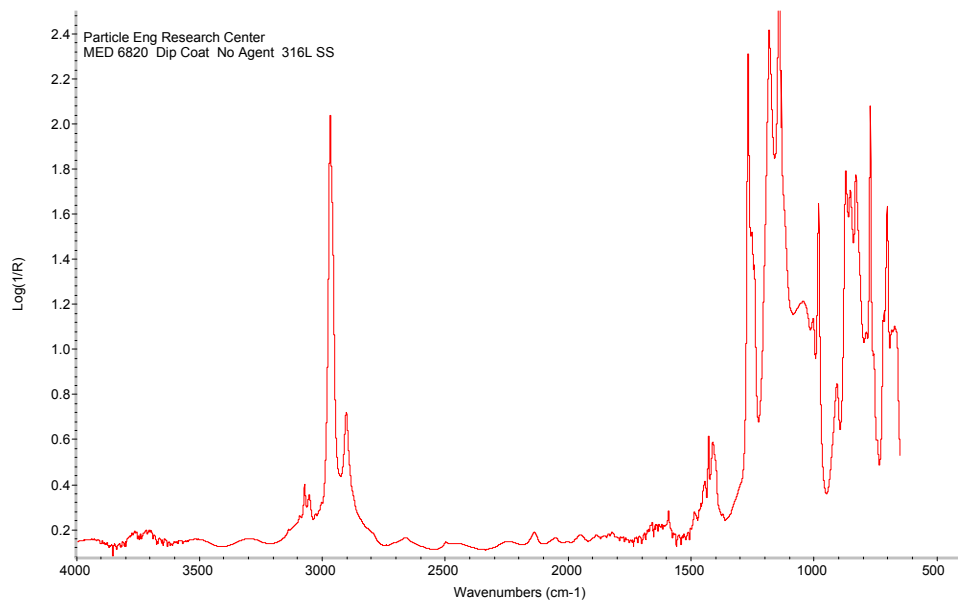


Figure 5.14 – FTIR-ATR spectra of MED 6820 SP coated untreated 316L stainless steel.

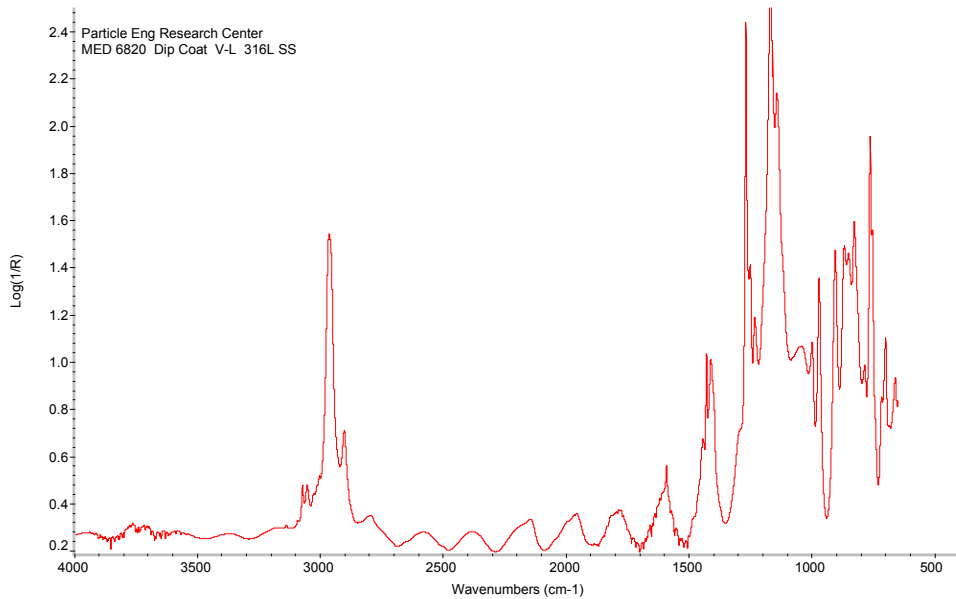


Figure 5.15 – FTIR-ATR spectra of MED 6820 SP coating on Volan[®] L treated 316L stainless steel.

XPS analysis was used to evaluate the SP coatings for elemental surface concentrations and possible shifting of binding energies associated with bonding changes. Substrates treated with Volan[®] L and coated in either 10 or 25% v/v MPC solutions exhibited P2p/N1s peak ratios in the range of ~ 1.5 for coatings on functionalized stainless steel and ~ 2.0 on untreated stainless steel. These treatment groups also showed reduced signal from Fe2p₃ and Cr2p₃, as well as no detectable shifting of the C1s peak indicating coverage of the stainless steel as shown in Table 5.1. NVP solution coatings exhibited N1s peaks, but 10% v/v treatments resulted in noticeable concentrations of Fe2p₃ and Cr2p₃ signals suggesting either a heterogeneous or very thin coating. SP coating solutions of 25% v/v NVP yielded lower concentrations of the surface metals; hence better coverage. Elemental analysis did not detect the stainless steel surface metals for the silicone coatings due to the thickness ($> 1 \mu\text{m}$) for these SP coatings.

Table 5.1 – XPS analysis of SP coated Volan[®] L and untreated 316L stainless steel.

	C1s	O1s	N1s	Fe2p3	Cr2p3	P2p	S2p3	K2p3	Si2p3
10% NVP – Untreated SS	50.0	37.8	4.3	3.9	3.9	-	-	-	-
10% NVP – Volan [®] L Treated SS	57.5	31.3	4.3	2.6	4.3	-	-	-	-
25% NVP – Untreated SS	67.0	24.9	3.6	1.9	2.4	-	-	-	-
25% NVP - Volan [®] L Treated SS	70.4	22.2	4.3	1.3	1.8	-	-	-	-
10% MPC – Untreated SS	63.5	23.9	3.9	0.4	0.4	7.7	-	-	-
10% MPC – Volan [®] L Treated SS	66.1	22.1	4.7	0.1	0.4	6.6	-	-	-
25% MPC – Untreated SS	64.4	22.3	3.0	0.4	0.3	9.7	-	-	-
25% MPC - Volan [®] L Treated SS	70.1	20.2	3.1	0.0	0.3	6.3	-	-	-
10% KSPA – Untreated SS	49.7	37.8	-	4.4	5.9	-	2.2	0.0	-
10% KSPA – Volan [®] L Treated SS	54.4	35.4	-	2.3	5.5	-	2.3	0.0	-
MED6820 – Untreated SS	46.3	20.6	-	0.0	0.6	-	-	-	32.6
MED6820 - Volan [®] L Treated SS	46.2	19.5	-	0.0	0.0	-	-	-	34.4

SEM micrographs indicated that surface modifications were thin and much of the 316L topography was discernable. XPS analysis suggests that SP coating with hydrophilic monomer resulted in surface modifications that are likely to be ~2 - 20 atomic layers in depth. SEM micrographs did not show any evidence of corrosion for SP coatings.

Summary

Stable, hydrophilic coatings were prepared using an *in situ* solution polymerization coating system. MPC based coatings were very hydrophilic for all conditions. However, 25% v/v NVP SP coatings on Volan[®] L treated 316L stainless were more stable and lubricious to the touch than other NVP treatments explored in this investigation. Concentration did not appear to affect MPC based coating, but did seem to be a factor for NVP based coatings. Hydrophilic stability of KSPA SP coatings, studied in the 10% v/v concentrations, was enhanced on trivalent chromium methacrylate (Volan[®] L) treated stainless steel. Other than differences in contact angle measurements, MED 6820 silicone SP coatings yielded similar results when characterized by FTIR-ATR, XPS or SEM. SEM micrographs did not reveal any evidence of corrosion for any treatment group in this study.

In situ solution polymerization coating has been shown to be effective for surface modifying 316L stainless steel with stable and hydrophilic coatings. Such surfaces may be useful for incorporation and controlled release of therapeutic agents from surface modified endovascular stents and keratome blades.

CHAPTER 6
LOADING AND RELEASE OF THERAPUETIC AGENTS FROM SURFACE
MODIFIED METAL ALKOXIDE TREATED STAINLESS STEEL

Introduction

Delivering therapeutic concentrations at the specific site that needs treatment is difficult to achieve with conventional systemic drug administration. Systemic drug delivery carries other problems, including systemic toxicity and drug residence issues, both of which can lead to further complications. Localized delivery of therapeutic drugs has been evaluated with devices such as endovascular stents where drugs were immobilized onto stents, chemically grafted or physically incorporated into coatings.^{8, 10, 11, 13, 14, 19} The results of these studies have been promising and indicate that targeted localized drug therapy can be achieved at therapeutic levels with low systemic effects. For keratome blades, there is a risk of infection due to incision in that any surgical intervention poses a potential risk of infection. Release of ofloxacin, an antimicrobial agent, from surface modified stainless steel has not been reported.

In this investigation, coating systems established from the previous chapters in this work were loaded with drugs following surface modification. Ofloxacin, a potent fluoroquinolone, was investigated as a surface eluted antimicrobial agent and dexamethasone, a glucocorticoid, was investigated as a surface eluted anti-inflammatory agent. The molecular structures of these drugs are illustrated in Figure 6.1. Drug loading of each coating system was determined by depletion assay analysis of the drug loading solutions. The depletion analysis was carried out assuming that the changes in drug

concentrations of the drug loading solutions are equal to the amount taken up by the coatings due to loading. Additionally, losses due to drug binding on glassware are not accounted for.

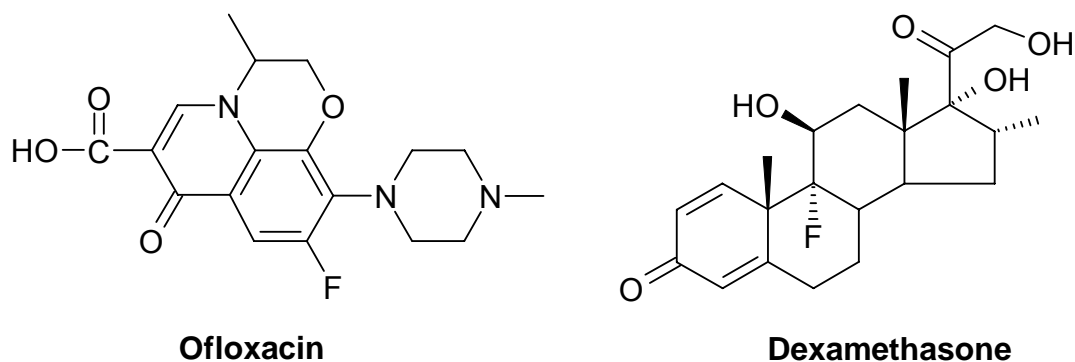


Figure 6.1 – Molecular structures for ofloxacin and dexamethasone.

Materials and Methods

Preparation of Substrates and Coatings

Stainless steel substrates (1 cm x 1 cm) with thicknesses of ~0.1 mm were cleaned by sequential sonication as described in Chapter 3, and dried in a vacuum oven at 60°C. Substrates were subsequently treated with 2% v/v Volan L[®] according to the procedure also described in Chapter 3. After chromium III methacrylate treatment, samples were coated as described below.

Controls consisted of untreated 316L stainless steel that underwent radiation grafting or solution coating and stainless steel that received neither chromium alkoxide treatment nor polymer coatings.

The monomers used in this study were 2-methacryloyloxyethyl phosphorylcholine (MPC; Dr. Ishihara, University of Tokyo) and n-vinyl-2-pyrrolidone (NVP; Polysciences, Inc). Treating volumes of 3 ml were used for each substrate with each gamma and solution polymerization (SP) coating condition. The coatings investigated in this study are summarized in Table 6.1.

For radiation grafted surface modifications, stainless steel substrates were deposited in MPC and NVP monomer solutions of 10% v/v concentrations that were prepared in 3 mL volumes in individual test tubes and degassed by mechanical vacuum pump. The samples were irradiated by a ^{60}Co gamma irradiator and exposed to a total dose of 0.1 Mrads at a dose rate of ~ 536 rads/min.

For solution polymerization (SP) coated surface modifications, cleaned Volan[®] L treated and untreated 316L stainless steel substrates were transferred to individual test tubes containing aqueous solutions of either 3 mL of 25% v/v NVP or MPC monomer plus Ultrapure[™] water with 0.125% v/v AIBN initiator or 45% MED 6820 oligomers that consisted of 1.5 mL of component A in chloroform and 1.5 mL of component B in chloroform. These solutions were then bubbled and backfilled with argon. Specimens in monomer solutions were placed in an oven that was heated to a minimum of 70°C for ~ 6 hours. Specimens contained in the dilute uncured silicone coating solutions were rotated in the solutions for 2 hours at $\sim 25^\circ\text{C}$, after which the samples were transferred to clean test tubes and cured at 60°C for 12 hours.

After coating the surfaces, samples were placed in new test tubes and tumble washed for one week with 5 mL of Ultrapure[™] water, which was decanted and replaced three times.

Post Loading Ofloxacin and Dexamethasone

Solutions of 3.0% (w/v) ofloxacin (Sigma-Aldrich) in 2% KOH were prepared. Methanol was used to prepare solutions of 0.5% (w/v) dexamethasone (Sigma-Aldrich). Table 6.1 lists the coatings conditions and drug that was investigated for each. The stainless steel specimens were placed into 3 mL volumes of these solutions and rotated

gently for 24 hrs, after which the samples were removed and dried at room temperature for 24 hrs.

Table 6.1 – Coating and metal alkoxide treatment conditions investigated for drug release where Oflox and Dex refers to ofloxacin and dexamethasone, respectively. 2% V-L refers to 2 % v/v Volan[®] L.

Coat	25% w/v MPC Solution Coated		10% w/v MPC Radiation Grafted		25% v/v NVP Solution Coated		45% v/v MED6820 Solution Coated		None
	2% V-L	None	2% V-L	None	2% V-L	None	2% V-L	None	
Oflox	✓	✓	-	-	✓	✓	-	-	✓
Dex	✓	✓	✓	✓	-	-	✓	✓	✓

Drug Loading Solution Depletion Study

Standard curves were established for both ofloxacin and dexamethasone using known drug concentrations from 1ppm to 50ppm in the loading solvents, KOH and methanol, where 1 ppm is equivalent to 1 µg/mL. These curves were used to calculate the concentration depletions for this study. The peaks of interest for ofloxacin and dexamethasone are 288 and 254 nm, respectively.

Aliquots of 1 mL were taken from stock solutions before drug loading and from drug soaking solutions after drug uptake, then transferred to UV-Visible Spectroscopy (UV-Vis) cuvettes to be measured immediately for depletion assay analysis. From the UV-Vis absorbance data, the difference in concentration of the drug stock solution and that of the solution following the loading procedure was calculated and recorded as the concentration of the drug loaded. These results were then normalized for substrate surface area and loading solution concentration.

Release of Drugs from Surface Modified 316L Stainless Steel

Ofloxacin release *in vitro* was conducted in phosphate buffered saline (PBS). PBS was prepared in our laboratory with a mixture of 50mM sodium monobasic with 50mM sodium dibasic solutions and adjusted to a pH of 7.4. The PBS stock was filtered through a 0.20 µm filter and autoclaved at 120°C. Dexamethasone release *in vitro* was conducted

in human blood plasma, donated from Shands Hospital Blood Bank, to better emulate the blood tissue environment of endovascular stents. The plasma was kept frozen until use, after which it was thawed and incubated for 5 minutes at 60°C, then centrifuged for 10 minutes. Precipitated proteins were removed and 0.02% of sodium azide was subsequently added to preserve the plasma, which was used immediately. The release media preparation procedures described here has been reported in previous work conducted by our laboratory.⁶⁵

Drug release studies were conducted out to 5 days. Drug loaded specimens were placed into 10 mL of respective release media contained in 15 mL capacity centrifuge tubes. Release was carried out at 37°C under continuous rotation. Aliquots of 1 mL were taken each hour for the first five hours and once a day through the fifth day and placed into either UV-Vis cuvettes (PBS) or 1.5 ml capacity centrifuge tubes (plasma). Removed aliquots were replaced with 1 mL of release media at each instance. Dexamethasone in plasma aliquots were sealed and frozen until HPLC analysis. Aliquots of ofloxacin release in PBS were sealed and refrigerated until UV-Vis analysis.

Dexamethasone release was quantified by HPLC assays with a system composed of a Perkin Elmer ISS-100 autosampler, a Consta Metric LDC Analytical high pressure pump, 25 μ L injection loop, an LDC Analytical Spectro Monitor 3200 UV Detector, a Discovery C-18 column (150 x 4.6 mm, 5 μ) and HP 3392-A III integrator. A standard curve for the range of 0.25 – 6 μ g/mL was prepared from a 100 μ g/mL solution of dexamethasone in acetonitrile. These standards were tested with 0.5, 2, and 6 μ g/mL concentrations of dexamethasone in plasma. Due to conducting dexamethasone release studies in plasma, the actual aliquots of released drug were first extracted from the media

by mixing 150 μL of the plasma release media with 10 μL of triamcinolone acetonide, which was used as an internal standard, and 500 μL of ethyl acetate to precipitate the proteins. This combination was mixed for 30 seconds and centrifuged for 10 minutes at 10,000 rpm. The supernatant was then removed, vacuum dried, reconstituted in 150 μL of acetonitrile, mixed and immediately analyzed by HPLC at a flow rate of 1.2mL/min with an injection volume of 25 μL at a temperature of 40°C and a set UV detection at 254nm.^{55, 66}

Preparation of Bacterial Cultures for Zone of Inhibition

Bacterial cultures were prepared by spreading 10 μL of either *s.epidermidis* or *s.aureus* cultures onto plate count agar prepared culture dishes. The concentration of both bacterial cultures were 10^8 colony forming units/mL. Post loaded ofloxacin in 25% v/v NVP SP coated samples of Volan[®] L and untreated stainless steel were placed into the prepared cultures. Silver acrylate functionalized stainless steel was also investigated for antimicrobial properties in cultures of both bacterial species. Samples were placed in bacteria seeded dishes and incubated at 37°C for 24 hours, after which the zones of inhibition were measured and photographed. The zones are reported as the distance from the sample edge to the edge of the zone that is perpendicular to the sample edge where bacterial growth was inhibited.

Analysis

Drug depletion assays were used to calculate the amount of drug that was loaded into the coatings. The depletion studies were analyzed by UV-Vis spectroscopy. Aliquots of drug release media from loaded coatings and controls were characterized by examination of sustained release profiles with UV-Vis for ofloxacin release into PBS and HPLC for dexamethasone release into human blood plasma. Reported values for drug

release analysis included three samples for each coating condition. Zones of inhibition were measured metrically using a ruler, where two samples were measured for each condition coating condition.

The controls consisted of post loaded and non-loaded samples of unmodified 316L stainless steel and surface modified 316L stainless steel without Volan[®] L treatment.

Results and Discussion

The drug solution depletion study was performed to determine the concentrations of ofloxacin and dexamethasone uptake by the coating from the drug loading procedure. To calculate the loaded drug concentrations, the surface area of the samples were measured and included in the analysis. Table 6.2 and 6.3 list the UV-Vis measured concentrations and sample surface areas as well as concentration conversions from ppm to $\mu\text{g}/\text{mm}^2$ for both the ofloxacin and dexamethasone depletion assays analyses.

Table 6.2 – Ofloxacin depletion UV-Vis absorption measurements in terms of concentration with adjustments for surface area and conversions, all values are reported as averages.

	Total Loaded (ppm)	Loading Vol. (mL)	Total Loaded (μg)	Surface Area (cm^2)	Uptake ($\mu\text{g}/\text{cm}^2$)	Uptake ($\mu\text{g}/\text{mm}^2$)
25% NVP Volan [®] L	5830	3	17491	3.59	4872	48.7
25% NVP No Agent	3241	3	9723	2.95	3295	33.0
25% MPC Volan [®] L	3648	3	10944	3.94	3132	31.3
25% MPC No Agent	3030	3	9091	3.61	2518	25.2
316L SS Control	4048	3	12142	3.45	3515	35.2

Table 6.3 – Dexamethasone depletion UV-Vis absorption measurements in terms of concentration with adjustments for surface area and conversions, all values are reported as averages.

	Total Loaded (ppm)	Loading Vol. (mL)	Total Loaded (μg)	Surface Area (cm^2)	Uptake ($\mu\text{g}/\text{cm}^2$)	Uptake ($\mu\text{g}/\text{mm}^2$)
25% MPC Volan [®] L	1896	3	5689	3.69	1541	15.4
25% MPC No Agent	1741	3	5222	3.64	1436	14.4
10% MPC Volan [®] L	1896	3	5689	3.33	1710	17.1
10% MPC No Agent	869	3	2607	3.69	774	7.7
45% MED Volan [®] L	1231	3	3694	2.90	1276	12.8
45% MED No Agent	1831	3	5492	3.21	1712	17.1
316L SS Control	1620	3	4888	3.23	1502	15.0

Chromium (III) methacrylate treated 316L stainless steel substrates that were surface modified generally exhibited increased drug uptake values relative to surface specimen surface area as shown in Tables 6.2 and 6.3.

The highest ofloxacin uptake value was $48.7 \mu\text{g}/\text{mm}^2$, corresponding to 25% v/v NVP SP coatings on Volan[®] L treated 316L stainless steel. 25% v/v NVP SP coatings on untreated stainless steel failed to yield increased ofloxacin loading compared with control values. 25% v/v MPC SP coatings on Volan[®] L treated stainless steel resulted in increased uptake ($\sim 31.3 \mu\text{g}/\text{mm}^2$) compared with MPC SP coated stainless steel that was not treated with Volan[®] L which was $\sim 25.2 \mu\text{g}/\text{mm}^2$. However, 25% v/v MPC SP coatings on Volan[®] L treated 316L stainless steel resulted in similar uptake compared with controls; and MPC SP coatings on untreated stainless steel had decreased uptake relative to uptake values for controls. The polarity of the MPC structure may contribute to these slightly lower drug uptake values.

Dexamethasone uptake values were lower than those seen for ofloxacin uptake, which correlates well with the lower loading solution concentrations. MPC SP coatings

on Volan[®] L treated stainless steel had dexamethasone loadings of $\sim 15.4 \mu\text{g}/\text{mm}^2$ that were comparable with unmodified stainless steel (control) with uptake values of $\sim 15.0 \mu\text{g}/\text{mm}^2$ and coatings on untreated stainless steel yielded values of $\sim 14.4 \mu\text{g}/\text{mm}^2$. Interestingly, radiation grafted 10% v/v MPC at 0.1 Mrads resulted in higher uptake values ($\sim 17.1 \mu\text{g}/\text{mm}^2$) for the Volan[®] L treated samples and much lower values than controls for coatings on untreated stainless steel ($\sim 7.7 \mu\text{g}/\text{mm}^2$). Furthermore, MED 6820 SP coatings on Volan[®] L treated stainless steel yielded in lower uptake values than MED 6820 SP coatings on untreated stainless steel. This could be attributed to a decrease propensity for swelling when the elastomeric material is bound at the coating-substrate interface limiting chain mobility.

Sustained release studies were conducted for the drug loaded specimens described here. Release from all coatings for both drugs was apparent to at least 5 days, which is a significant improvement from studies of the same drugs released from radiation grafted hydrophilic coatings in high pH solutions and without metal alkoxide surface treatments, where drug release was completed in the first two hours.

As shown in Figure 6.2, ofloxacin cumulative release from NVP SP coatings in the first 48 hours were $0.98 \mu\text{g}/\text{mm}^2$ and $0.66 \mu\text{g}/\text{mm}^2$ for Volan[®] L and untreated stainless steel, respectively. Cumulative release from controls yielded $0.95 \mu\text{g}/\text{mm}^2$, which was similar to released quantities seen for NVP SP coatings on Volan[®] L untreated stainless steel. While controls released a greater fraction of the loaded drug, this could result in shorter release times overall. Furthermore, as discussed in Chapter 3, the 316L stainless steel used in these studies were not electropolished, therefore having characteristically rougher surfaces. The roughness of these surfaces can also contribute to increase drug

physical-adsorption onto surfaces. However, extended studies would be necessary to confirm this.

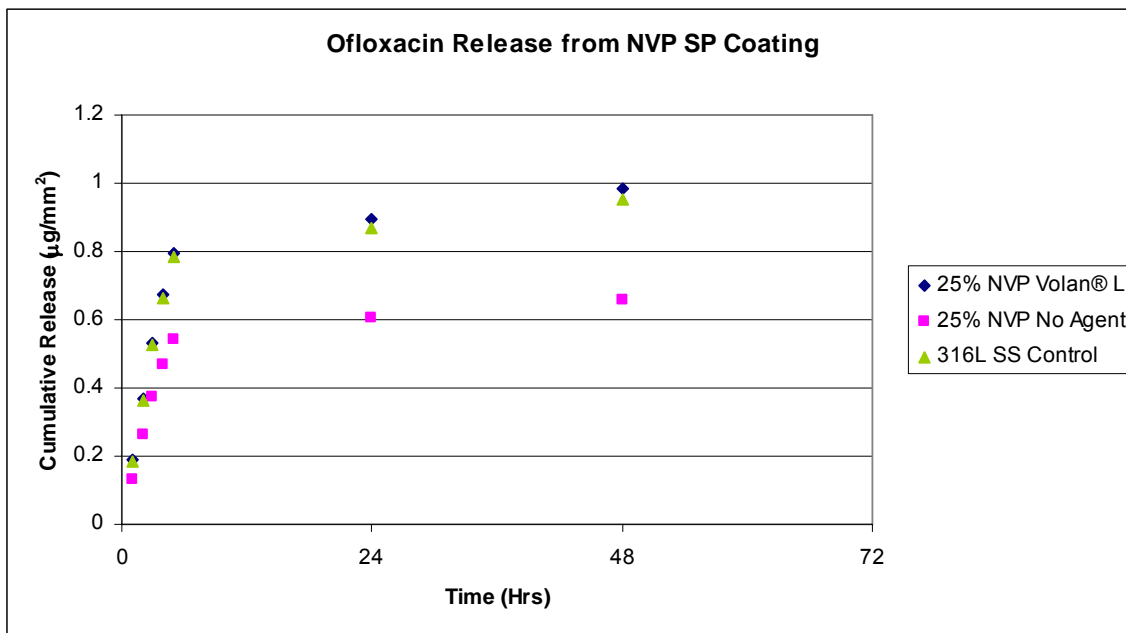


Figure 6.2 – Ofloxacin release from 25% v/v NVP SP coated Volan® L and untreated 316L stainless steel compared with unmodified controls.

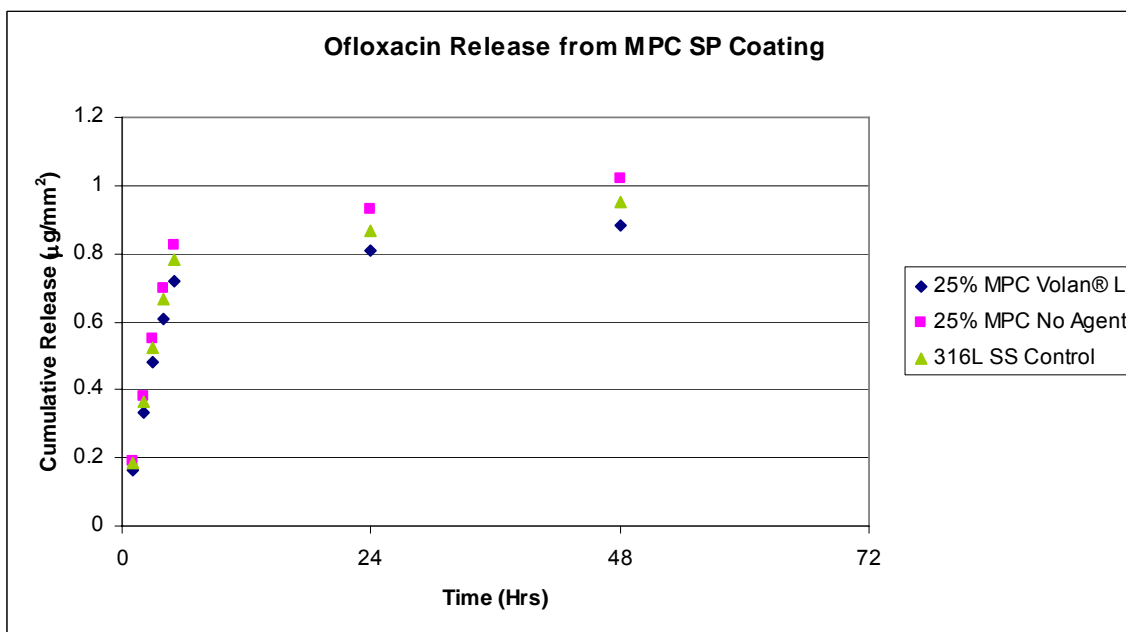


Figure 6.3 – Ofloxacin release from 25% v/v MPC SP coated Volan® L and untreated 316L stainless steel compared with unmodified controls.

Ofloxacin cumulative release from MPC SP coated surface modifications (Figure 6.3) were $0.88 \mu\text{g}/\text{mm}^2$ and $1.02 \mu\text{g}/\text{mm}^2$ for Volan[®] L and untreated stainless steel, respectively, in the first 48 hours. MPC coatings on untreated stainless steel released greater fractions of the loaded drugs, which could be related to increased release rates and/or the surface roughness.

Dexamethasone cumulative release from MPC SP coated, MPC gamma irradiation grafted, and MED6820 SP coated surface modifications (Figure 6.4-6) were 0.33, 0.33 and $0.31 \mu\text{g}/\text{mm}^2$ for Volan[®] L treated stainless steel, respectively, in the first 120 hours. Cumulative dexamethasone releases from these polymer coatings on untreated stainless steel were 0.31, 0.26 and $0.24 \mu\text{g}/\text{mm}^2$, respectively. Release from stainless steel controls were also measured, where cumulative values for these uncoated surfaces were $0.19 \mu\text{g}/\text{mm}^2$. All measured release concentrations below the limit of detection of $0.25 \mu\text{g}/\text{mL}$ (or approximately $0.01 \mu\text{g}/\text{mm}^2$) were not included in these analyses.

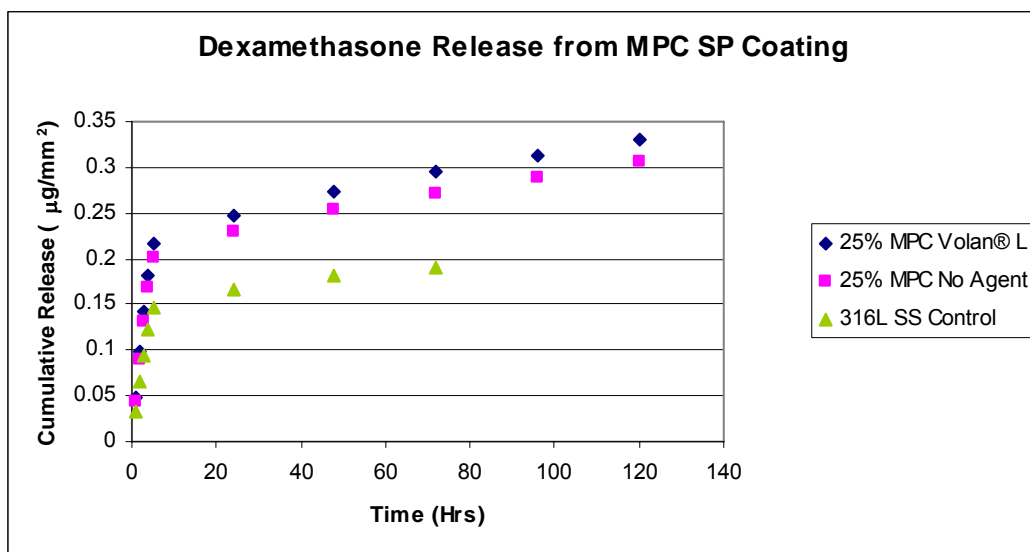


Figure 6.4 – Dexamethasone release from 25% v/v MPC SP coated Volan[®] L and untreated 316L stainless steel compared with unmodified controls.

Illustrated graphically in Figure 6.4, MPC SP coatings on Volan[®] L treated and untreated stainless steel released similar quantities of loaded dexamethasone, which had longer release times with cumulatively more released drug than controls. In Figure 6.5, MPC gamma irradiation grafted coating on Volan[®] L treated stainless steel yielded increased cumulative release values compared with both untreated stainless steel that was coated and controls. As shown in Figure 6.6, MED6820 SP coatings on Volan[®] L treated stainless steel yielded the greatest cumulative release values, where the control and MED6820 coated untreated stainless steel resulted in similar releases of dexamethasone.

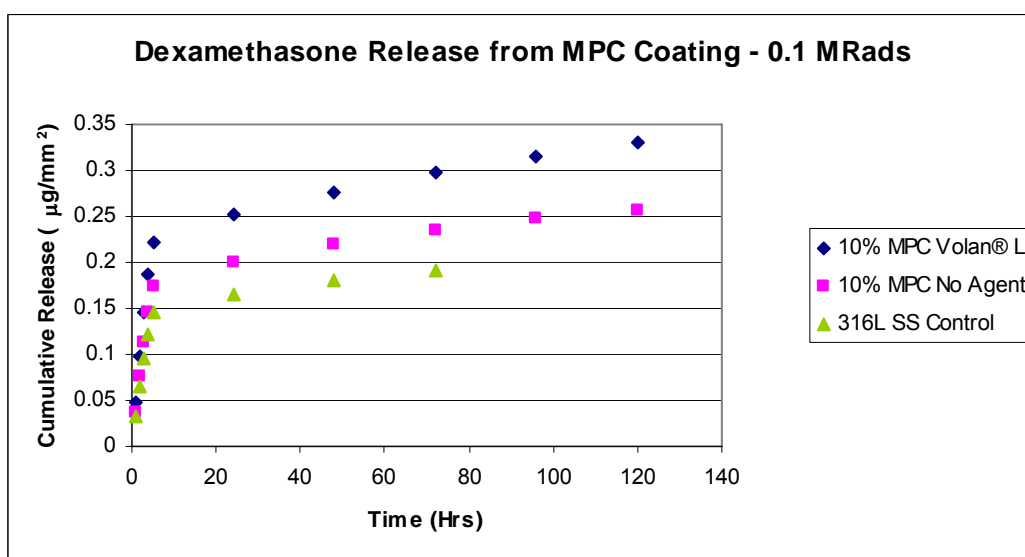


Figure 6.5 – Dexamethasone release from 10% v/v MPC gamma irradiation graft coated Volan[®] L and untreated 316L stainless steel compared with unmodified controls.

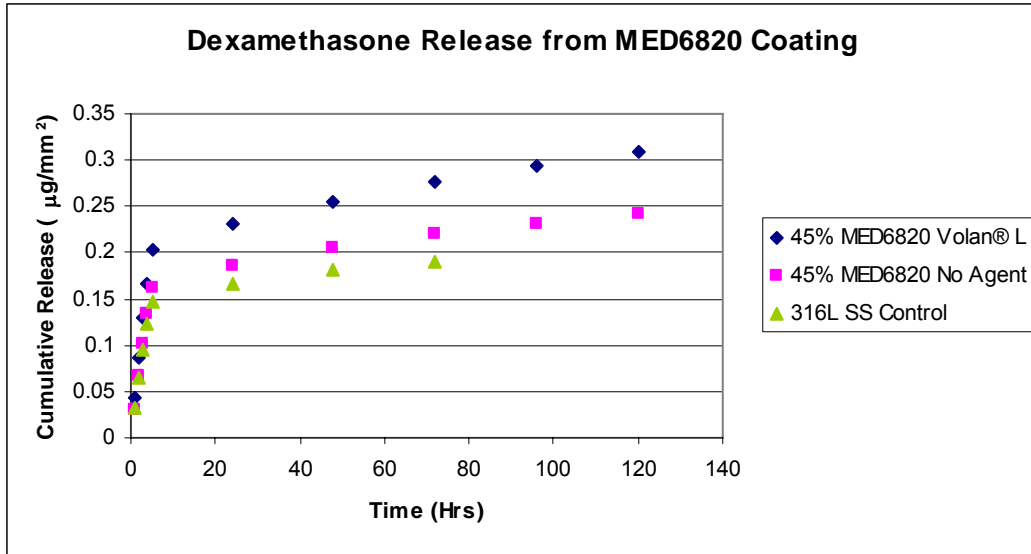


Figure 6.6 – Dexamethasone release from 45% v/v MED6820 SP coated Volan[®] L and untreated 316L stainless steel compared with unmodified controls.

Zones of inhibition were measured for specimens incubated in *s.epidermidis* and *s.aureus* cultures. As shown in Table 6.3, very little difference in inhibition zones were seen in *s.epidermidis* cultures for ofloxacin release from 25% v/v NVP SP coated Volan[®] L and untreated stainless steels, with zones of 15.5 and 16 mm, respectively. A slightly greater difference in zones was seen for cultures in *s.aureus*. Silver acrylate treatments did not yield a measurable zone in all culture plates. However, one specimen in an *s.aureus* culture resulted in a 2 mm zone. Unmodified 316L stainless steel in these bacterial cultures did not yield zones of inhibition. Examples of these zones are shown in Figure 6.7-6.9. These results suggest that therapeutic doses of ofloxacin were released from the drug loaded coatings.

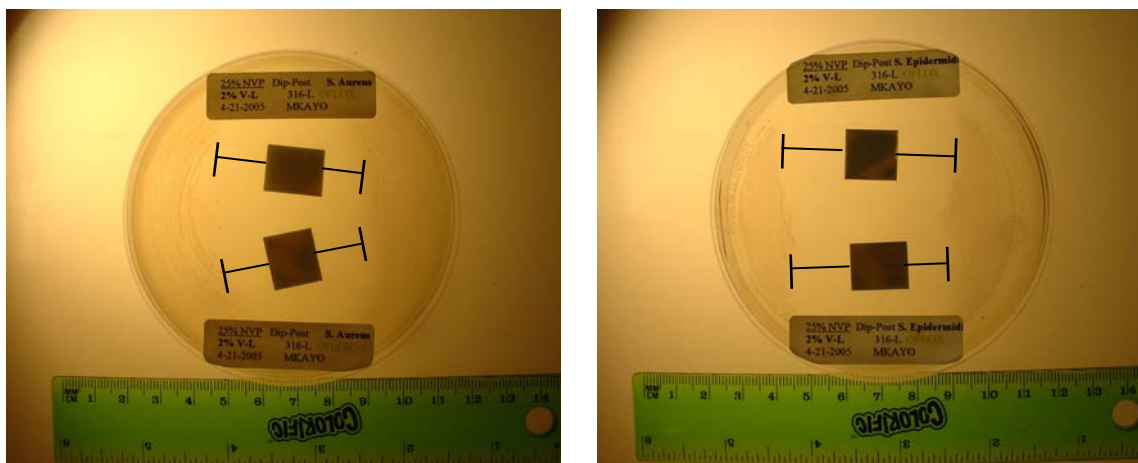


Figure 6.7 – Zone of inhibition of ofloxacin release from 25% NVP solution coated Volan[®] L treated 316L stainless steel. Left-S.Aureus. Right-S.Epidermidis.

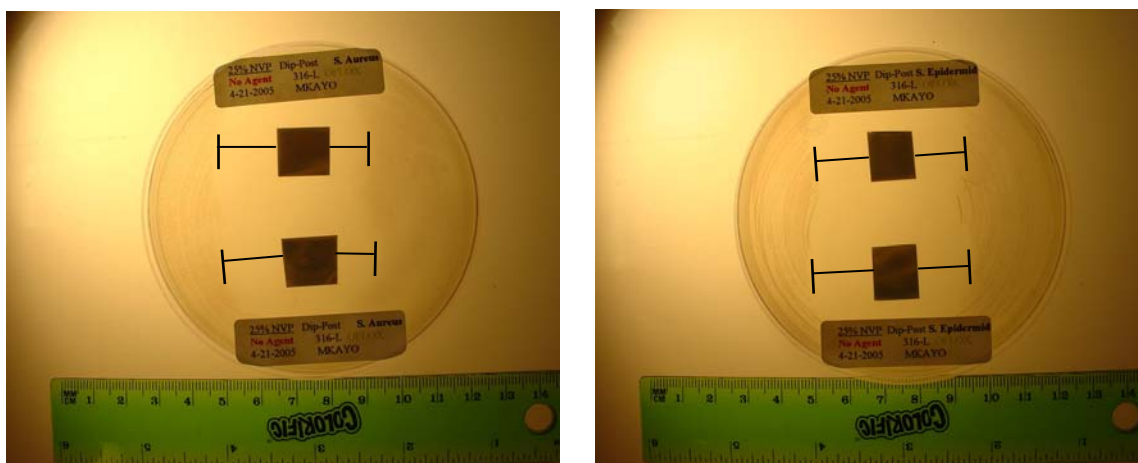


Figure 6.8 – Zone of inhibition of ofloxacin release from 25% NVP solution coated untreated 316L stainless steel. Left-S.Aureus. Right-S.Epidermidis.

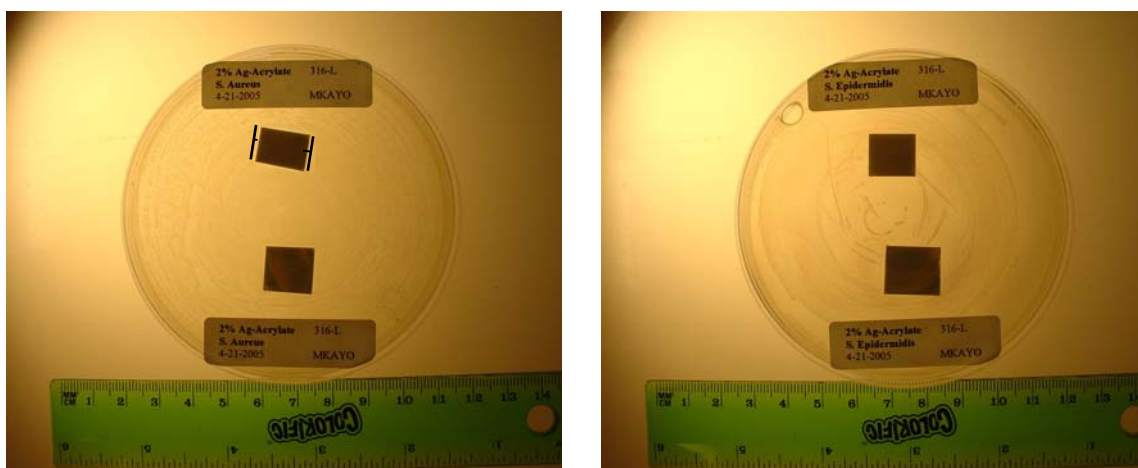


Figure 6.9 – Zone of inhibition of ofloxacin release from 2% silver acrylate functionalized 316L stainless steel. Left-S.Aureus. Right-S.Epidermidis.

Summary

The stainless steel surface modifications developed here have been shown to be capable of loading with antimicrobial agent, ofloxacin, and anti-inflammatory agent, dexamethasone. Ofloxacin release from surface modified stainless steel has not been reported before. Ofloxacin loading concentrations of $48.7 \mu\text{g}/\text{mm}^2$ were observed for 25% v/v NVP SP coatings on chromium (III) methacrylate activated stainless steel. 25% v/v MPC SP coatings on activated stainless steel exhibited $31.3 \mu\text{g}/\text{mm}^2$ of ofloxacin loading.

Previous research conducted in this laboratory reported dexamethasone loadings of $4.3 \mu\text{g}/\text{mm}^2$ for gamma radiation grafted polymers prepared at high pH.⁵⁵ Coatings studies hence have higher drug loadings of dexamethasone, where 25% v/v MPC SP solution coatings on chromium (III) methacrylate activated stainless steel had $15.4 \mu\text{g}/\text{mm}^2$ uptake and 10% v/v MPC radiation grafted modifications on chromium (III) methacrylate treated stainless steel yielded $14.4 \mu\text{g}/\text{mm}^2$ uptake. These values are approximately three times greater than what was previously reported. Additionally, these new values are much greater than loading values reported in the Study of Antirestenosis with the BiodivYsio Dexamethasone-Eluting Stent (STRIDE) human multicenter pilot trial, which reported a loading of $0.5 \mu\text{g}/\text{mm}^2$ for phosphorylcholine coated stents.²³

Non-linear release of these drugs was observed in a 5 day test. Ofloxacin release in PBS and dexamethasone release in human blood plasma was evident past five days. Previously reported *in vitro* release studies for dexamethasone indicated complete release within 24 hours.^{23, 55} The highest cumulative release of dexamethasone was seen for 25% MPC SP coated and 10% MPC gamma irradiation grafted Volan[®] L treated stainless

steel. Similar release quantities were also recorded for MPC SP coatings on untreated stainless steel.

These results suggest the improved, stable hydrophilic coatings on stainless steel prepared in this study may enhance the loading and prolong the release of drugs such as dexamethasone and ofloxacin.

CHAPTER 7 CONCLUSIONS

Implanted medical devices often lead to complications associated with tissue-material interfacial interactions. The overall objective of this research was therefore to study the influence of chromium alkoxide coupling agents on the adhesion of polymers commonly used in bioactive coatings with the ultimate goal of developing improved methods for surface modification of metallic medical devices such as endovascular stents and keratome blades to improve biocompatibility.

1. New surface coating methods based on 2% v/v trivalent chromium alkoxide functionalization of 316L stainless steel followed by gamma radiation grafting, pulsed laser ablation deposition, radio frequency plasma, and solution polymerization coating were developed.
2. Chromium (III) fatty acid and chromium (III) methacrylate treatments were adapted for 316L stainless steel surface functionalizations. This surface activation is simpler than most other surface activation methods.
3. Chromium alkoxide treatments were shown to provide corrosion free functionalization of stainless steel surfaces.
4. Chromium alkoxide functionalized stainless steel surfaces were coated with hydrophilic vinyl monomers such as MPC and NVP to yield greater stability and increased coating hydrophilicity compared to non-surface functionalized stainless steel.

5. MPC and NVP that were radiation grafted and solution polymerization coated on Volan[®] L metal alkoxide functionalized 316L stainless steel yielded hydrophilic contact angles that were maintained or recovered throughout a drying and rehydrating process.
6. MPC and MPC/DMA surface modifications of stainless steel using chromium alkoxide treated substrates were compared with the untreated stainless steel. Surfaces that were more stable, hydrophilic, and lubricious to the touch were achieved. These coatings maintained excellent hydrophilic properties without measurable recovery time after dehydration.
7. Stable hydrophilic coatings were prepared by gamma irradiation of monomer solutions on chromium alkoxide functionalized 316L stainless steel. Single monomer formulations of NVP, MPC and KSPA were comparable to copolymers of these monomers with DMA.
8. Crosslinked medical grade resin-filled silicone was deposited by Pulsed Laser Ablation Deposition (PLAD) to surface modify stainless steel. Parameters such as fluence, oxygen content and base pressure were varied to deposit PDMS-like or silica-like coatings.
9. PLAD results differ from previous reports in that higher base pressures such as 30 mTorr yielded hydrophilic coatings at fluences above 200 mJ/cm² and lower base pressures such as 5.0×10^{-5} mTorr produced hydrophobic coatings at fluences higher than 125 mJ/cm².

10. Homogeneous RF-plasma surface modifications with NVP, DMA and NVP/DMA at 50 Watts for 5 minute treatment times were prepared with vertical orientation of samples; a geometry that treated both sides of the substrates.
11. RF plasma surface modifications with NVP, DMA, and NVP/DMA resulted in contact angles that were hydrophilic, but not stable.
12. Solution polymerization coating of chromium (III) methacrylate functionalized 316L stainless steel by NVP, MPC and KSPA was shown to be effective for surface modifying 316L stainless steel to yield stable hydrophilic coatings that were lubricious to the touch. Concentrations of MPC in the range of 10% v/v and 25% v/v did not appear to affect the lubricity or stability of these coatings. For NVP based coatings, a higher concentration of 25% v/v was preferred. KSPA solution polymerization coatings at 10% v/v concentration exhibited improved hydrophilic stability on Volan[®] L functionalized stainless steel.
13. The surface modifications prepared in this research were shown to be capable of loading with therapeutic agents for sustained local drug release. Loading concentrations of 48.7 $\mu\text{g}/\text{mm}^2$ of ofloxacin and 17.1 $\mu\text{g}/\text{mm}^2$ of dexamethasone were achieved. Some increases in drug loading were seen for surface modified stainless steel with metal alkoxide treatments. Drug release at therapeutic levels was demonstrated with ofloxacin (antimicrobial) and dexamethasone (anti-inflammatory). Release of these drugs from the surface modifications developed here suggests that such treatments may be tailored for application to a variety of implantable medical devices.

CHAPTER 8 FUTURE WORK

Based on this research, several opportunities for future studies are suggested:

1. Modifications with Increased Thicknesses on Chromium Alkoxide Functionalized Stainless Steel
 - a. Further modifying initial radiation grafts, solution coatings, with additional radiation grafting to yield IPNs.
 - b. Add crosslinker, such as ethylene glycol dimethacrylate (EGDMA), in solution coating systems.
 - c. Investigate monomers with ionic functionality.
 - d. Use electropolished stainless steel or cobalt-chromium formulation metals to determine if coating adhesion is thereby affected.
2. Surface Testing
 - a. Study the method of the coupling agent reactions with substrate surfaces and coating solutions.
 - b. Measure adhesive strength of surface modifications using nanoscratch and nanoindentation methods.
 - c. Apply additional methods for surface thickness measurement.
3. Delivery of Therapeutic Agents
 - a. Study release characteristics as a kinetic process including examination of chemistry relative to time, stress, and strain on the tested system to mimic dynamic *in vivo* conditions that stents would be subject to.

- b. Investigate *in situ* loading methods and release of ofloxacin, dexamethasone, and other drugs to achieve sustained release beyond 14 days.
- c. Investigate the use of 17β -estradiol, a smooth muscle cell growth modulator, as a restenosis inhibitor agent released from hydrophilic coatings for stents treated with metal alkoxides.
- d. Study combination loading and release of drugs such as dexamethasone and 17β -estradiol.

4. *In vitro* Studies

- a. Examine *in vitro* cell culture proliferation of endothelial cells on drug loaded and unloaded surface modified materials.
- b. Examine *in vitro* cell culture proliferation of vascular smooth muscle cells on drug loaded and unloaded surface modified materials.

5. *In vivo* Studies

- a. Implant various stent treatment groups in rabbits

LIST OF REFERENCES

1. Ratner BD, Hoffman AS, Schoen FJ, Lemons JE, Editors. Biomaterials Science: An Introduction to Materials in Medicine, Academic Press, San Diego, CA 1996:484 pp.
2. Kirchengast M, Munter K. Endothelin and restenosis. Cardiovascular Research 1998; 39:550-555.
3. Sahin NO, Burgess DJ. Competitive interfacial adsorption of blood proteins. Farmaco 2003; 58:1017-21.
4. Wang F, Stouffer GA, Waxman S, Uretsky BF. Late coronary stent thrombosis: early vs. late stent thrombosis in the stent era. Catheter Cardiovasc Interv 2002; 55:142-7.
5. Glanze WDe. The Mosby Medical Encyclopedia. New York: Plume, Penguin Books USA Inc, 1992:926 pp.
6. American Heart Association. www.americanheart.org, 2004.
7. Serruys PW, de Jaegere P, Kiemeneij F, et al. A comparison of balloon-expandable-stent implantation with balloon angioplasty in patients with coronary artery disease. Benestent Study Group. New England Journal of Medicine 1994; 331:489-95.
8. Dzau VJ, Braun-Dullaeus RC, Sedding DG. Vascular proliferation and atherosclerosis: New perspectives and therapeutic strategies. Nature Medicine 2002; 8:1249-1256.
9. Welt FG, Rogers C. Inflammation and restenosis in the stent era. Arterioscler Thromb Vasc Biol 2002; 22:1769-76.
10. Indolfi C, Mongiardo A, Curcio A, Torella D. Molecular mechanisms of in-stent restenosis and approach to therapy with eluting stents. Trends in Cardiovascular Medicine 2003; 13:142-148.
11. Nakatani M, Takeyama Y, Shibata M, et al. Mechanisms of restenosis after coronary intervention: difference between plain old balloon angioplasty and stenting. Cardiovascular Pathology 2003; 12:40-48.

12. Schuessler A, Strobel M, Steegmueller R, Piper M. Stent materials and manufacturing: requirements and possibilities/opportunities. ASM Materials & Processes for Medical Devices Conference, Anaheim, CA, 2003.
13. Babapulle MN, Eisenberg MJ. Coated stents for the prevention of restenosis: part II. *Circulation* 2002; 106:2859-66.
14. Hofma SH, van Beusekom HM, Serruys PW, van Der Giessen WJ. Recent developments in coated stents. *Curr Interv Cardiol Rep* 2001; 3:28-36.
15. Endovascular Today: Drug-Eluting Stent Update. www.evtoday.com, 2004.
16. Duda SH, Poerner TC, Wiesinger B, et al. Drug-eluting stents: potential applications for peripheral arterial occlusive disease. *Journal of Vascular and Interventional Radiology* 2003; 14:291-301.
17. Sehgal SN. Rapamune (Sirolimus, rapamycin): an overview and mechanism of action. *Ther Drug Monit* 1995; 17:660-5.
18. Ruygrok PN, Muller DW, Serruys PW. Rapamycin in cardiovascular medicine. *Internal Medicine Journal* 2003; 33:103-109.
19. Sousa JE, Serruys PW, Costa MA. New frontiers in cardiology: drug-eluting stents: part II. *Circulation* 2003; 107:2383-9.
20. Lewis AL, Leppard SW. Stents with drug-containing amphiphilic polymer coating. *PCT Int Appl Wo: (Biocompatibles Limited, UK)*. 2002:51 pp.
21. Abizaid A, Albertal M, Costa Marco A, et al. First human experience with the 17-beta-estradiol-eluting stent: the estrogen and stents to eliminate restenosis (EASTER) trial. *Journal of the American College of Cardiology* 2004; 43:1118-21.
22. Joung YK, Kim HI, Kim SS, Chung KH, Jang YS, Park KD. Estrogen release from metallic stent surface for the prevention of restenosis. *Journal of Controlled Release* 2003; 92:83-91.
23. Liu X, Huang Y, Hanet C, et al. Study of antirestenosis with the BiodivYsio dexamethasone-eluting stent (STRIDE): a first-in-human multicenter pilot trial. *Catheterization and cardiovascular interventions : official journal of the Society for Cardiac Angiography & Interventions* 2003; 60:172-8; discussion 179.
24. Kallinteri P, Antimisiaris SG, Karnabatidis D, Kalogeropoulou C, Tsota I, Siablis D. Dexamethasone incorporating liposomes: an in vitro study of their applicability as a slow releasing delivery system of dexamethasone from covered metallic stents. *Biomaterials* 2002; 23:4819-26.

25. Lincoff AM, Furst JG, Ellis SG, Tuch RJ, Topol EJ. Sustained local delivery of dexamethasone by a novel intravascular eluting stent to prevent restenosis in the porcine coronary injury model. *Journal of the American College of Cardiology* 1997; 29:808-816.
26. Wu Z, Bai X. Vertical vibration method for the measurement of drug release rate of levonorgestrel in contraceptive vaginal rings in vitro. *Shengzhi Yu Biyun* 1986; 6:18-21.
27. Sarkar NN. Low-dose intravaginal estradiol delivery using a Silastic vaginal ring for estrogen replacement therapy in postmenopausal women: a review. *European Journal of Contraception & Reproductive Health Care: Official Journal of the European Society of Contraception* 2003; 8:217-24.
28. Matlin SA, Belenguer A, Hall PE. Progesterone-releasing vaginal rings for use in postpartum contraception. I. in vitro release rates of progesterone from core-loaded rings. *Contraception* 1992; 45:329-41.
29. Malcolm RK. The intravaginal ring. *Drugs and the Pharmaceutical Sciences* 2003; 126:775-790.
30. Jackanicz T, Croxatto AHB, Drexler LG, Zegers-Hochschild F. Progesterone vaginal ring for treatment of infertility. US Patent Application. Us: (The Population Council, USA). 1999:6 pp.
31. Englund DE, Victor A, Johansson ED. Pharmacokinetics and pharmacodynamic effects of vaginal oestradiol administration from silastic rings in post-menopausal women. *Maturitas* 1981; 3:125-33.
32. Holmgren PA, Lindskog M, von Schoultz B. Vaginal rings for continuous low-dose release of oestradiol in the treatment of urogenital atrophy. *Maturitas* 1989; 11:55-63.
33. Smith P, Heimer G, Lindskog M, Ulmsten U. Oestradiol-releasing vaginal ring for treatment of postmenopausal urogenital atrophy. *Maturitas* 1993; 16:145-54.
34. Zhang C-X, Sheng J, Ma J-T. Drug release system based on silicone rubber and levo-norgestrel. *Yingyong Huaxue* 2002; 19:597-599.
35. Chauhan PS, Varma KC. In vitro release of progestogens from contraceptive implants. *Indian Journal of Pharmaceutical Sciences* 1986; 48:29-33.
36. Marotta JS, Goldberg EP, Habal MB, et al. Silicone gel breast implant failure: evaluation of properties of shells and gels for explanted prostheses and meta-analysis of literature rupture data. *Annals of Plastic Surgery* 2002; 49:227-42; discussion 242-7.

37. Schopflin G, Fuchs P, Kolb KH. Pharmaceutical preparations containing silicon rubber. Brit Gb: (Schering A-G, Fed Rep Ger.). 1975:6 pp Addn to Brit 1,412,969.
38. Widenhouse CW, Goldberg EP. Method for the surface modification of silicone surfaces for medical goods. PCT Int Appl Wo: (University of Florida, USA; Jabar H; Urbaniak D). 2003:22 pp.
39. Widenhouse CW, Goldberg EP, Seeger JM. Antithrombogenic coatings for biomedical devices. US Pat Appl Publ Us (USA) 2002:11 pp, Cont.-in-part of US Ser No 113,375, abandoned.
40. Akura J, Funakoshi T, Kadonosono K, Saito M. Differences in incision shape based on the keratome bevel. J Cataract Refract Surg 2001; 27:761-5.
41. European Society of Cataract and Refractive Surgeons: www.escrs.org, 2005.
42. Kwei JZ-h. Adhesion promoter comprising chromium methacrylate-hydrochloride complexes and poly(vinyl alcohol) for bonding metals and thermoset resins. US Patent Application. Us (E I Du Pont de Nemours & Co, USA). 1999:4 pp, Cont of US Ser No 599,826, abandoned.
43. Keeley C, Kwei JZ-h. Dupont (R) Volan L (R) Bonding Agent Inquiries: Zaclon, Inc. & Dupont, 2004.
44. Goldberg EP, Yahiaoui A, Mentak K, Erickson TR, Seeger J. Polymer grafting for enhancement of biofunctional properties of medical and prosthetic surfaces. US Us (University of Florida, USA). 2002:29 pp, Cont-in-part of US 5,376,400.
45. Seeger JM, Ingegno MD, Bigatan E, et al. Hydrophilic surface modification of metallic endoluminal stents. Journal of Vascular Surgery 1995; 22:327-35; discussion 335-6.
46. Ishihara K, Nomura H, Mihara T, Kurita K, Iwasaki Y, Nakabayashi N. Why do phospholipid polymers reduce protein adsorption? Journal of Biomedical Materials Research 1998; 39:323-330.
47. Nakaya T, Li Y. Recent progress of phospholipid polymers. Designed Monomers and Polymers 2003; 6:309-351.
48. New G, Moses Jeffrey W, Roubin Gary S, et al. Estrogen-eluting, phosphorylcholine-coated stent implantation is associated with reduced neointimal formation but no delay in vascular repair in a porcine coronary model. Catheterization and Cardiovascular Interventions 2002; 57:266-71.
49. Whelan DM, van der Giessen WJ, Krabbendam SC, et al. Biocompatibility of phosphorylcholine coated stents in normal porcine coronary arteries. Heart (British Cardiac Society) 2000; 83:338-45.

50. Clough RL. High-energy radiation and polymers: A review of commercial processes and emerging applications. *Nuclear Instruments & Methods in Physics Research Section B-Beam Interactions with Materials and Atoms* 2001; 185:8-33.
51. Brook MA. *Silicon in Organic, Organometallic, and Polymer Chemistry*. New York: John Wiley & Sons, Inc., 2000:680 pp.
52. Arkles B. *Gelest: A Survey of Properties and Chemistry*. Tullytown: Gelest, Inc., 1998:544 pp.
53. Bertrand OF, Sipehia R, Mongrain R, et al. Biocompatibility aspects of new stent technology. *J Am Coll Cardiol* 1998; 32:562-71.
54. Wieneke H, Schmermund A, von Birgelen C, Haude M, Erbel R. Therapeutic potential of active stent coating. *Expert Opin Investig Drugs* 2003; 12:771-9.
55. Urbaniak DJ. *Surface Modification of Medical Implant Materials with Hydrophilic Polymers for Enhanced Biocompatibility and Delivery of Therapeutic Agents*. Gainesville: University of Florida, 2004:176 pp.
56. Campbell D, Pethrick RA, White JR. *Polymer Characterization : Physical Techniques*. Cheltenham, UK: S Thornes, 2000:viii, 481 pp.
57. Sheets JW. *Hydrophilic polymer coatings to prevent tissue adhesion*, 1983:xiv, 172 pp.
58. Bityurin N, Muraviov S, Alexandrov A, Malyshev A. UV laser modifications and etching of polymer films (PMMA) below the ablation threshold. *Applied Surface Science* 1997; 110:270-274.
59. Rau K, Singh R, Goldberg E. Nanoindentation and nanoscratch measurements on silicone thin films synthesized by pulsed laser ablation deposition (PLAD). *Materials Research Innovations* 2002; 5:151-161.
60. Rau K, Singh R, Goldberg E. Synthesis and characterization of cross-linked silicone thin films by pulsed laser ablation deposition (PLAD). *Materials Research Innovations* 2002; 5:162-169.
61. Laude LD, Soudant S, Beauvois S, Renaut D, Jadin A. Laser ablation of charged polymers. *Nuclear Instruments & Methods in Physics Research Section B-Beam Interactions with Materials and Atoms* 1997; 131:211-218.
62. Yahiaoui A. Surface modification of intraocular lens polymers by hydrophilic graft polymerization for improved ocular implant biocompatibility, 1990:xvii, 235 pp.
63. Biagtan EC. Effects of gamma radiation on polymer degradation and surface graft polymerization, 1995:xii, 169 pp.

64. Odian GG. Principles of Polymerization. New York: Wiley, 1991:xxii, 768 pp.
65. Urbaniak DJ, Mauldin J, Goldberg EP. Nanoscratch characterization of polymeric coatings under aqueous conditions. Society for Biomaterials 28th Annual Meeting Transactions. Tampa, FL, 2002:569A.
66. Derendorf H, Rohdewald P, Hochhaus G, Mollmann H. Hplc determination of glucocorticoid alcohols, their phosphates and hydrocortisone in aqueous-solutions and biological-fluids. Journal of Pharmaceutical and Biomedical Analysis 1986; 4:197-206.

BIOGRAPHICAL SKETCH

The author was born in Bronx, NY, lived in Taiwan for two and a half years and in Orlando, FL until she graduated from Lake Brantley High School. She pursued her undergraduate education at University of Florida College of Engineering in the Department of Materials Science and Engineering with a focus in Polymers. After a few years in this program, the author also chose to pursue studies in fine arts to further explore her creative talents at the same institution. In August 2001, Margaret was awarded a Bachelors of Science degree, which was followed by a Masters of Science in April 2004 both from University of Florida College of Engineering in the Department of Materials Science and Engineering. Finally after numerous evenings in MAE 234D and several bottles of wine, the author defended her dissertation thesis on June 9th, 2005 and passed.

The author was highly involved with extra curricular activities. For the University of Florida Benton Engineering Council, she served as Society For Biomaterials Representative (2002-03), Assistant Treasurer (2002-03), Finance Committee Member (2002-05), and Treasurer (2003-04). For Society For Biomaterials, Margaret served as Secretary (2002-04) of University of Florida Student Chapter, Secretary (2002-04) of SFB National Student Section, Student Representative (2003-05) of the Long Range Planning Committee, Co-Programs Chair (2003-05) of Ophthalmologic Biomaterials SIG, Student Representative (2003-05) of Membership Committee, Treasurer (2004-05) of University of Florida Student Chapter, Abstract Reviewer & Moderator (2004-05) for

the 30th Annual Society For Biomaterials Meeting & Expo., Memphis, TN, and Chair (2005-06) of Membership Committee.

The author's hobbies include first and foremost wine tasting, college basketball, and dancing to any music that moves her. Additionally, she enjoys oil painting, sculpture, rubber stamping, and jewelry design. Furthermore, she has been known to cook exotic dishes, eat large amounts of salted pork products, spoil her Abyssinian cats, have success with fix-it-herself projects, and she has also been spotted at the driving range from time to time.